University of Alberta

Conversion of Protein-Rich Waste Biomass into Value-Added Polymers

by

Nayef El-Thaher

A thesis submitted to the Faculty of Graduate Studies and Research
in partial fulfillment of the requirements for the degree of

Doctor of Philosophy

in

Chemical Engineering

Chemical & Materials engineering

Spring 2014
Edmonton, Alberta

ABSTRACT

Conversion of protein-rich biomass waste into value-added industrial products via chemical cross-linking reactions was explored. Two types of cross-linking reagents were investigated: dialdehydes and epoxy resins. Reaction chemistry was the main focus of this investigation and the main reaction parameters selected for study were electrolytes and protein molecular weight since raw material modification usually involves these two parameters. First, the reaction chemistry of glutaraldehyde was investigated. Glutaraldehyde is a cheap and highly reactive cross-linking reagent. Its reaction chemistry, however, is poorly understood. At low reaction temperatures, protein amine groups form Schiff bases with carbonyl groups of glutaraldehyde. The resulting C═N bond is weak and can be easily broken by heat or dissolution in water. As the reaction temperature is increased, the more stable C—N bond is formed. A network with low water solubility and significantly improved thermal stability is produced. The presence of water has a dual effect. Water acts as a medium to disperse hydrolyzed proteins into glutaraldehyde and is also a hydrogen source to drive the reaction forward. However, water is a byproduct. Its presence suppresses the reaction from the standpoint of thermodynamic equilibrium, and it must therefore be driven off. Epoxy-protein reaction chemistry was also investigated. The effects of salt, molecular weight and viscosity, and mass ratio on the apparent activation energy of the cross-linking reaction of epoxy resins and protein hydrolysate were studied by nonisothermal differential scanning calorimetry. The presence of salts contributed to an increase in the apparent

activation energy. The curing of epoxy resins with lower molecular weight protein hydrolysates was found to have lower activation energy and order of reaction. An increase in the concentration of curing groups resulted in a small increase in the order of reaction. The activation energy of curing bisphenol A diglycidyl ether, with viscosity 500–700 cP, was found to be significantly higher than the curing activation energy of polypropylene glycol diglycidyl ether (viscosity ~50 cP). Denaturant addition was also investigated and was found to be an energetically efficient alternative to higher degrees of protein hydrolysis for subsequent reactions.

ACKNOWLEDGMENTS

I am grateful to my supervisor Professor Phillip Choi for his guidance and help during the course of my research and for his guidance in the write-up of this thesis.

I am also grateful to the support staff and professors at the University of Alberta for all the information and help given to me during my studies at the university.

I am also grateful to Professors David Bressler and Jonathan Curtis, as well as members of their research groups for their collaboration and technical support over the past four years.

I am also grateful to PrioNet, *Alberta Prion Research Institute* (APRI), and the Alberta Livestock and Meat Agency (ALMA) for their financial support during the research.

TABLE OF CONTENTS

LIST OF TABLES

LIST OF FIGURES

NOMENCLATURE

α: extent of reaction (degree of cure)

α_M: extent of reaction at maximum value of y(α)

α_p: extent of reaction at peak temperature

dα/dt: reaction rate with respect to time

dα/dT: reaction rate with respect to temperature

$f(\alpha)$: function of extent of reaction

$h(P)$: function of pressure dependence

y(α): special function of extent of reaction

β: heating rate (DSC scan)

ΔH: enthalpy of reaction

A_o: pre-exponential factor

BSE: Bovine Spongiform Encephalopathy

CFIA: Canadian Food Inspection Agency (Canada)

DGEBA: bisphenol A diglycidyl ether

DSC: differential scanning calorimetry

E_a: activation energy

E_α: activation energy at an extent of reaction

FDA: Food and Drug Administration (USA)

GPI: Glycosyl Phosphatidylin Isotol

$k(T)$: temperature-dependent rate constant

m, n, p: reaction order parameters

P: pressure

PAGE: polyacrylamide gel electrophoresis

PEP180: SRM hydrolyzed at 180 ºC, water extracted

PEP180SA: SRM hydrolyzed at 180 ºC, salt-solution extracted

PEP220: SRM hydrolyzed at 220 ºC, water extracted

PEP220SA: SRM hydrolyzed at 220 ºC, salt-solution extracted

PMCA: Protein Misfolding Cyclic Amplification

PrP: Prion, *pro*teinaceous *i*nfectious *on*ly

PrP^{C}: normally folded protein

PrP^{Sc}: misfolded prion, scrapie

PPGDE: polypropylene glycol diglycidyl ether

Q_T: total heat of reaction

d*Q*/d*t*: heat flow measured by DSC

r: correlation coefficient

R: universal gas constant

SDS: sodium dodecyl sulfate

SRM: Specified Risk Material

T: temperature

T_α: peak temperature at extent of reaction (DSC exotherm)

T_{eq}: temperature at which two different reactions have the same reaction rate

T_p: peak temperature (DSC exotherm)

TEA: triethylamine

TGA: thermogravimetric analysis

TSE: Transmissible Spongiform Encephalopathy

vCJD: variant Creutzfeldt-Jakob Disease

w/w: mass fraction

x: reduced activation energy

CHAPTER 1

1.0 INTRODUCTION

This study explored the hydrolysis of Specified Risk Material (SRM) as per Canadian Food Inspection Agency (CFIA) safe disposal guidelines and the subsequent chemical treatment of hydrolyzed materials. SRM consists of the skull, brain, trigeminal ganglia, eyes, tonsils, spinal cord & column, dorsal root ganglia, and distal ileum for cows older than 30 months. For the younger cows, SRM consists of only the tonsils and distal ileum [1]. The end-goal of the project is the value-added conversion of hydrolyzed SRM into a stable product.

This body of work constitutes an investigation of the chemical and physical properties of hydrolyzed proteins in order to facilitate a better understanding of protein biomass behavior in general. The benefit of such an approach lies in the transferability of findings for any type of protein-based waste material in an attempt to standardize research methods for the evaluation of the suitability of protein-rich materials for subsequent utilization in industrial, non-food applications regardless of the source of the biomass.

Hydrolysis of SRM is mandated by government regulations as a suitable disposal method due to the specific occurrence of BSE. Nonetheless, protein hydrolysis is also useful for denaturing and breaking down large molecules of

proteins that may otherwise be insufficiently soluble or their reactive groups are inaccessible due to the presence of tertiary structures in their folded state. The destruction of bacteria and enzymes in the native biomass is also needed in order to avoid degradation of the final product. Previously, rendering plants processed beef by-products into cattle feed. The outbreak of Bovine Spongiform Encephalopathy (BSE) resulted in new guidelines for processing beef waste material. In Europe, by-products are mostly incinerated. In Canada, the use of most beef by-products was banned to utilization as cattle feed since 1997, and in 2007 the measure expanded to ban SRM from all animal foods and fertilizers [2]. The two factors of increased disposal cost and reduced value generation combine to necessitate finding a novel value-generating process to convert animal by-products into stable materials that can be used for industrial applications.

Hydrolyzed proteins contain poly-functional units that can react with adequate cross-linking reagents to form infinite network structures. We studied the cross-linking of hydrolyzed proteins with glutaraldehyde and epoxy resins and also carried out experiments to gain more insight into the physical behavior of hydrolyzed proteins under various conditions. The main methodology employed assesses the effect of every parameter in the hydrolysis, extraction, and cross-linking steps on the efficiency of the overall system.

Proteins in the body are folded into characteristic conformations in order to carry out specific functions. Many processes within living organisms assist in the process of protein folding. Misfolding of proteins causes various types of diseases. Bovine Spongiform Encephalopathy, also known as the mad cow disease, Creutzfeldt-Jakob disease in humans, scrapie in sheep, and Chronic Wasting Disease in deer and elk are generally referred to as Transmissible Spongiform Encephalopathies (TSEs). The causing agent has been linked to a single protein in the brain, called *pro*teinaceous *i*nfectious *on*ly, or prion (PrP). This protein is found in the brains of all mammals and can cause illness when the conformation of the normal PrP, denoted as PrP^{C}, is altered.

The misfolded protein, PrP^{Sc}, can then interact with PrP^{C} and transform the conformation of the normal protein into the misfolded one, creating a domino effect which causes more brain proteins to misfold into the disease-causing form [3]. The N-terminus of the normal prion in humans and other species such as apes usually consists of five repeating sequences of eight amino acids (often referred to as octapeptide repeats or octarepeats) with a strong affinity to copper [4] (p. 45), a finding that has an implication on the role of PrP^{C} in copper metabolism. For example, PrP^{C} deficiency in mice showed more than 10-fold copper reduction in infected brains relative to wild-types, resulting in increased sensitivity to copper toxicity and oxidative stress in cerebellar cells from PrP^{C} deficient mice [5]. The difficulty in predicting secondary and tertiary structures from amino acid sequence stems from the fact that proteins consist of 20 different amino acids that

can be assembled into similar structures from different sequences. The number of different sequences that can be formed from these 20 amino acids exceeds the number of atoms in universe. Hence, how proteins fold or misfold remains a mystery [6] (pp. 2-3).

Recent research has shown that prions can linger in the environment in their misfolded state after the death of the carrying organism and can adsorb to minerals commonly found in soil such as montmorillonite clay. Oral infectivity has also been examined and it has been found that oral transmission of the disease-causing proteins is possible. In fact, transmission is enhanced due to the association of prions with inorganic micro-particles relative to the unbound prion [7]. The risk of transmission is the reason behind the enhanced bans of rendering by-products and regulations on disposal methods the CFIA has put into effect.

1.1 PRION DISEASE

1.1.1 Historical Background

The 1985 outbreak of the “mad cow disease” in the United Kingdom brought global awareness to the previously obscure set of TSEs as hundreds of the thousands of cattle were found to have been infected by BSE and human exposure to BSE-infected meat caused a variant Creutzfeldt-Jakob disease (vCJD) in humans, a fatal neurodegenerative form of TSE. The full effect of BSE infections

on human beings due to consumption cannot be determined at this point due to variations in incubation of the disease prior to detection. Additionally, available tests do not detect PrP^{Sc} at low levels, necessitating extreme measures such as complete bans on imports from high-risk regions, massive culling of livestock when few cases of infection are detected within a herd, and total destruction of prions via costly disposal methods of SRM [4] (pp. 5-6).

A similar disease in humans, known as kuru, has been studied [4, 8, 9]. Kuru is similar to CJD and originated in Papua New Guinea. According to burial rituals of the Fore Tribes, women and children eat the brain of the deceased. This practice, referred to as endo-cannibalism, resulted in illness within the tribe that had symptoms akin to other TSE illnesses, and women had a far higher rate of infection than men. Since the discovery of kuru in 1957 and the subsequent ban of cannibalism, kuru cases declined. Additionally, scientists demonstrated through inoculation of chimpanzees with brain suspensions from kuru patients that spongiform encephalopathy is transmissible across different species [4] (pp. 39-41).

A genetic study by Mead et al. [9] on more than 3,000 people from the Fore Tribes and neighboring communities with whom they intermarried was conducted in 2009. Among the individuals who were exposed to kuru but escaped infection, the majority were found to have a resistance factor at codon 129 of the

prion protein gene. The variant, G127V, was found exclusively among kuru-resistant individuals in regions were the disease is known to occur and was not found among kuru patients who lived in unaffected areas, indicating that the variant is an acquired resistance factor in response of the epidemic which hit the Fore Tribes, not a mutation that triggered it. The immune system is not believed to recognize PrP^{Sc}, which has the same primary structure (amino acid sequence) as PrP^{Sc} [4] (pp. 47-48).

Numerous studies on the interactions between normal and abnormal prions have also shown transmissibility among species. Chesebro, who isolated mice the cDNA clones corresponding to the full-length PrP sequence [4] (p. 42), summarized research [10] on transmissibility in cell-free biochemical systems as follows: abnormal prions from cattle had positive interactions with normal prions from mice, sheep, cattle, and humans. No positive interactions were detected with normal prions from hamsters. Furthermore, inoculation with mice from either human or cattle TSE resulted in similar lesion patterns in their brains. Prusiner [8], who won the Nobel Prize in Physiology or Medicine in 1997 for his contributions to the field of prions, also argued for the transmissible nature of the disease. Goats inoculated from brain tissue of humans suffering from TSE developed scrapie within 3 to 4 years in five out of ten cases. The disease caused by inoculation was found to be not neuropathologically different from natural scrapie. No evidence has been found that scrapie leads to illness in humans. Chimpanzees were also susceptible to CJD but resistant to scrapie. Hamsters,

resistant to BSE, were also found to be susceptible to scrapie. Nonetheless, the dose required for oral transmission is 10^9 greater than the dose that causes illness by inoculation.

Transmissibility is not entirely an unexpected phenomenon due to mere coincidence. As protein research made substantial advances over the past few decades with the determination of protein structures by x-ray crystallography or nuclear magnetic resonance and amino acid sequences, the preservation of protein domains was found to be transcending different species, including mammals and plants. While amino acid sequences diverged considerably among species, the three dimensional structure of proteins that carries out the same functions was preserved. Active sites do not necessarily contain the same amino acids. Mutations may replace one amino acid with another in the active site provided residues have similar hydrophobic or hydrophilic character [6] (pp. 41-43).

1.1.2 Prion Destruction/Inactivation

Six procedures known to attack nucleic acids have been tested on the agent that causes scrapie. Nucleases, UV radiation, acidic attack, chemical modification, and divalent cation hydrolysis have been determined to be ineffective in deactivating the scrapie agent. These results suggest that nucleic acids are not involved in TSE illnesses. Only alkaline resulted in inactivity that was not reversed by subsequent acidic neutralization, possibly due to the hydrolysis of the causative agent. The

use of denaturizing reagents and other compounds that can alter protein structures such as proteases, phenol, chaotropic ions (e.g. guanidinium thiocyanate), sodium dodecyl sulfate, and urea also resulted in the deactivation of the scrapie agent, in addition to extreme temperatures [8], again possibly due to the breakdown of protein molecules. The lack of evidence that nucleic acids are involved and the indication that illness is due to a misfolded protein have led to the "protein-only" hypothesis [3, 11]. The notion that nucleic acids are not involved in illness is supported by Prusiner's work just described here as well as by reconstitution studies recently carried out that show in vitro propagation of prions in mice does not require nucleic acids [12].

1.1.3 Cofactor Hypothesis

Although molecular mechanism by which PrP^{C} is converted into PrP^{Sc} remains unknown [13], the "protein-only" hypothesis for infection has not been proven to be correct and doubt has been cast on the idea. For example, when pure PrP^{C} has been used as a substrate, only relatively low infectivity has been detected. The addition of lipid molecules and nucleic acid pure PrP^{C} resulted in moderate levels of infectivity whereas the removal of these cofactors reduced infectivity back to undetectable levels [14].

Deleault et al. determined, by employing Protein Misfolding Cyclic Amplification (PMCA) [15], that PrP^{Sc} can be propagated from the native PrP^{C}

and purified lipid molecules only after the addition of accessory polyanion molecules. These polyanion molecules are believed to lower the energy barrier for the generation of PrP^{Sc} by destabilizing PrP^{C} [13]. No pre-existing prions are needed for the *de novo* formation of PrP^{Sc} in this method, and the formed prions caused scrapie in hamsters inoculated with these samples [15].

PMCA was first used by Saborio et al. for *in vitro* reproduction of PrP^{C} into PrP^{Sc} in the presence of minute PrP^{Sc} quantities. The procedure is as follows: PrP^{Sc} is diluted to barely detectable levels by the proteinase K digestion. The solution is then incubated with PrP^{C}, leading to an increase in the PrP^{Sc} signal. Sonication is then carried out in order to disrupt the formed aggregates of PrP^{C} and PrP^{Sc} and form smaller units for continued growth of the disease agent. Five cycles of incubation/sonication have led to ~98% conversion rate of normal PrP into the misfolded form [16].

Attempts to replace PrP^{C} with truncated recombinant PrP in PMCA did not lead to the generation of PrP^{Sc} despite attempts involving rPrP conversion into conformations rich in abnormal β-sheets. This result is possible because rPrP lacks Glycosyl Phosphatidylin Isotol (GPI) anchor that prevents rPrP from attaching to the cell surface the same way PrP^{Sc} does. rPrP is also not fully compatible with PrP^{C} [11]. Briefly, the GPI anchor is added to the PrP^{C} molecule when the C-terminus amino acids are removed during transamidation and two

cystine amino acid residues form a tight bond [4] (p. 43). In conclusion, the Co-Factor Hypothesis is based on results that indicate normal prions cannot misfold on their own into the disease causing agent when present only in their pure form. Gheoghegan et al. proposed that negatively charged lipids, protein chaperones, and polyanionic molecules (such as RNA and heparan sulfate proteoglycans) may be recruited from pre-existing cellular pools (hence their replication is not needed) to cause misfolding [13].

Given the difficulty in isolating PrP^{Sc} and determining its structure in order to design a suitable inhibitor for its active site, the validity of the Cofactor Hypothesis provides a possibility that research on other molecules associated with misfolding offers an alternative approach: determine which molecules are responsible for the conversion for further study on early detection and antibody binding [4] (pp. 62-63).

1.1.4 Implication of Hypotheses & TSE Research Challenges

For proponents of the "Protein-only" hypothesis, the misfolded protein is the TSE infectious agent. For other researchers who hypothesize that other molecules are needed for infectivity, the term prion refers to TSE infectivity but it is not equated with PrP^{Sc}. Consequently, literature may often use the phrase "infectious agent of TSE" when researchers are not engaged in promoting either theory but merely presenting general findings and maintaining neutrality [4] (pp. 39-40). Progress is

expected to be slow due to long incubation periods in animal models, difficulty in obtaining standardized disease reagents, the high cost of setting up laboratories equipped to handle biohazardous material, and the lack of a specific immune response from prion carriers [4] (p. 54). Protein folding, as earlier discussed, is also poorly understood.

1.1.5 Hydrolysis

Hydrolysis is a safe method to irreversibly break down prions and prevent them from reverting back into the original PrP^{Sc} conformation. Prions are long-chain peptides folded in a specific way which induces illness. Large molecules have thousands of different conformations they can attain while simultaneously achieving an energy minimum. There are also many energy minima: global (for the entire protein) or local (for certain sections of the protein) [17]. The misfolded conformation state is one of many states a molecule can attain. In order for the protein to fold and aggregate into the precise state of the disease-causing agent, every single stable conformation of every part of the protein which leads to a harmless molecule must be ruled out. Previous work has demonstrated that proteins cannot reach a specific conformation by exhaustively traversing the entire conformational space they can possibly attain [18]. This means once the protein attains a particular stable state, it is unable to unfold itself and proceed to another state until it eventually "finds" itself misfolded as PrP^{Sc}. This leaves the protein with only one alternative: the protein must follow a precise and controlled

pathway in order to fold and aggregate in a defined conformation. This pathway is impossible without the presence of chaperones, proteins which assist other proteins in attaining specific conformations and then aggregating at the desired state [4, 19] (p. 46). Since hydrolysis also breaks down chaperones into smaller molecules, and their reconstruction into their exact previous state is likewise impossible due to the same reasoning just mentioned, the protein is left without a reasonable pathway to fold into the disease causing agent. Once prions are destroyed, they are completely deprived of the kinetic (chaperones) and thermodynamic (stable conformations) means required in order to form the disease-causing agent again.

Among all TSE agents, BSE was found to be the most resistant to inactivation by either heat or steam sterilization [20]. Denaturation of biological macromolecules by heat or pH modification may lead to inactivation, but there are limitations in cases where dehydration (e.g. by incubation) merely converts a protein into a more thermally stable form. Hydrolysis at high pressure, on the other hand, breaks the BSE agent irreversibly, thereby avoiding this problem, as high pressure keeps water in the system at high temperatures to avoid mere dehydration of the BSE agent and enhance hydrolysis [21]. Murphy et al. [22] also demonstrated that rendering SRM at 130 ºC did not completely destroy the scrapie agent and recommended the use of alkaline to hydrolyze SRM. Inoculation of mice with material rendered at 130 ºC only delayed clinical signs of illness but did not prevent infection. Heating alone is not sufficient since

methods used for protein stabilization (tissue fixation or dehydration) have been suggested to compromise the destruction of TSE agents [20]. Canada-based company Biosphere Technology Inc. developed and promoted the high-pressure thermal hydrolysis method at 180 ºC for 40 minutes [21] which is now one of the methods approved by CFIA for safe disposal of SRM [2].

Alkaline hydrolysis employs high temperatures as well as increased concentration of hydroxyl ions. This is expected to result in a higher degree of protein breakdown compared to thermal hydrolysis. Additionally, the use of basic solutions means an acidic solution needs to be added at the end of the process for neutralization; not only an added cost to the process but also results in peptones containing electrolytes. Using caustic also has adverse effects on equipment, a major concern for the industry.

Thermal hydrolysis may require additional energy to break down SRM to the same levels alkaline hydrolysis, but its advantages are likely to provide adequate compensation. Not only thermal hydrolysis does not damage reactors and other equipment or severely break down SRM to very small molecules, we can also control the degree of hydrolysis, and by extension, the molecular size distribution of hydrolyzed proteins, by increasing the hydrolysis temperature or duration to prepare different sets of hydrolyzed proteins. Concentration of salts in hydrolyzed proteins can also be controlled: by using distilled water extraction (for

salt-free hydrolyzed proteins) or salt-solution extraction we can study the effect of salts on various parameters. The effect of the molecular size on the cross-linking reactions as well as the properties of the final products can be investigated. Obtaining salt-free hydrolyzed materials from alkaline hydrolysis is challenging and costly. The entire process includes the addition of NaOH and subsequent neutralization by HCl and then stripping NaCl from the extracted material.

1.2 CROSS-LINKING

1.2.1 Cross-linked Networks

The reaction of bi-functional compounds always occurs at the terminal ends via linear addition and, irrespective of the reaction extent, the product always has a finite molecular weight. In contrast, reactants which possess functionality exceeding two, such as proteins, have the ability to grow in more than just the two directions from the terminal ends. The process is called cross-linking. The result is a complex network in which molecules are continuously added to the initial network. The molecular weight is extremely large and is said to be infinite. Cross-linked polymers are often called infinite networks. During the early stages of the reaction, the polymer is fusible and soluble in suitable solvents. As the reaction proceeds forward, the molecular size of the product keeps increasing, resulting in higher viscosity. Eventually, a point is reached where the viscous liquid turns into a gel that is neither fusible nor entirely soluble. The changes of the physical properties beyond the gel point are due to the formation of three-dimensional

structures in which the mobility of the molecules is restrained. The soluble portion of a cross-linked polymer consists of molecules that have not been cross-linked to a point where the resultant molecular weight exceeds the threshold for insolubility [23] (p. 377), the gelation point. This implies that a higher number of cross-linkages are needed for gelation as the molecular weight of the linear polymer is smaller. Gelation may not necessarily be achieved by merely reacting compounds of higher functionality if the extent of the reaction is limited or reactant mass ratios are far from stoichiometric requirements [23] (pp. 46-47).

1.2.2 Criteria for Infinite Network Formation

Flory proposed that three general conditions must be met in order for polymers to form infinite networks via cross-linking. The first criterion is that each molecule must be able to join with more than two other molecules. The second criterion is that as molecules join into more complex structures, the resulting network must have a higher capacity to link up with more than two other molecules. This means that the initial molecules must be poly-functional. Multi-chain molecules with just two terminal reaction ends do not have an increasing capacity to form more complex networks. The third criterion requires that any molecule previously joined to another molecule must be able to join at least one additional molecule. If the terminal units of a molecule are reactive, the number of additional reactive units needed to join with two other molecules is two. The ability of a system to

form an infinite network thus depends on the reactivity of branching units versus the reactivity of terminal units [23] (p. 361).

1.2.3 Glutaraldehyde Cross-linking

Glutaraldehyde is a clear, oily liquid with a linear 5-carbon dialdehyde structure. It is soluble in water, alcohol, and organic solvents in all proportions. Its commercial availability, low cost, and high reactivity with amine groups at around neutral pH make glutaraldehyde a suitable cross-linker for protein-based materials. On the other hand, cross-linking reactions involving glutaraldehyde are poorly understood due to the controversial nature of its reaction pathway, particularly when used as a solution in water. Glutaraldehyde does not remain as a monomer but rather forms linear and cyclic oligomers. The implication of using impure glutaraldehyde in cross-linking reaction hindered the complete understanding of the reaction mechanism and is the reason why different groups obtain different results [24].

Olde Damink et al. [24] summarized various groups' findings into the schematic diagram shown in Figure 1-1.

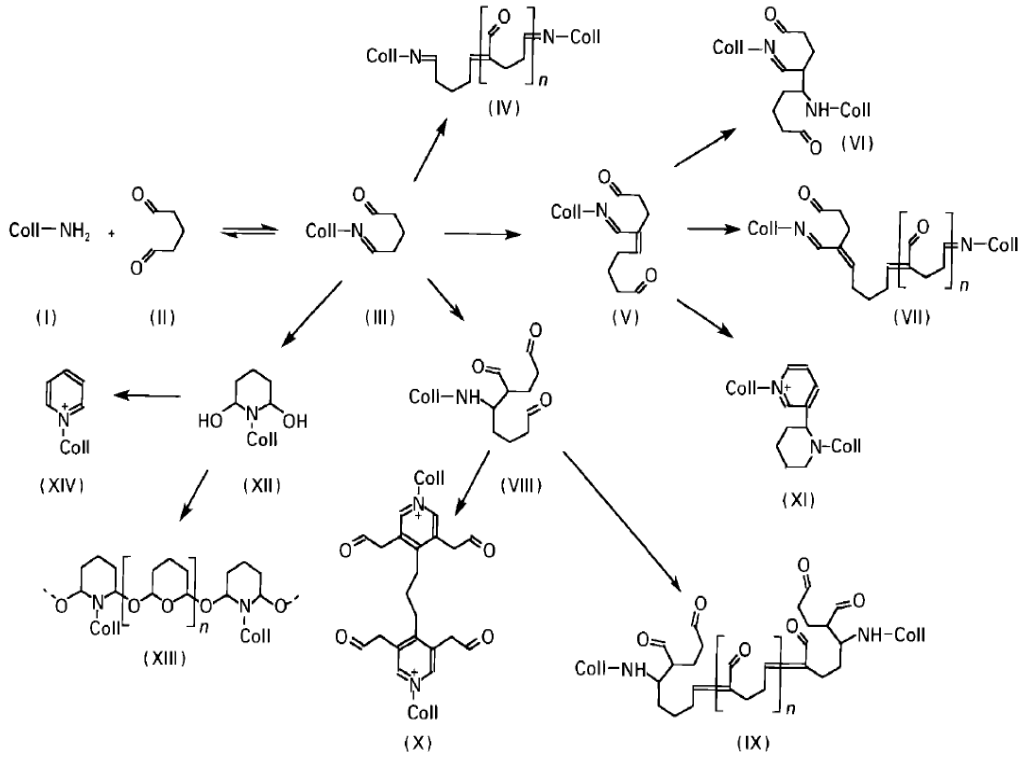

Figure 1-1. Glutaraldehyde reaction scheme with amines as proposed by Olde Damink et al.

Migneault et al. [25] later summarized scientific findings on the structure of glutaraldehyde in aqueous solutions, explaining that the structure and reaction mechanism of cross-linking agents are important for their efficient utilization. The proposed oligomerization of glutaraldehyde in aqueous solution is shown in Figure 1-2.

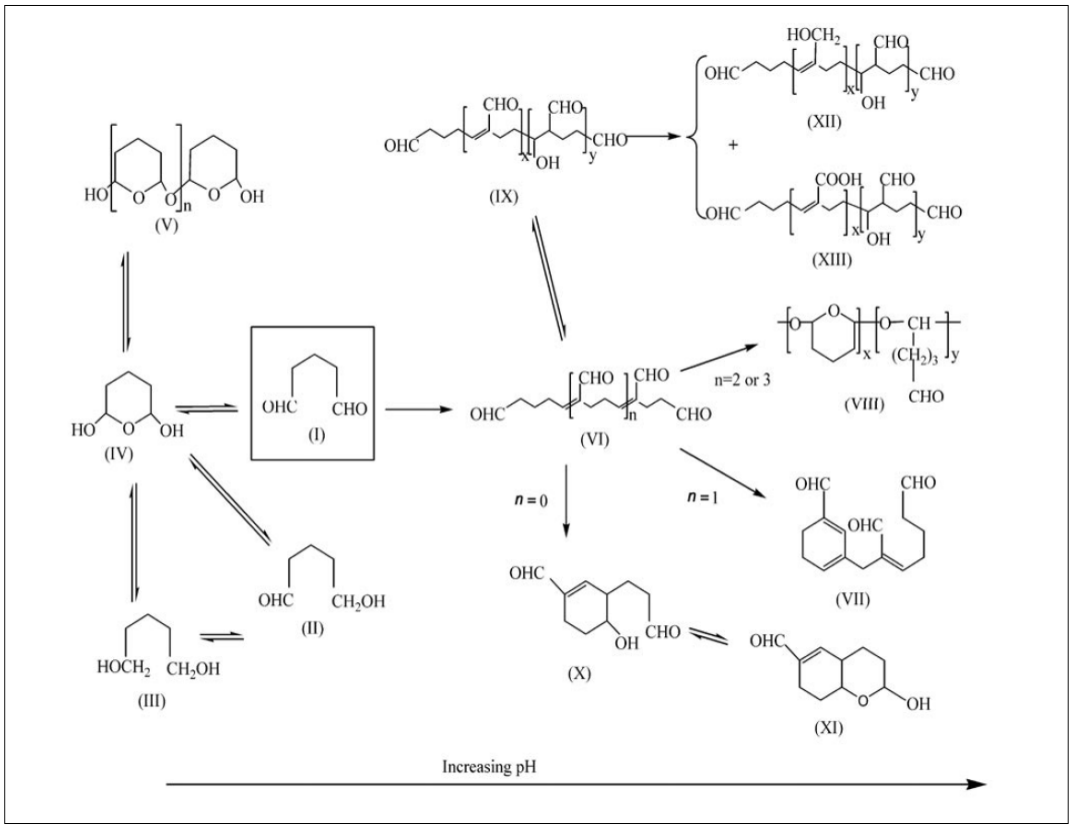

Figure 1-2. Glutaraldehyde behavior in aqueous solutions as proposed by Migneault et al.

As shown in Figures 1-1 and 1-2, reaction mechanism for glutaraldehyde cross-linking with amine is rather complex. Effective cross-linking of proteins with glutaraldehyde depends on the understanding of their reaction mechanisms. In this work, we took a theoretical approach to further simplify reaction pathways and then experimentally confirm the simplified pathway.

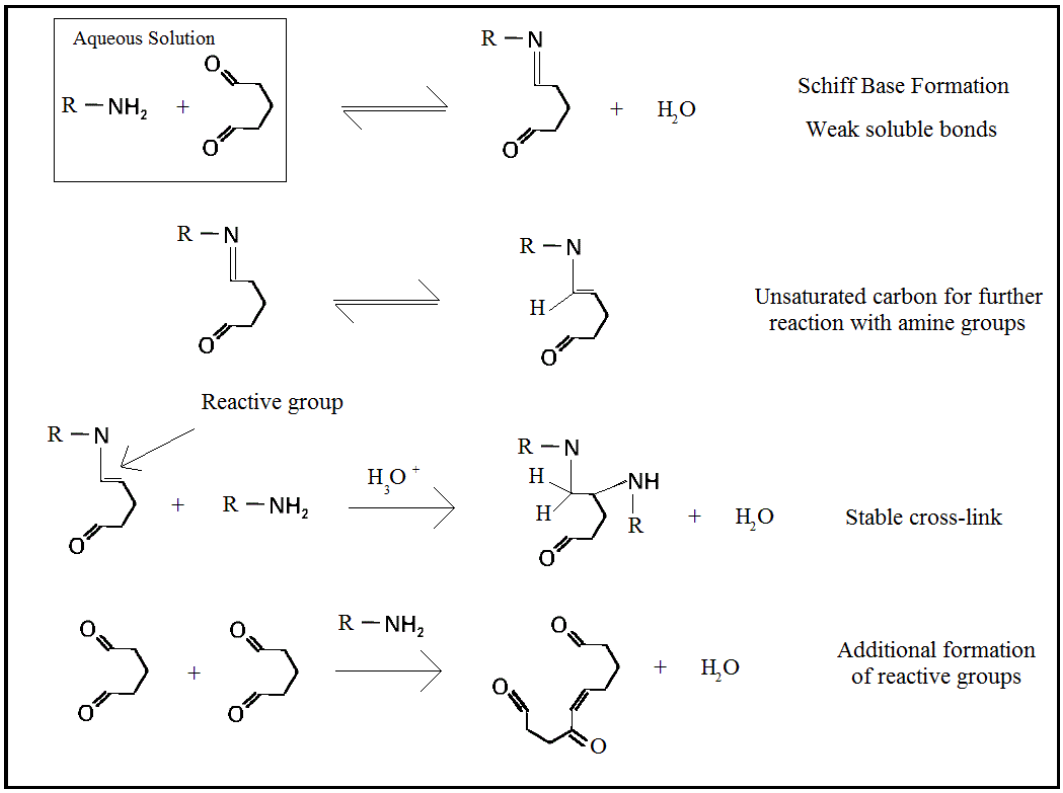

Figure 1-3. The proposed reaction mechanisms of Glutaraldehyde with amines in aqueous media

Combing through literature on amine-aldehyde reactions, we list five main types of reactions which are known to occur: Schiff base formation [24, 25, 26], aldol condensation [24, 25], Michael addition [27], Mannich reaction [24, 27], and Stork enamine reaction [27]. It is worth mentioning that aldol condensation is the polymerization of glutaraldehyde in aqueous solutions, not its reaction with amine groups. It is included here for two reasons: first, amine groups of proteins aid in catalyzing this reaction. The second reason is that this reaction converts glutaraldehyde to a more reactive structure, thereby aiding its cross-linking of

protein molecules. As an illustration, Figure 1-3 is the summary of the theoretical work described earlier.

1.2.4 Epoxy Resin Cross-linking

Epoxy resins are widely used in the fabrication of thermosetting polymers due to the good thermal, mechanical, and electrical properties of the formed network [28]. They are extremely reactive with groups that contain hydrogen. A proton attack opens the epoxy ring and forms a hydroxyl group that can in turn also react with another oxirane. The epoxy arm can react with primary and secondary amine groups, converting them into secondary and tertiary amines, respectively [29]. Similarly, they can react with hydroxyl and carboxylic groups to convert them into ethers and esters, respectively [30]. These groups are abundantly present in proteins. Though commercially available epoxy resins are mostly petroleum-derived materials, current research is focusing on synthetic epoxy resins produced from renewable resources. Sefose, for example, is a bio-based epoxy resin commercialized by Procter & Gamble (P&G) Chemicals. It is produced by esterifying sucrose with fatty acids [31]. Epoxidation of triglycerides [32] and soy-based materials such as methyl soyate and allyl soyate [33] has also been reported. While petroleum-based epoxy resins, in particular Araldite 506, remain cheaper than green epoxy resins today, future advances in technology may open the door to bio-based epoxy resins at a competitive price. In anticipation, we have decided to investigate curing behavior of commercially available epoxy resins

with proteins. The first step is to replace petroleum-based hardeners with materials derived from protein-rich biomass. The second step is the utilization of bio-based epoxy resins in order to produce thermosetting polymers entirely derived from renewable resources.

The study of the reaction kinetics for the cross-linking of epoxy resins can also provide answers related to the effect of various parameters on protein reactions. This is because epoxy resins have well understood reaction mechanisms, no by-products, and no solvent medium is required for their reactions with proteins. The advantage is therefore in the fact the reaction is a binary system. Consequently, the reaction heat flow is predominantly a measurement of the heat released from the cross-linking reactions, i.e. no evaporation.

1.2.5 Methodology

The process of value recovery from waste proteins involves three steps: hydrolysis, extraction, and cross-linking. In order to optimize the overall process, the parameters from each step need to be investigated. Activation energy measurements were carried out to quantify the effect of the process parameters.

At the hydrolysis step, the degree of hydrolysis affects the molecular weight of the protein-rich feedstock. The degree of hydrolysis is proportional to the hydrolysis duration, temperature, and pressure. Therefore, the degree of hydrolysis is proportional to the cost of the overall process. At the extraction step, proteins can be extracted by either a salt-water solution or distilled water solution. The latter method yields salt-free protein-rich material. The effect of the presence of salts, which may aid miscibility with many cross-linking reagents, can be studied. At the cross-linking step, the effect of viscosity and miscibility can also be evaluated.

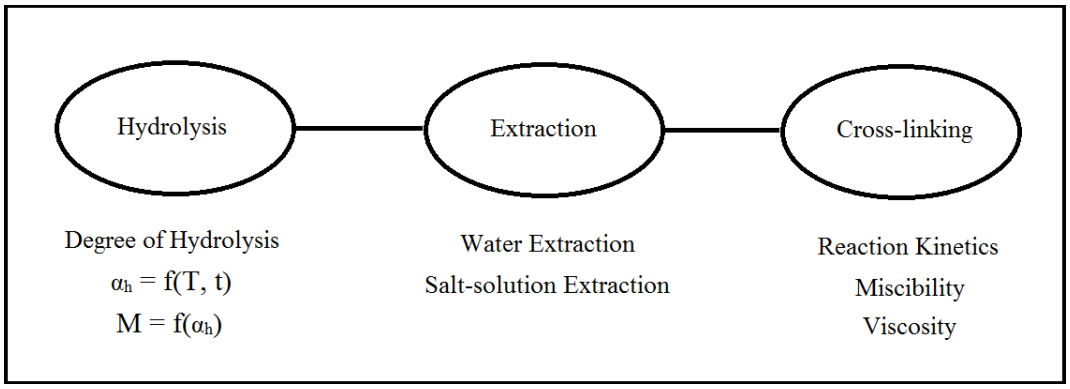

Figure 1-4. The overall process consisting of hydrolysis, extraction, and cross-linking

Figure 1-4 summarizes the overall process and the parameters that shall be evaluated.

1.3 REFERENCES

(1) Fedorowicz, E. M.; Miller, S. F.; Miller, B. G. Biomass Gasification as a Means of Carcass and Specified Risk Materials Disposal and Energy Production in the Beef Rendering and Meat Packing Industries. *Energy Fuels.* **2007**, *21*, 3225-3232.

(2) Canadian Food Inspection Agency. *Enhanced Animal Health Protection from BSE.* **2010**, Canada. [Online] Available at: http://www.inspection.gc.ca/animals/terrestrial/animals/diseases/enhanced-feed-ban/eng/1299870250278/1334278201780 [Accessed 26 November 2012].

(3) Nelson, D.; Cox, M. Lehninger Principles of Biochemistry, 5th Edition, New York: W.H. Freeman & Company, 2008.

(4) Erdtmann, R.; L. Sivitz, L. Advancing Prion Science, Washington: The National Academics Press, 2004.

(5) Viles, J. H.; Cohen, F. E.; Prusiner, S. B.; Goodin, D. B.; Wright, P. E. Copper Binding to the Prion Protein: Structural Implications of Four Identical Cooperative Binding Sites. *Proc. Natl. Acad. Sci.U. S. A.* **1999**, *96*, 2042-2047.

(6) Branden, C.; J. Tooze, J. Introduction to Protein Structure, Second Edition, New York: Garland Science, 1999.

(7) Johnson, C.; Pederson, J.; Chappell, R.; McKenzie, D.; Aiken, J. Oral Transmissibility of Prion Disease Is Enhanced by Binding to Soil Particles. *PLoS Pathog.* **2007**, *3*, 874-881.

(8) Prusiner, S. B. "Novel Proteinaceous Infectious Particles Cause Scrapie. *Science* **1982**, *216*, 136-144.

(9) Mead, S.; Whitfield, J.; Poulter, M.; Shah, P.; Uphill, J.; Campbell, T.; Al-Dujaily, H.; Hummerich, H.; Beck, J.; Mein, C.; Verzilli, C.; Whittaker, J.; Alpers, M.; Collinge, J. A Novel Protective Prion Protein Variant that Colocalizes with Kuru Exposure. *N. Engl. J. Med.* **2009**, *361*, 2056-2065.

(10) Chesebro, B. BSE and Prions: Uncertainties About the Agent. *Science* **1998**, *279*, 42-43.

(11) Makarava, N.; Kovacs, G. G.; Bocharova, O.; Savtchenko, R.; Alexeeva, I.; Budka, H.; Rohwer, R. G.; Baskakov, I. V. Recombinant Prion Protein Induces a New Transmissible Prion Disease in Wild-type Animals. *Acta Neuropathol.* **2010**, *119*, 177-187.

(12) Deleault, N. R.; Piro, J. R.; Walsh, D. J.; Wang, F.; Ma, J.; Geoghegan J. C.; Supattapone, S. Isolation of Phosphatidylethanolamine as a Solitary Cofactor for Prion Formation in the Absence of Nucleic Acids. *Proc. Natl. Acad. Sci.U. S. A.* **2012**, *109*, 8546-8551.

(13) Geoghegan, J. C.; Valdes, P. A.; Orem, N. R.; Deleault, N. R.; Williamson, R. A.; Harris, B. T.; Supattapone, S. Selective InIncorporation of Polyanionic Molecules into Hamster. *J. Biol. Chem.* **2007**, *282*, 36341-36353.

(14) Deleault, N. R.; Walsh, D. J.; Piro, J. R.; Wang, F.; Wang, X.; Ma, J.; Rees, J. R.; Supattapone, S. Cofactor Molecules Maintain Infectious Conformation and

Restrict Strain Properties in Purified Prions. *Proc. Natl. Acad. Sci.U. S. A.* **2012**, *109*, E1938-E1946.

(15) Deleault, N. R.; Harris, B. T.; Rees, J. R.; Supattapone, S. Formation of Native Prions from Minimal Components in vitro. *Proc. Natl. Acad. Sci.U. S. A.* **2007**, *104*, 9741-9746.

(16) Saborio, G. P.; Permanne B.; Soto, C. Sensitive Detection of Pathological Prion Protein by Cyclic Amplification of Protein Misfolding. *Nature* **2001**, *411*, 810-813.

(17) Schlick, T. Molecular Modeling & Simulation, New York: Springer, 2002.

(18) Levinthal, C. How to Fold Graciously, in *Mossbauer Spectroscopy in Biological Systems*, Monticello, 1969.

(19) Fenton W.; Horwich, A. GroEL-mediated Protein Folding. *Protein Sci.* **1997**, *6*, 743-760.

(20) Fernie, K.; Hamilton, S.; Somerville, R. A. Limited Efficacy of Steam Sterilization to Inactivate vCJD Infectivity. *J. Hosp. Infect.* **2012**, *80*, 46-51.

(21) Somerville, R. A.; Fernie, K.; A. Smith; Andrews, R.; Schmidt E.; Taylor, D. M. Inactivation of a TSE Agent by a Novel Biorefinement System. *Proc. Biochemistry* **2009**, *44*, 1060-1062.

(22) Murphy, R.; Scanga, J.; Powers, B. J.; Vercauteren, K.; Nash, P.; Smith G.; Belk, K.; Alkaline Hydrolysis of Mouse-adapted Scrapie for Inactivation and Disposal of Prion-positive Material. *J. Anim. Sci.* **2009**, *87*, 1787-1793.

(23) Flory, P. J. Principles of Polymer Chemistry, New York: Cornell University Press, 1953.

(24) Olde Damink, L. L. H.; Dijkstra, P. J.; van Luyn, M. J. A.; van Wachem, P. B.; Nieuwenhuis, P.; Feijen, J. Glutaraldehyde as a Cross-linking Agent for Collagen-based Biomaterials. *J. Mater. Sci. – Mater. Med.* **1995**, *6*, 460-472.

(25) Migneault, I.; Dartiguenave, C.; Bertrand, M. J.; Waldron, K. C. Glutaraldehyde: Behavior in Aqueous Solution, Reaction with Proteins, and Application to Enzyme Cross-linking. *BioTechniques.* **2004,** *37*, 790-802.

(26) Tomimatsu, Y.; Jansen, E. F.; Gaffield, W.; Olson, A. C. Physical Chemical Observations on the α-Chymotrypsin Glutaraldehyde System during Formation of an Insoluble Derivative. *J. Colloid Interface Sci.* **2012,** *36*, 51-64.

(27) McMurry, J. Organic Chemistry, fifth ed., Pacific Grove: Brooks/Cole Thomson Learning, 1999.

(28) Roşu, D.; Caşcaval, C. N.; Mustaţă, F.; Ciobanu, C. Cure Kinetics of Epoxy Resins Studied by non-isothermal DSC Data. *Thermochim. Acta.* **2002,** *383*, 119-127.

(29) Grenier-Loustalot, M. F.; Grenier, P.; Horny, P.; Chenard, J. Y. Reaction Mechanism, Kinetics and Network structure of the DGEBA-DDS System. *Brit. Polym. J*. **1988**, *20*, 463-476.

(30) Stevens, G. C. Cure Kinetics of a Low Epoxide/Hydroxyl Group-Ratio Bisphenol A Epoxy Resin-Anhydride System by Infrared Absorption Spectroscopy. *J. Appl. Polym. Sci.* **1981,** *26,* 4259-4278.

(31) Pan, X.; Sengupta, P.; Webster, D. C. High Biobased Content Epoxy-Anhydride Thermosets from Epoxidized Sucrose Esters of Fatty Acids. *Biomacromolecules* **2011**, *12,* 2416-2428.

(32) Crivello J. V.; Narayan, R. Epoxidized Triglycerides as Renewable Monomers in Photoinitiated Cationic Polymerization. *Chem. Mat.* **1992**, *4*, 692–699.

(33) Zhu, J.; Chandrashekhara, K.; Flanigan V.; Kapila, S. Curing and Mechanical Characterization of a Soy-based Epoxy Resin System. *J. Appl. Polym. Sci.* **2004**, *91*, 3513-3518.

CHAPTER 2

2.0 DIFFERENTIAL SCANNING CALORIMETRY

Various groups investigated the reaction kinetics of epoxy resin curing by employing the technique of differential scanning calorimetry (DSC) [1, 2, 3]. This is because heat flow measured during the reaction can be used to obtain the reaction rate, $d\alpha/dt$ [4]:

$$dQ/dt = Q_T \, d\alpha/dt \tag{2-1}$$

where Q_T is the total heat of the reaction when an uncured sample is cured to completion, dQ/dt is the heat flow, and α is the degree of conversion. The reaction rate, $d\alpha/dt$, can be expressed in terms of the temperature-dependent reaction rate constant, $k(T)$, as follows:

$$d\alpha/dt = k(T)f(\alpha)h(P) \tag{2-2}$$

where $f(\alpha)$ is a function of the extent of reaction and $h(P)$ is the function of pressure dependence of the reaction, important for reactions involving gases as reactants and/or by-products [5]. The term $h(P)$ can be dropped for the purpose of this study since no gases are involved in reactions involving the curing of epoxy resins. The reaction rate can then be expressed as:

$$d\alpha/dt = A_o \exp(-E_a/RT)f(\alpha) \tag{2-3}$$

where E_a is the activation energy, A_o is the frequency factor, R is the universal gas constant, and T is the temperature. For non-isothermal DSC experiments, it is mathematically convenient to carry out scans at constant heating rates, β_i, in order to express the degree of cure, α, as a function of temperature:

$$d\alpha/dt = (d\alpha/dT)(dT/dt) \tag{2-4}$$

where dT/dt is the heating rate, β_i. For constant heating rates, Equation 2-3 can be expressed as:

$$\beta_i \, d\alpha/dT = A_o \exp(-E_a/RT) f(\alpha) \tag{2-5}$$

This is important because obtaining $d\alpha/dt$ is much more difficult than obtaining $d\alpha/dT$ from thermal data [5]. By taking the natural log of both sides in Equation 2-5, we arrive at:

$$\ln[(\beta_i \, d\alpha/dT)/f(\alpha)] = \ln A_o - E_a/RT \tag{2-6}$$

Therefore, a plot of $\ln[(\beta_i \, d\alpha/dT)/f(\alpha)]$ vs. $1/T$ for constant values of α and an adequate model for $f(\alpha)$ is expected to yield a straight line. The slope is $-E_a/R$ and the y-intercept is $\ln A_o$. It is clear from Equation 2-6 that the correct selection of a suitable mathematical model for $f(\alpha)$ is necessary for obtaining the

parameters that best model the reaction. It is generally recommended that 3 to 5 different heating rates be used, keeping in mind that extremely low heating rates may yield excessive base-line noise and extremely high heating rates may result in self-heating such that the rate of temperature change with respect to time, dT/dt, is not necessarily constant [5].

There are three main types of reactions: accelerating, decelerating, and sigmoidal, and their models are, respectively, as follows [5]:

$$f(\alpha) = n\alpha^{(n-1)/n} \tag{2-7a}$$

$$f(\alpha) = (1-\alpha)^n \tag{2-7b}$$

$$f(\alpha) = n(1-\alpha)[-\ln(1-\alpha)](n-1)^{/n} \tag{2-7c}$$

The Sestak-Berggren model, $f(\alpha) = \alpha^m(1-\alpha)^n[-\ln(1-\alpha)]^p$, can adequately model autocatalytic reactions. The truncated form is obtained by setting p = 0. It can be simplified further by adding a constraint, m + n = 2, since reactions rarely have an order exceeding 2 [1, 5, 6]. This leads to:

$$\ln[(\beta_i\, d\alpha/dT)/\alpha^{2-n}(1-\alpha)^n] = \ln A_o - E_a/RT \tag{2-8}$$

where n is the reaction order. While the condition (m + n = 2) was demonstrated to be adequate for epoxy-amine reactions, epoxy-hydroxyl reactions had better

model fits when the condition (m + n = 1.5) was selected [7]. For scans at different heating rates, the degrees of cure, α, at different temperatures and $d\alpha/dT$ are then used to plot values for $\ln[(\beta_i\, d\alpha/dT)/\alpha^{2-n}(1-\alpha)^n]$ vs. $1/T$. The numerical value for n is selected such that the correlation coefficient, r, is at its maximum value [6].

It is also not necessary to place any conditions on the sum of m and n to model experimental data. The constraint can be imposed initially to determine the value of n for the best fit, and then optimize the model by changing one parameter at a time while keeping the other one constant until the maximum value of r is obtained [5]. Another method to obtain the values of m and n involves the use of a special function, $y(\alpha)$, as follows:

$$y(\alpha) = (d\alpha/dt)e^x \qquad (2\text{-}9)$$

where x is the reduced activation energy, E_a/RT. This method requires estimating the value of by another E_a method first and then obtaining a plot for $y(\alpha)$ vs. α [1]. An example is shown in Figure 2-1.

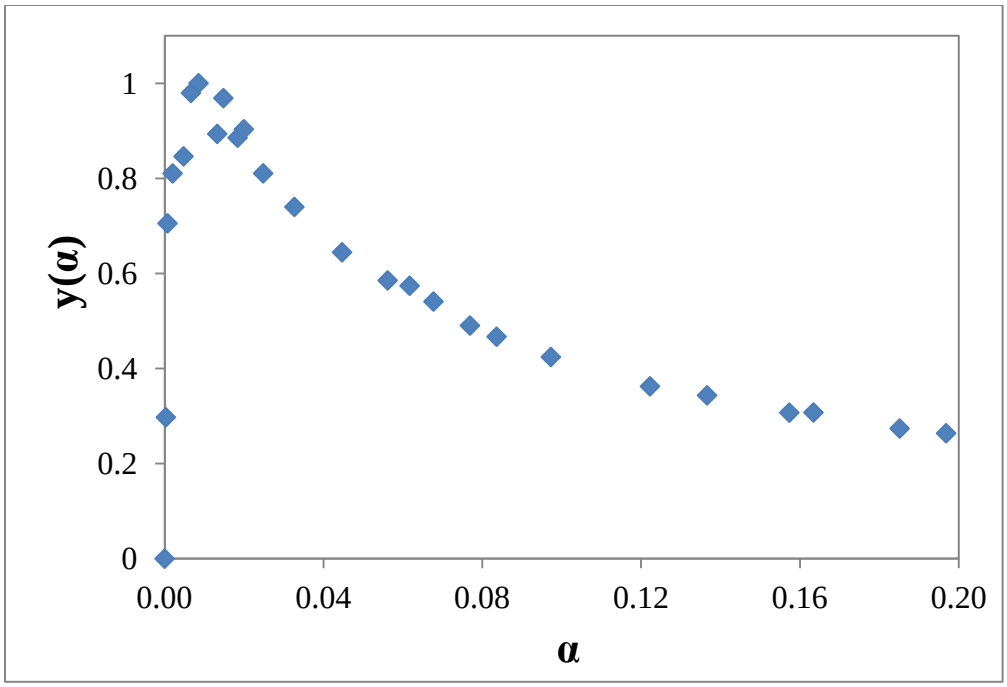

Figure 2-1. Plot of the normalized special function, y(α), vs. α

The value at which y(α) is maximum, α_M, can then be used in order to obtain a ratio parameter, p, to obtain values for m and n as follows:

$$p = \alpha_M/(\alpha_M - 1) \quad (2\text{-}10)$$

$$n = m/p \quad (2\text{-}11)$$

This method is not expected to have an effect on calculated values greater than acceptable experimental errors (10%) [1].

2.1 ISOCONVERSIONAL METHOD

Thermal data can also be analyzed by a model-free method, also called the isoconversional method, which does not require determining the model function, $f(\alpha)$. Dependence of activation energy on the degree of curing, α, is useful to understand the reaction. For example, if the values of activation energy do not change with α, the reaction can best be described by a single-step kinetics equation. In cross-linking, a sharp decrease in the activation energy as curing progresses towards completion indicates a vitrification process; the rate-determining reaction has changed from a kinetic-controlled to a diffusion-controlled as a glassy state has been reached such that molecules are locked in and need to "jump" to find the next reaction site – values for the activation energy of diffusion processes are in the order of 20 – 30 kJ/mol, significantly less than the values for reaction processes [5].

Analogous to Equation 2-6, the activation energy at various values of α are obtained from

$$\ln[(\beta_i/T^2_{\alpha,i})] = \text{Constant} - E_\alpha/RT_{\alpha,i} \quad (2\text{-}12)$$

where E_α is the activation energy at α and $T_{\alpha,i}$ is the temperature at which α is attained for curing scans at different heating rates. It is generally recommended to calculate E_α at increments of α no greater than 0.05 [5]. Generally, the most

accurate values are usually for curing degrees in the range 0.30-0.6 [1], and the average value in this window of cure may be used as an acceptable estimate to determine the reaction parameters in Equations 2-9 to 2-11 [5].

It is worth noting that the model-free method assumes that the activation energy does not depend on the degree of curing. Therefore, it is recommended to use the method with care. For reactions in which the change of activation energy values is small as the extent of the reaction is increased, the error is expected to be minimal. This method was recently shown to be inadequate for reactions in which there is a significant change [8].

2.2 METHOD OF KISSINGER

A special case of the isoconversional method, the Kissinger method is used to obtain one activation energy value, evaluated from the temperature at the peak of the curing curve, $T_{p,I}$ [5].

$$\ln[(\beta_i/T^2_{p,i})] = \text{Constant} - E_a/RT_{p,I} \quad (2\text{-}13)$$

At the peak of the curve, the rate of the reaction, $d\alpha/dt$, is maximum. This means the derivation of the reaction rate, $d^2\alpha/dt^2$, can be set to zero [9]. Equation 2-3 can then be rearranged as follows:

$$\beta_i/T_p^2 = (A_o R/E_a)[n(1-\alpha_p)^{n-1}]\exp(-E_a/RT_p) \quad (2\text{-}14)$$

where α_p is the extent of cure at the maximum reaction rate, $d\alpha/dt$. The assumptions so far made in order to arrive at Equation 2-14 are that the pressure term, $h(P)$, is negligible and the reaction model fits the n^{th} order kinetics. With respect to the term $[n(1-\alpha_p)^{n-1}]$, Kissinger demonstrated that it is independent of the heating rate and nearly equal to unity [10]. Therefore, by taking the natural log of Equation 2-14, Equation 2-13 is obtained after three approximations. It is worth pointing out that the activation energy value obtained from the Kissinger method may or may not agree with any of the values obtained from the isoconversional method. Usually, α_p is 0.5 and may slightly vary with the heating rate, in which case $E_a = E_\alpha$. However, α_p may not necessarily be the same as the heating rate is changed [1], in which case activation energy from the Kissinger method would not be expected to match any activation energy value obtained from the isoconversional method for any degree of cure.

2.3 REFERENCES

(1) Roşu, D.; Caşcaval, C. N.; Mustaţă, F.; Ciobanu, C. Cure Kinetics of Epoxy Resins Studied by non-isothermal DSC Data. *Thermochim. Acta.* **2002,** *383*, 119-127.

(2) Pan, X.; Sengupta, P.; Webster, D. C. High Biobased Content Epoxy-Anhydride Thermosets from Epoxidized Sucrose Esters of Fatty Acids. *Biomacromolecules* **2011**, *12*, 2416-2428.

(3) Zhu, J.; Chandrashekhara, K.; Flanigan V.; Kapila, S. Curing and Mechanical Characterization of a Soy-based Epoxy Resin System. *J. Appl. Polym. Sci.* **2004**, *91*, 3513-3518.

(4) Jubsilp, C.; Punson, K.; Takeichi, T.; Rimdusit, S. Curing Kinetics of Benzoxazine-epoxy Copolymer Investigated by Non–isothermal Differential Scanning Calorimetry. *Polym. Degrad. Stabil.* **2010**, *95*, 918-924.

(5) Vyazovkin, S.; Burnham, A. K.; Criado, J. M.; Perez-Maqueda, L. A.; Popescu, C.; Sbirrazzuoli, N. ICTAC Kinetics Committee Recommendations for Performing Kinetic Computations on Thermal Analysis Data. *Thermochim. Acta.* **2011,** *520*, 1-19.

(6) Hong, I.; Lee, S. Cure Kinetics and Modeling the Reaction of Silicone Rubber. *J. Ind. Eng. Chem.* **2013,** *19*, 42-47.

(7) Oh, J. H.; Jang, J.; Lee, S. H. Curing Behavior of Tetrafunctional Epoxy Resin/Hyperbranched Polymer System. *Polymer* **2001**, *42*, 8339-8347.

(8) Šimon, P.; Thomas, P.; Dubaj, T.; Cibulková, Z.; Peller, A.; Veverka, M. The Mathematical Incorrectness of the Integral Isoconversional Methods in Case of Variable Activation Energy and the Consequences. *J. Therm. Anal. and Calorim.* **2013**, In Press, DOI: 10.1007/s10973-013-3459-7.

(9) Prime, R. B. Differential Scanning Calorimetry of the Epoxy Cure Reaction. *Polym. Eng. Sci.* **1973,** *13*, 365-371.

(10) Kissinger, H. E. Reaction Kinetics in Differential Thermal Analysis. *Anal. Chem.* **1957,** *29*, 1702-1706.

CHAPTER 3[1]

3.0 GLUTARALDEHYDE CROSS-LINKING

This study explored the reaction chemistry of cross-linking Specified Risk Material (SRM), hydrolyzed according to Canadian Food Inspection Agency (CFIA) safe disposal guidelines, with glutaraldehyde into stable materials for potential industrial applications. Previously, rendering plants processed beef byproducts into cattle feed. The outbreak of Bovine Spongiform Encephalopathy (BSE) resulted in new guidelines for processing beef waste materials. In Europe, byproducts are mostly incinerated. In Canada, most proteins have been banned from cattle feed since 1997, and in 2007, the ban was expanded to exclude SRM from all animal foods and fertilizers [1]. SRM consists of the skull, brain, trigeminal ganglia, eyes, tonsils, spinal cord and column, dorsal root ganglia, and distal ileum for cows older than 30 months. For younger cows, SRM consists of only the tonsils and distal ileum [2].

There are four methods approved by the CFIA for the destruction of SRM: incineration, gasification, alkaline hydrolysis, and thermal hydrolysis. Incineration and gasification result in the total destruction of peptide bonds to the point where cross-linking the product into anything useful is almost impossible.

[1] A version of this chapter has been published. El-Thaher et al. *Industrial and Engineering Chemistry Research*. **2013**, *52*, 4987-4993.

The CFIA-approved procedures for the two hydrolysis processes are as follows: Thermal hydrolysis must be conducted at 180 °C and 1200 kPa for 40 min. Alkaline hydrolysis must be conducted at 150 °C and 400 kPa for 180 min (using 15% weight/volume of NaOH).

These two hydrolysis methods were shown by Somerville et al. [3] and Murphy et al. [4] to inactivate prions and can be used to safely dispose of SRM. Hydrolysis breaks down proteins into molecules large enough to be cross-linked. Nonetheless, both methods utilize energy. The bans have reduced the value generated from rendering processes. Additional regulations regarding disposal have also increased the cost for dealing with rendering byproducts. These two factors of increased cost and reduced value generation combine to necessitate that a novel value-generating process for converting rendering byproducts into stable materials that can be used for other industrial applications be found. Cross-linked polymers are one type of material that can be produced from byproducts. Proteins contain polyfunctional units that provide the possibility of forming infinite network structures. The aim of this work was the cross-linking of hydrolyzed SRM into a stable material that can then be used for an industrial application.

Glutaraldehyde is a clear liquid oil that has a linear five-carbon dialdehyde structure. One of its earliest applications, for the fixation of protein tissues, was identified 50 years ago when Sabatini et al. [5] experimented with a few organic

solvents, including glutaraldehyde and glyoxal, as fixatives for electron microscopy and cytochemistry. Since then, glutaraldehyde has been widely used and studied in cross-linking applications because of its commercial availability, low cost, and high reactivity with amine groups at approximately neutral pH. Studies on collagen cross-linking with various dialdehydes consisting of two to six carbon atoms demonstrated that reactivity is maximized when a five-carbon dialdehyde is used [6]. Glutaraldehyde is also soluble in water, alcohol, and organic solvents in all proportions.

The main difficulty with glutaraldehyde is the controversial nature of its reaction pathway, particularly when used as a solution in water. Glutaraldehyde does not remain as a monomer but rather forms linear and cyclic oligomers. The implication of using impure glutaraldehyde in cross-linking reactions hinders the complete understanding of the reaction mechanism and is why different groups obtain different results [7].

Migneault et al. [6] published an excellent review article on glutaraldehyde-protein research carried out over the past 40 years. The review included work on glutaraldehyde behavior in aqueous solutions, as well as its use in enzyme cross-linking and tissue fixation, and covered various applications such as cytochemistry and biomedical sciences. In this work, we do not aim to review or thoroughly study the various theories put forth by numerous groups on the

subject but rather use current knowledge and experimentation to cross-link hydrolyzed proteins into an insoluble, thermally stable network and provide additional insight based on our empirical work regarding glutaraldehyde reactivity with proteins. Insolubility is an important parameter because it is a strong indication of covalent cross-linking. According to the theoretical work of Paul J. Flory for large molecules, it takes very few cross-links (one per molecule) to form an infinite network [8]. If the molecules are covalently bonded, the polymer is expected to be insoluble, at least to some degree, in solvents that do not break down the covalent bonds. Because peptones and glutaraldehyde are readily soluble in water, insolubility of the product indicates the extent of covalent bond formation.

Glutaraldehyde has been used by various groups in the past for cross-linking of proteins. Olde Damink et al. [7] cross-linked sheep skin collagen with glutaraldehyde at 40 °C, and Cheung and Nimni [9] also carried out cross-linking with collagen, obtained from rat skin, at room temperature. Park et al. [10] used glutaraldehyde for cross-linking defatted soy protein at room temperature. Payne also worked at room temperature to cross-link albumin into larger molecules for use as high-molecular-weight markers in sodium dodecyl sulfate polyacrylamide gel electrophoresis (SDS-PAGE) [11]. Fernandez-Lorente et al. [12] studied the stabilization of different lipase enzyme structures by glutaraldehyde in the presence and absence of detergent. Cross-linking of lipases was carried out at room temperature. Bolivar et al. [13] stabilized a polyethylenimine composite

with glutamate dehydrogenase, an enzyme, through glutaraldehyde cross-linking at 4 °C by immobilizing the composite onto a weak cationic exchanger.

The vast majority of research on protein cross-linking has been focused on proteins in their native or denatured states, generally insoluble, and has required only a low degree of cross-linking for the numerous applications for which the studies were conducted, such as tissue fixation or increase in tensile strength or shrinkage temperature. Additionally, low temperatures are preferred when dealing with labile molecules [6], an important consideration in some areas of research. Our work focuses on proteins that have been broken down into smaller molecules by vigorous hydrolysis, are completely denatured, and are highly soluble in water. Therefore, the degree of cross-linking needed is significantly higher to produce stable, insoluble materials. Reactions at higher temperatures are less cumbersome because of the absence of labile molecules. The main considerations with increased temperatures are further hydrolysis of the protein, the boiling point of glutaraldehyde, and energy costs for mass production - a practical consideration outside the scope of the research presented here.

3.1 REACTION TYPES

Five types of reactions are expected to occur when dialdehydes and amine groups of proteins are present: Schiff base (imine) formation, aldol condensation, Mannich reaction, Michael addition, and Stork enamine reaction. Because there is

no general consensus on the chemical nature of the glutaraldehyde reaction with protein, we can only speculate how any of these reactions, independently or together, corresponds best to our experimental results.

3.1.1 Schiff Base Formation

Among the expected reactions between aldehydes and proteins/peptones is nucleophilic attack by the lysine ε-amino groups on the carbonyl group to form Schiff bases. The bond is weak and can be broken down by heat or acidic conditions. The reversibility of this bond means that reactants are readily regenerated and the cross-linked network is not considered to be stable [6, 14]. Regardless of whether Schiff bases are stable cross-links, they are generally believed to be intermediates for subsequent reactions that then result in stable cross-links [7].

3.1.2 Aldol Condensation

Proteins can also catalyze the polymerization of glutaraldehyde through aldol condensation. Subsequent reaction of the product with proteins leads to cross-linked networks consisting of linear glutaraldehyde oligomers with branches of Schiff base groups linked to the main chain [6]. It is worth mentioning that water is a byproduct of aldol condensation reactions [15].

3.1.3 Mannich Reaction

The Mannich reaction involves three components: a ketone, an amine, and an aldehyde. A two-step reaction, it commences in a first step in which the aldehyde and amine react to form a Schiff base intermediate, with a structure of —C═NR_2^+. As is the case with aldol condensation, water is a byproduct of the first step. The second step is the subsequent reaction of the intermediate with ketone [15]. The ketone in this step is a glutaraldehyde-related enol obtained from aldol condensation [7].

3.1.4 Michael Addition

The Michael reaction involves a nucleophilic group and an α,β-unsaturated carbonyl compound such as polymeric aldehydes formed by aldol condensation. Just as in the Mannich reaction, the first step involves the formation of a Schiff base that further reacts to form a stable bond. Unlike in the Mannich reaction, however, the Schiff base intermediate is not protonated [15].

3.1.5 Stork Enamine Reaction

A special case of the Michael reaction, the Stork enamine reaction involves a ketone/aldehyde and a secondary amine, present in proline and histidine residues of proteins. This leads to the formation of enamine instead of imine or a Schiff

base, which are both unstable because of the presence of C═N bonds. This pathway makes no contribution to cross-linking [15].

3.1.6 Role of Water

To summarize the five types of reactions and the role of water, the following observations are made: Water is needed to form oligomeric glutaraldehyde into an α,β-unsaturated carbonyl compound to enhance its reaction with protein amino groups. Water is also a byproduct of many reactions. Its presence is likely to suppress reactions by shifting equilibria toward the reactants' side. Reactions of alcohols [16] and aldehydes [17] (e.g., glutaraldehyde) with amines have been studied previously and were found to be thermodynamically uphill. It is therefore necessary to drive off byproducts, H_2 and/or H_2O, to shift equilibria toward cross-linked networks.

Schiff base formation, aldol condensation, and the Stork enamine reaction make no contribution to the formation of insoluble cross-linked polymers. Only two pathways, the Mannich reaction through a protonated Schiff base intermediate and the Michael addition through an unprotonated one, lead to the desired product.

3.2 EXPERIMENTAL SECTION

3.2.1 Thermogravimetric Analysis (TGA)

Experiments were conducted with a Thermal Analysis Instruments TGA Q50 apparatus under a flow of nitrogen to study the effects of heating only, without oxidation (which occurs when air or oxygen is used as the carrier gas). Platinum pans were used as sample holders because they withstand high temperatures and can be easily cleaned. The temperature range was from room temperature to 300 °C. Peptide bonds generally break apart at higher temperatures, so there was no need to run longer experiments. Samples were heated to 100 °C in the TGA apparatus and kept at that temperature for 10–15 min to allow for the removal of moisture. The purpose of the isothermal mode is to distinguish mass change observations from one another based on the component that is being lost. All results were reproduced to 5% error or better. The heating regimen was as follows: (1) ramp from room temperature to 100 °C at 10 °C/min, (2) isothermal conditions at 100 °C for 10–15 min, and (3) ramp from 100 to 300 °C at 5 °C/min.

3.2.2 Differential Scanning Calorimetry (DSC)

To corroborate the results obtained by TGA with the results obtained by DSC, nitrogen was used as the carrier for all experiments. A Thermal Analysis Instruments DSC 2910 instrument was utilized in this work. Aluminum hermetic sample pans and lids were used for experiments. The lids were inverted and

sealed on top of the pans. The sample and reference were manually placed in the DSC cell. Aluminum pans are inexpensive but cannot be used for more than one run because they are difficult to clean and they easily deform under heating. The DSC instrument was routinely calibrated with indium and zinc standards.

3.2.3 Hydrolysis and Peptone Extraction

Thermal hydrolysis was conducted in a dedicated 2 L stainless steel pressure vessel (Parr Instrument, Moline, IL) capable of handling pressures up to 2000 psi. SRM samples, mainly composed of coarse brownish colored granulated meat and bone particles, were hydrolyzed in aqueous solution in accordance with techniques approved by the CFIA [18] and U.S. Food and Drug Administration (FDA) [19]. Thermal hydrolysis was conducted by adding 100 mL of distilled water to 100 g of dry SRM in the pressure vessel. SRM sample handling and reactor loading were performed in a biosafety cabinet of a biosafety level II laboratory with special approval from the CFIA for handling such materials. The cabinet and reactor vessels were decontaminated with 5% Environ LpH for 30 min [20] followed by 70% ethanol after each SRM handling. Peptones were extracted from the insoluble components of hydrolyzed SRM with a salt solution consisting of 100 g of the hydrolyzed sample with 450 mL of salt solution containing 18 g of NaCl, 0.23 g of $MgCl_2$, 4.10 g of KH_2PO_4, and 4.30 g of Na_2HPO_4 according to the method of Park et al.[21] by agitating at 200 rpm for 30 min in a shaker (Innova laboratory shaker, New Brunswick, Canada). The supernatant was separated from the residue by centrifugation (7000*g*for 30 min)

on a Beckman centrifuge, followed by hexane extraction to remove fats and lipid residues. The raffinate was then collected, vacuum-filtered (Whatman filter paper no. 4), and freeze-dried. Salt-free peptones were extracted by the dissolution of 40 g of hydrolyzed protein in 180 mL of Milli-Q water, agitated at 200 rpm for 30 min, centrifuged at 7000*g* for 30 min, and then vacuum filtered (Whatman filter paper no. 4) to remove insoluble tissues and bone particles. The filtered supernatant was then extracted with 540 mL of hexane to remove lipids. The raffinate was then freeze-dried under reduced pressure, and the total nitrogen was quantified by the Dumas method [22].

The breakdown of protein into smaller molecules was evident, as most of the hydrolyzed proteins were concentrated below the 25 kDa marker. As reported in our previous work [23], peptones from thermally hydrolyzed SRM smeared uniformly between 15 and 5 kDa. Peptones from caustic hydrolysis are more broadly distributed from approximately 15 to less than 1 kDa. Alkaline hydrolysis is more severe because of a combination of time, pressure, and the catalytic effect of the alkali. The disadvantages of alkaline hydrolysis are not limited to the generation of smaller molecules for cross-linking, but the use of caustic is generally avoided by industry because of its effects on equipment. Therefore, we proceeded to work with peptones obtained from thermal hydrolysis.

3.2.4 Materials

SRM samples with a total protein content of 44.05% on a dry-weight basis were obtained from Sanimax Industries, Inc. (Montreal, QC, Canada). The samples were handled in a biosafety level II laboratory, according to CFIA protocol for safe handling, hydrolysis, and disinfection of SRM material. NaCl (99%, 58.44 g/mol), Na_2HPO_4 (99.6%, 268.07 g/mol), KH_2PO_4 (99.8%, 136.09 g/mol), $MgCl_2$ (99%, 95.21 g/mol), glutaraldehyde (50% w/w aqueous solution), and hexane (99.9%, HPLC-grade, 86.18 g/mol) were purchased from Fisher Scientific Co. SDS (>99%, 288.38 g/mol) was obtained from Sigma-Aldrich (St. Louis, MO). Filter paper (Whatman no. 4; diameter, 11 cm; pore size, 20–25 μm) was purchased from Whatman (Maidstone, Kent, U.K.). Peptones were obtained by thermal hydrolysis of SRM using the method described earlier. Two sets of peptones were obtained and differed by method of extraction: One set was salt-extracted and therefore contains salts. The other set was salt-free, as it was water-extracted.

3.3 RESULTS AND DISCUSSION

As discussed earlier, research on glutaraldehyde–protein cross-linking has mostly dealt with proteins in native or denatured states, with experiments carried out at low temperatures. We performed the cross-linking of 5 g of salt-extracted peptones with 25 g of glutaraldehyde solution (50% w/w) at 37 °C for 24 h. The mass ratio employed (2.5:1 glutaraldehyde/peptones) was due to the low bulk

density of peptones. The amount of glutaraldehyde solution was just enough to dissolve the entire peptone sample. Preliminary experimental results on amine group analysis showed that this ratio of peptones to glutaraldehyde led to a significant reduction of free amine groups. We initially started with salt-extracted peptones because of their better miscibility with glutaraldehyde solutions. Solubility tests (ASTM D 570, 24-h immersion in water to measure mass loss) on the resultant samples showed that they readily dissolved in water (>90%), indicating that cross-linking did not occur. Experiments were repeated several times at the same temperature but increased reaction time. Even after 2 weeks, the solubility remained the same. Given that cross-linked networks are insoluble except when the solvent breaks down covalent bonds, the most likely explanation for what was observed is that only Schiff bonds were formed between the amino groups of the peptones and the carbonyl groups of glutaraldehyde. The TGA curves also indicated that the desired outcome was not obtained from this reaction. As Figure 3-1 demonstrates, the thermal stability of the end product was poor compared to that of peptones, the starting material. This is due to the retention of unreacted glutaraldehyde (bp 187 °C).

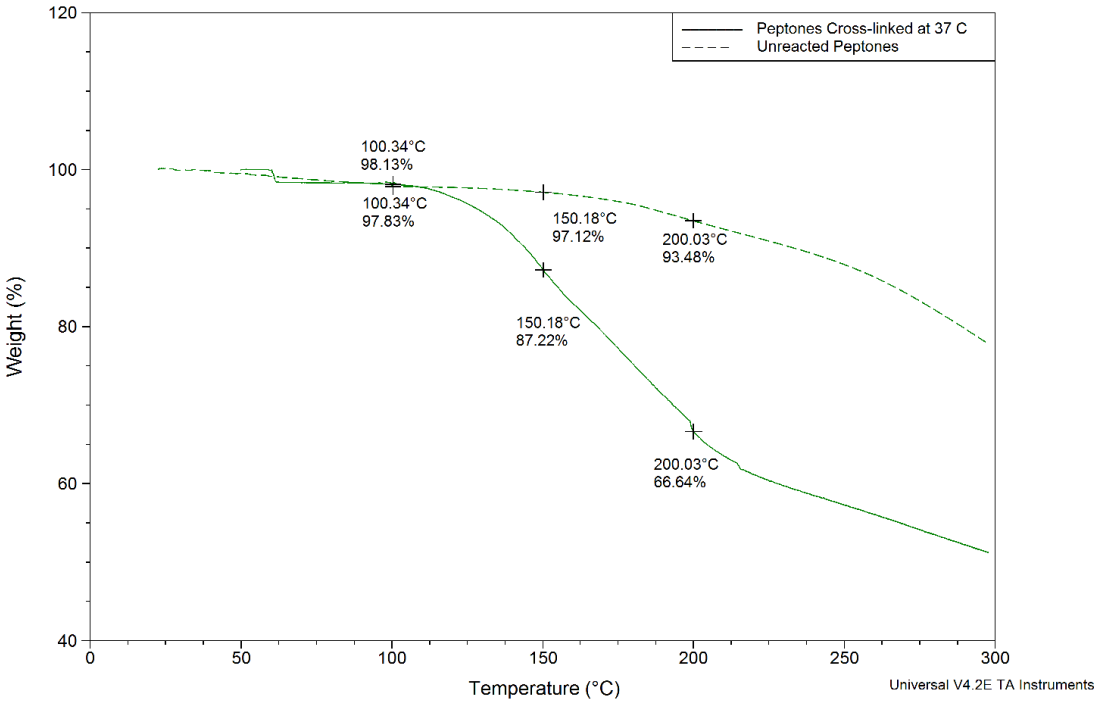

Figure 3-1. TGA curves at 5 ºC/min for salt-extracted peptones reacted with glutaraldehyde at 37 ºC and un-reacted peptones indicating mass at 150 ºC, 200 ºC, and the end of the isothermal run at 100 ºC

DSC analysis of the end product provides additional information. The DSC curve in Figure 3-2 shows an endothermic peak (onset ~100 °C) followed immediately by an exothermic peak. Similar results were reproduced in DSC scans at 2, 5, and 15 °C/min.

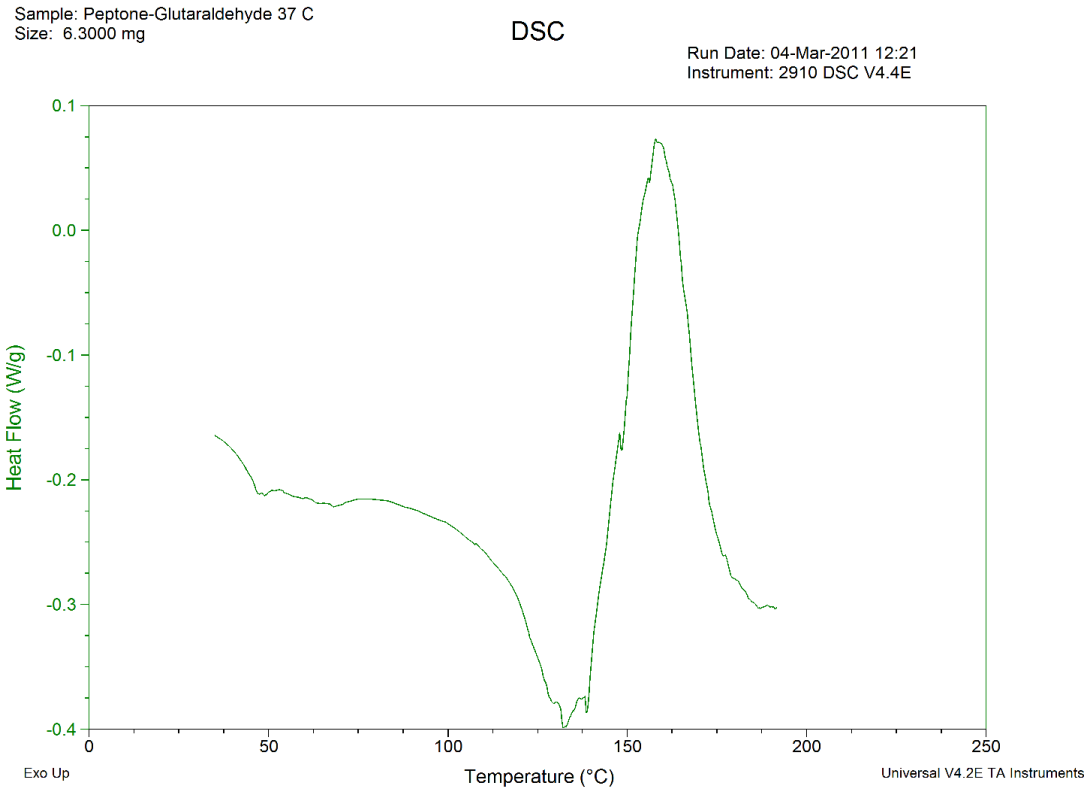

Figure 3-2. DSC curve at 10 ºC/min for peptones reacted with glutaraldehyde at 37 ºC

The endothermic peak is attributed to water evaporation. Cross-linking of polymeric molecules is exothermic as a result of bond formation. Because there is an overlap between the endothermic peak for water evaporation and the exothermic peak for cross-linking, it is difficult to determine a narrow range for the onset cross-linking temperature. The exothermic peak exhibits a sharp rise at ~140 °C. Having determined the temperature range for cross-linking, we carried out experiments by varying the temperature at 10 °C intervals in the range of 100-150 °C.

The solubility values, reported in Table 3-1, indicate considerable improvement in comparison to cross-linking at 37 °C but remain higher than what is acceptable for industrial applications (5% or better). The cross-linking time for the same sample mass was significantly shorter: 12-15 h was sufficient to produce dry materials. Persistent solubility of a fraction of the formed polymer can be attributed to unreacted peptones and/or glutaraldehyde, as well as water trapped within the network. It can also be attributed to intramolecular cross-linking competing with intermolecular cross-linking, where the former involves reactive sites within the same molecule being cross-linked to each other by one glutaraldehyde chain. The net effect of this phenomenon is that there is less intermolecular cross-linking (among different molecules), suppressing the formation of infinitely large networks.

Table 3-1. Solubilities of Salt-Extracted Peptones Cross-Linked at Various Temperatures.

Temperature, ºC	Solubility, %	# samples	t-test[a]
37	92.8 ± 0.8	3	< 0.001
100	20.6 ± 3.4	3	0.040
110	11.8 ± 0.8	3	
120	16.9 ± 2.0	6	0.029
130	31.9 ± 5.0	3	0.021
140	23.0 ± 0.6	5	< 0.001
150	20.3 ± 0.8	3	< 0.001

[a]*Unpaired, two-tailed t-tests are reported for solubility results compared to network formed at 110 ºC.*

One important observation is that there was an optimal cross-linking temperature. As mentioned earlier, water is a byproduct of the reaction, and

therefore, removing water shifts the equilibrium toward the products. However, water is also a reaction medium and hydrogen source for the reaction [24]. At low temperatures, water removal is slow, and the energy in the system is lower. Both factors lead to a lower extent of reaction. As temperature is increased, water removal in the system is enhanced, diffusion is increased, and there is more energy for a higher reaction rate/extent. As the temperature is further increased, water removal becomes so fast that it deprives the reaction of the medium and hydrogen source. As the temperature is increased even further to 140 °C, the solubility begins to decrease again. Although water is being removed at a significantly higher rate, the high-energy molecules compensate for it. This trend was not surprising, as the DSC scans showed exothermic peaks for cross-linking in the temperature range of 140–150 °C.

An optimal cross-linking temperature was again observed for salt-free peptones that were extracted with water following the same hydrolysis conditions. As Table 3-2 shows, the solubility of the resulting cross-linked networks was lower than that of the salt-containing networks. This result is surprising because, during sample preparation and mixing, we consistently observed that the miscibility of the glutaraldehyde solution with the peptones was better in the presence of salts. Therefore, reactivity was expected to be improved in the presence of salts.

Table 3-2. Solubilities of Water-Extracted Peptones Cross-Linked at Various Temperatures.

Temperature, ºC	Solubility, %	# samples	t-test[a]
100	11.3 ± 2.5	3	0.022
110	6.0 ± 3.0	4	0.019
120	6.0 ± 1.0	4	0.003
135	7.0 ± 0.6	3	0.015
150	9.5 ± 2.0	4	< 0.001

[a]*Unpaired, two-tailed t-tests are shown for solubility results compared to salt-extracted networks reported in Table 3-1.*

The presence of ions enhances reactions with charged intermediates but hinders reactions with neutral intermediates [25]. Our results demonstrate that salts have a small but negative effect on the overall reaction. There are two reasonable explanations for this effect that are not mutually exclusive. Salts might bind water to peptones and slow its removal from the system (boiling point elevation). Because water is a byproduct, this would impede the shift in equilibrium toward the products. The second explanation is based on reaction chemistry: If reaction intermediates are neutral, an increase in ionic strength is detrimental to the overall reaction. As discussed earlier, the two pathways that lead to a cross-linked network are the Mannich reaction (charged intermediate) and Michael addition (neutral intermediate). Because the results obtained with and without salts are not dramatically different, the Mannich reaction cannot be ruled out, but one can infer that the Michael addition reaction is the more favorable pathway.

The DSC curves for the final products of salt-extracted and water-extracted networks did not show any exothermic peaks, suggesting that cross-linking was completed during reactions at higher temperatures.

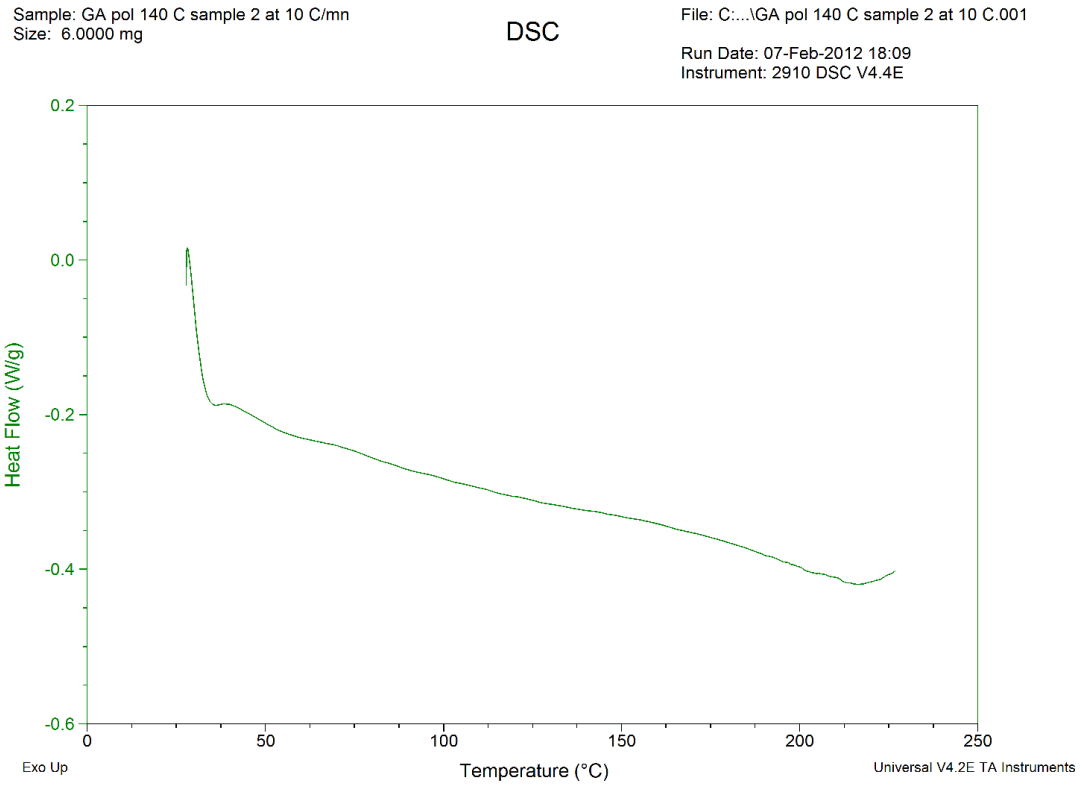

Figure 3-3. DSC curve at 10 ºC/min for salt-extracted peptones reacted with glutaraldehyde at 140 ºC

As an example, Figure 3-3 shows the DSC curve for the product of cross-linking carried out at 140 °C with no endothermic (water evaporation) or exothermic (cross-linking) peaks. This scan was repeated for all samples prepared at elevated temperatures, and the same outcome was observed.

Thermal stability was also found to be significantly better. The networks were stable up to 200 °C, whereas previous results (for cross-linking at 37 °C) showed breakup/degradation at 120 °C and reached 67% of the initial weight by 200 °C. Unlike the solubility measurements, the TGA results for thermal stability did not exhibit an optimum temperature for cross-linking (Figure 3-4). The thermal stability of the cross-linked networks increased as the cross-linking temperature was increased because of the increased evaporation of unreacted glutaraldehyde and/or water.

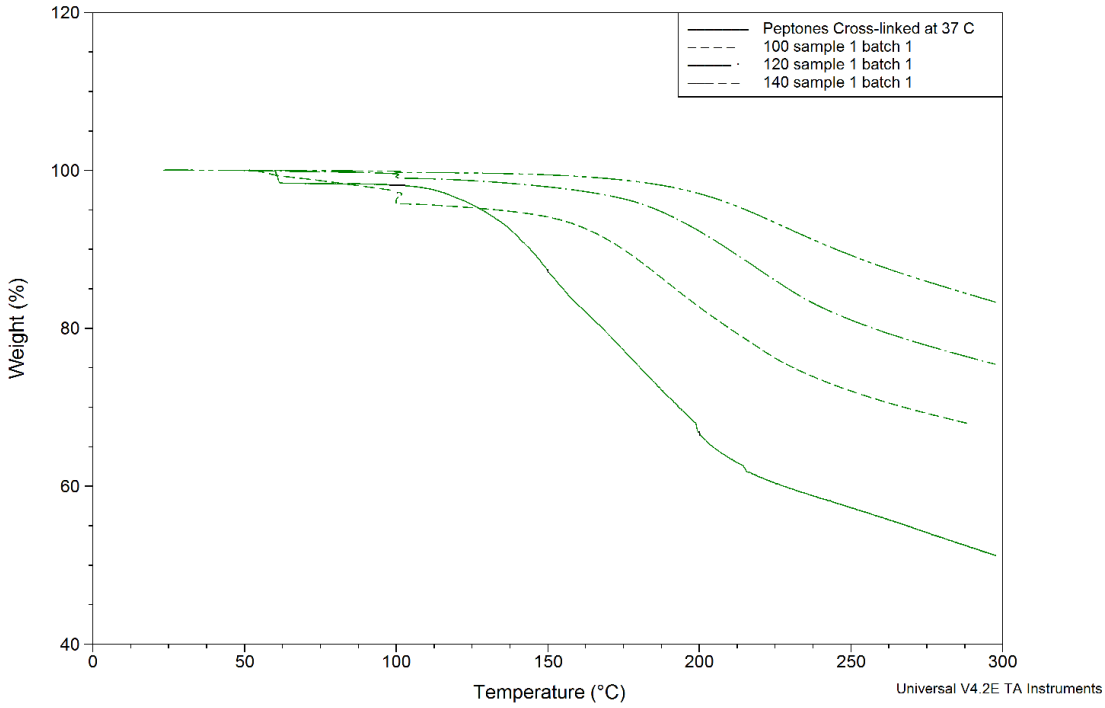

Figure 3-4. TGA curves at 5 ºC/min for salt-extracted peptones reacted with glutaraldehyde at 37, 100, 120, and 140 ºC

The TGA curves for networks formed at 110, 130, and 150 °C were very similar to the curves for cross-linking at 100, 120, and 140 °C, respectively.

Table 3-3 summarizes the results discussed earlier. Listed are the mass losses obtained for two reference temperatures after subtraction of the mass loss at the end of the isothermal run at 100 °C for the removal of moisture and/or absorbed water. The TGA results indicate that higher cross-linking temperatures yielded improved thermal stability. The lower thermal stabilities of some polymers compared to hydrolyzed protein might also indicate the evaporation of excess reactants.

Table 3-3. Additional mass loss observed after the conclusion of the isothermal run for salt-extracted peptones cross-linked at various temperatures.

Compound	Mass Loss at 150 ºC	Mass Loss at 200 ºC
Hydrolyzed Protein	1.0%	4.0%
Reacted at 37 ºC	11%	28%
Reacted at 100 ºC	1.7%	13%
Reacted at 110 ºC	1.9%	16%
Reacted at 120 ºC	1.0%	7.0%
Reacted at 130 ºC	0.3%	5.0%
Reacted at 140 ºC	0.3%	2.3%
Reacted at 150 ºC	0.2%	1.6%

Similar results were obtained for glutaraldehyde-cross-linked salt-free peptones. Thermal stability (Table 3-4) also improved as the cross-linking temperature increased. These results are statistically the same as those for the cross-linked salt-extracted peptones (Figure 3-5). Only at temperatures above 220 °C did the salt-containing networks have better thermal stability.

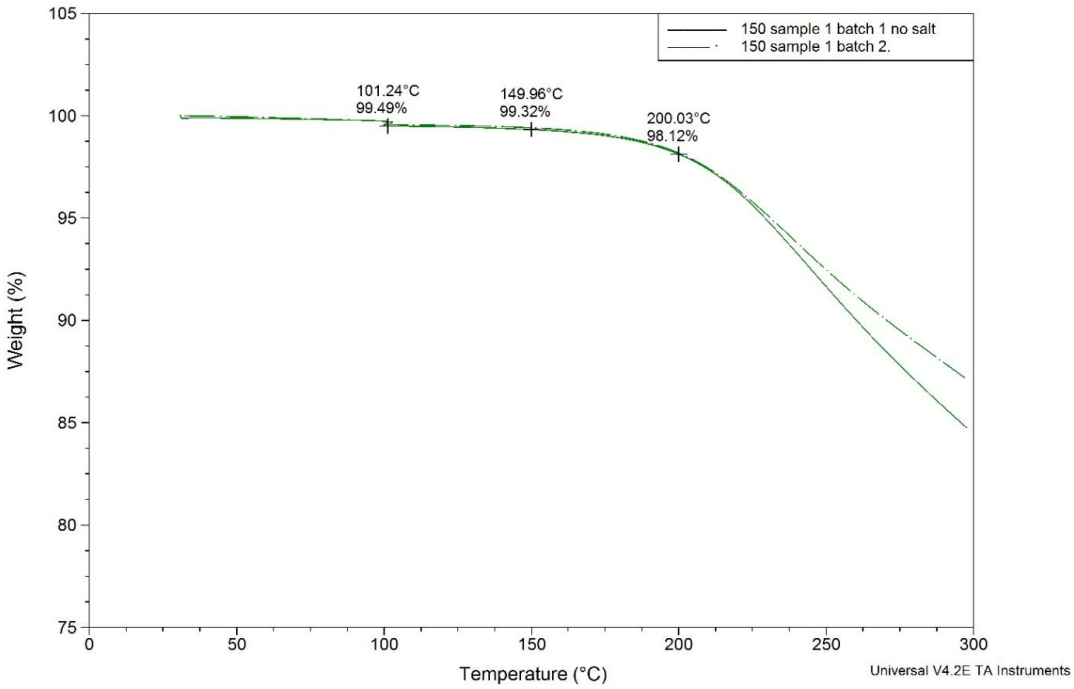

Figure 3-5. TGA curves at 5 ºC/min for salt-extracted (dashed line) and water-extracted (solid line) peptones reacted with glutaraldehyde at 150 ºC

The slightly improved thermal stability above 220 °C of salt-extracted peptone networks was reproduced for networks cross-linked at all temperatures. Biobased products are not generally expected to be utilized in applications above 200 °C because of degradation. The improved thermal stability of the formed

networks, compared to that of the starting material, clearly shows that chemical cross-linking was achieved.

Table 3-4. Additional mass loss observed after the conclusion of the isothermal run for water-extracted peptones cross-linked at various temperatures.

Compound	Mass Loss at 150 ºC	Mass Loss at 200 ºC
Reacted at 100 ºC	3.1%	22%
Reacted at 110 ºC	1.9%	12%
Reacted at 120 ºC	1.1%	8.7%
Reacted at 135 ºC	1.0%	6.0%
Reacted at 150 ºC	0.2%	1.5%

We also tested the effect of byproduct removal by carrying out cross-linking at 80 °C. Although there was a sufficient energy increase in the system compared to that at 37 °C, water removal was slow compared to that for reactions carried out at temperatures higher than 100 °C. Figure 3-6 illustrates the inhibition of water by comparing products from reactions at 80 and 37 °C. The results here show no improvement in thermal stability of the product when reacted at 80 °C. This illustrates that merely increasing the temperature was not sufficient to increase reactivity and that the presence of water prevented the reaction from proceeding to the desired extent. Solubility also exceeded 50%.

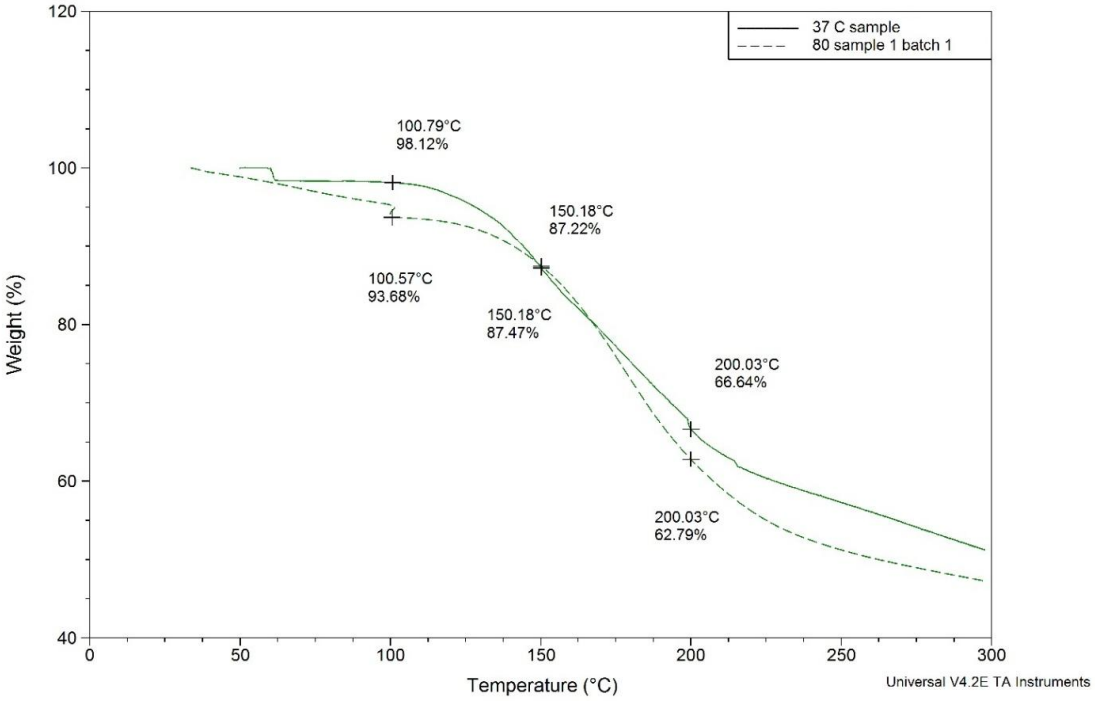

Figure 3-6. TGA curves at 5 ºC/min for salt-extracted peptones reacted with glutaraldehyde at 37 and 80 ºC indicating mass at 150 ºC, 200 ºC, and the end of the isothermal run at 100 ºC

3.4 CONCLUSION

Positive results have been obtained by employing glutaraldehyde as a cross-linking agent to form cross-linked networks from hydrolyzed Specified Risk Material. Reaction conditions leading to cross-linked networks with only 5–10% solubility and thermal stability up to 200 °C were determined. The temperature range for effective cross-linking was found to be 110–150 °C. As different regimes of hydrolysis result in different molecular weight distributions of peptones, our measurements are reproducible mainly for the materials obtained

under the conditions outlined in this article. However, the qualitative findings of our work are expected to be applicable to a wide range of biobased materials. In this work, it was shown that there is an optimum temperature at which cross-linking is most efficient because competing effects are balanced out. The presence of water is useful as a medium to disperse the peptones into glutaraldehyde, which would otherwise be very difficult to mix and would form a very viscous material, and a hydrogen source for the reaction. Longer presence of water was achieved at lower temperatures. Water is also a byproduct that needs to be removed from the system to shift the equilibrium toward the product side. Higher temperatures enhance water removal and reactant miscibility and provide more energy for higher reactivity. However, for temperatures below 100 °C, the lack of removal of water leads to poor final products. Salts can enhance the mixing of peptones and glutaraldehyde, but better results are obtained if no salts are used.

3.5 REFERENCES

(1) Canadian Food Inspection Agency. *Enhanced Animal Health Protection from BSE*. **2010**, Canada. [Online] Available at: http://www.inspection.gc.ca/animals/terrestrial-animals/diseases/enhanced-feedban/eng/1299870250278/1334278201780 [Accessed 26 November 2012]

(2) Fedorowicz, E. M.; Miller, S. F.; Miller, B. G. Biomass Gasification as a Means of Carcass and Specified Risk Materials Disposal and Energy Production in the Beef Rendering and Meat Packing Industries. *Energy Fuels.* **2007**, *21*, 3225-3232.

(3) Somerville, R. A.; Fernie, K.; A. Smith; Andrews, R.; Schmidt E.; Taylor, D. M. Inactivation of a TSE Agent by a Novel Biorefinement System. *Proc. Biochemistry* **2009**, *44*, 1060-1062.

(4) Murphy, R.; Scanga, J.; Powers, B. J.; Vercauteren, K.; Nash, P.; Smith G.; Belk, K. Alkaline Hydrolysis of Mouse-adapted Scrapie for Inactivation and Disposal of Prion-positive Material. *J. Anim. Sci.* **2009**, *87*, 1787-1793.

(5) Sabatini, D. D.; Bensch, K.; Barnett, R. J. Cytochemistry & Electron Microscopy. The Preservation of Cellular Ultra-structure & Enzymatic Activity by Aldehyde Fixation. *J. Cell. Biol.* **1963**, *17*, 19-58.

(6) Migneault, I.; Dartiguenave, C.; Bertrand, M. J.; Waldron, K. C. Glutaraldehyde: Behavior in Aqueous Solution, Reaction with Proteins, and

Application to Enzyme Cross-linking. *BioTechniques.* **2004,** *37,* 790-802.

(7) Olde Damink, L. L. H.; Dijkstra, P. J.; van Luyn, M. J. A.; van Wachem, P. B.; Nieuwenhuis, P.; Feijen, J. Glutaraldehyde as a Cross-linking Agent for Collagen-based Biomaterials. *J. Mater. Sci. – Mater. Med.* **1995**, *6*, 460-472.

(8) Flory, P. J. *Principles of Polymer Chemistry*; Cornell University Press: Ithaca, 1953.

(9) Cheung, D. T.; Nimni, M. E. Mechanism of Cross-linking of Proteins by Glutaraldehyde II. Reaction with Monomeric and Polymeric Collagen. *Connect. Tissue Res.* **1982**, *10*, 201-216.

(10) Park, S. K.; Bae; D. H.; Rhee, K.C. Soy Protein Biopolymers Cross-Linked with Glutaraldehyde. *J. Am. Oil Chem. Soc.* **2000**, *77*, 879-884.

(11) Payne, J. W. Polymerization of Proteins with Glutaraldehyde. *Biochem. J.* **1973**, *135*, 867-873.

(12) Fernandez-Lorente, G.; Palomo, J. M.; Mateo, C.; Munilla, R.; Ortiz, C.; Cabrera, Z.; Guisan, J. M.; Fernandez-Lafuente, R. Glutaraldehyde Cross-Linking of Lipases Adsorbed on Aminated Supports in the Presence of Detergents Leads to Improved Performance. *Biomacromolecules.* **2006**, *7,* 2610-2615.

(13) Bolivar, J. M.; Rocha-Martin, J.; Mateo, C.; Cava, F.; Fernandez-Lafuente, R.; Guisan, J. M. Coating of Soluble and Immobilized Enzymes with Ionic Polymers: Full Stabilization of the Quaternary Structure of Multimeric Enzymes.

Biomacromolecules. **2009**, *10*, 742-747.

(14) Tomimatsu, Y.; Jansen, E. F.; Gaffield, W.; Olson, A. C. Physical Chemical Observations on the α-Chymotrypsin Glutaraldehyde System during Formation of an Insoluble Derivative. *J. Colloid Interface Sci.* **2012,** *36*, 51-64.

(15) McMurry, J. *Organic Chemistry*; Brooks/Cole Thomson Learning: Pacific Grove, 1999.

(16) Gunanathan, C.; Ben-David, Y.; Milstein, D. Direct Synthesis of Amides from Alcohols and Amines with Liberation of H2. *Science.* **2007,** *317*, 790-792.

(17) Tillak, A.; Rudloff, I.; Beller, M. Catalytic Amination of Aldehydes to Amides. *European J. Org. Chem.* **2001**, *2001*, 523-528.

(18) Canadian Food Inspection Agency. *Enhanced Feed Ban Decision Documents.* **2009**, Canada. [Online]. Available: http://www.inspection.gc.ca/english/anima/heasan/disemala/bseesb/enhren/decdoce.shtml. [Accessed 12 February 2010].

(19) Food & Drug Administration. Substances Prohibited From Use in Animal Food or Feed. *Federal Register.* **2008**, *73*, 22720-22758.

(20) Race, R. E.; Raymond, G. J. Inactivation of Transmissible Spongiform Encephalopathy (Prion) Agents by Environ LpH. *J. Virol*. **2004**, *78*, 2164-2165.

(21) Park, S. K.; Bae, D. H.; Hettiarachchy, N. S. Protein Concentrate and

Adhesives from Meat and Bone Meal. *J. Am. Oil Chem. Soc.* **2000**, *77*, 1223-1227.

(22) Garcia, R. A.; Rosentrater, K. A.; Flores, R. A. Characteristics of North American Meat and Bone Meal Relevant to the Development of non-feed Applications. *Appl. Eng. Agric.* **2006**, *22*, 729-736.

(23) Mekonnen, T.; Mussone, P.; Stashko, N.; Choi, P.; Bressler, D. Recovery and Characterization of Proteinacious Material Recovered from Thermal and Alkaline Hydrolyzed Specified Risk Materials. **2013**, *48*, 885-892.

(24) Mizuta, T.; Sakaguchi, S.; Ishii, Y. Catalytic Reductive Alkylation of Secondary Amine with Aldehyde and Silane by an Iridium Compound. *J. Org. Chem.* **2005**, *70*, 2195-2199.

(25) March, J. *Advanced Organic Chemistry: Reactions, Mechanisms, and Structure*; Wiley: New York, 1992.

CHAPTER 4[2]

4.0 EPOXY RESINS CROSS-LINKING

The outbreak of bovine spongiform encephalopathy (BSE) resulted in worldwide restrictions on beef rendering plants to dispose of tissues that may contain the BSE disease-causing agents (prions), commonly referred to as specified risk material (SRM). SRM must therefore be hydrolyzed at high temperatures in order to break down proteins into smaller molecules, protein hydrolysates. The two factors of increased disposal cost and reduced value generation combine to necessitate finding a novel value-generating process to convert animal byproducts into stable materials which can be used for industrial applications. In Canada, SRM is banned from all animal foods and fertilizers since 2007, resulting in lost revenue for the beef industry [1]. SRM consists of the skull, brain, trigeminal ganglia, eyes, tonsils, spinal cord and column, dorsal root ganglia, and distal ileum for cows older than 30 months. For the younger cows, SRM consists of only the tonsils and distal ileum [2]. Hydrolysis of SRM and extraction of protein hydrolysates have been reported in our previous work [3]. We have also studied the cross-linking of protein hydrolysates with glutaraldehyde [4] and bisphenol A diglycidyl ether (DGEBA) [5] to produce insoluble cross-linked polymers.

[2] A version of this chapter has been published. El-Thaher et al. *Industrial and Engineering Chemistry Research.* **2013**, *52*, 8189−8199.

In order to further study the behavior of hydrolyzed proteins in cross-linking reactions, we have employed the Kissinger method for differential scanning calorimetry (DSC) in order to calculate the apparent activation energy for a set of reactions, analyzed our results by the isoconversional method, and determined reactions models suitable to simulate reaction rates.

Epoxy resins have been shown to convert primary and secondary amine groups into secondary and tertiary amines, respectively, via the transfer of a proton from amine groups to the epoxy ring to form a hydroxyl group [6]. Likewise, hydroxyl and carboxylic groups react with epoxy rings via proton transfer from the hydroxyl (or carboxylic group) to the epoxy ring whereby the hydroxyl group is converted into an ether (or carboxylic group forms an ester) and the epoxy ring forms a hydroxyl group [7]. Sulfhydryl groups similarly react with epoxy rings: proton transfer from sulfur opens the epoxy ring and a hydroxyl group is formed [8]. Cysteine amino acids in proteins contain sulfhydryl groups; tyrosine, threonine, and serine contain hydroxyl groups; glutamic and aspartic acids contain carboxylic groups; asparagine, glutamine, lysine, arginine, and the protein hydrolysate main chain contain secondary amines; proline and histidine contain primary amines. These groups are abundantly present in proteins and hydrolyzed proteins, as has been shown in our previous work [3]. Figure 4-1 illustrates mechanisms of the expected reactions. It is worth noting that these reactions always convert the oxygen of an epoxy ring into a hydroxyl group, itself a curing group for epoxy rings. The reaction, therefore, is expected to exhibit

autocatalysis. There are no byproducts from these reactions. As there are no gases such as H_2 or H_2O emitted from the curing process, there is no pressure dependence or mass loss during experiments. Since no mass loss occurs, DSC scans are not affected by baseline shift or evaporation peaks.

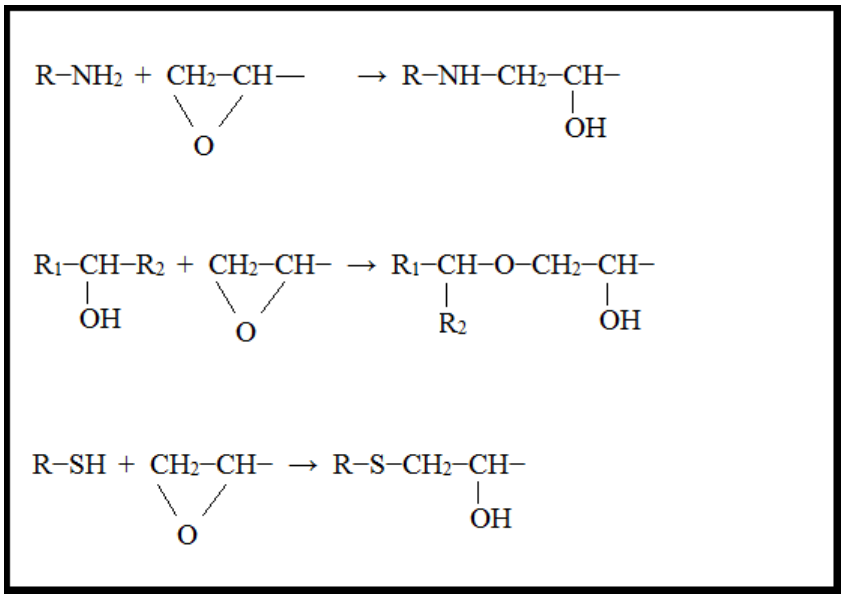

Figure 4-1. Reaction mechanisms for curing of epoxy rings

DSC has been previously used in kinetic studies of thermosetting polymers. Roşu et al. [9] varied the heating rate in order to determine the model and parameters which best describe the curing of two epoxy resins, one of which is DGEBA, with triethylenetetramine. They also studied the effect of adding a reactive diluent (diglycidyl aniline) on the apparent activation energy. Hong and Lee [10] also employed the dynamic technique in order to study the kinetics of cross-linking polydimethylsiloxane as well as to compare four different methods (Flynn−Wall−Ozawa, Kissinger, Ozawa, and Friedman) for calculating apparent

activation energy. Friedman's method led to a slightly lower (6%) activation energy than the three other methods, which were within 4% of one another. Boey and Qiang [11] also compared the Kissinger and Ozawa methods for DGEBA curing with hexaanhydro-4-methylphthalicanhydride and demonstrated that activation energy is nearly the same for both methods. This contribution reports the effect of epoxy mass ratio to protein hydrolysates, electrolytes, epoxy viscosity, and protein hydrolysate molecular weight on the apparent activation energy measured by the nonisothermal technique and calculated by the Kissinger method. The Ozawa method [12] is not as accurate as the Kissinger method, and it is generally recommended that only one method be used for analysis of thermal data [13].

4.1 DIFFERENTIAL SCANNING CALORIMETRY THEORY

The DSC nonisothermal technique was used in this work to obtain the curing thermal data. The Kissinger method was then used to calculate the apparent activation energy. The main advantage of this method is that activation energy can be calculated without the need to determine reaction mechanisms [10] and the frequency factor can also be estimated without determining the order of reaction [14]. When cross-linking is studied with a calorimetric instrument, released energy is recorded for the duration of the reaction. When constant heating is used, the temperature at which the exothermic peak is at its maximum, T_p, increases as the heating rate is increased. Kissinger [15] showed that, for solid → solid + gas

reactions, T_p can be used to calculate activation energy for reactions of any order since it is the temperature at which reaction rate is at a maximum. The correlation is as follows:

$$d(\ln[(\beta_i/T^2_{p,i})])/dT = -E_a/RT_{p,I} \quad (4\text{-}1)$$

where R is the universal gas constant, β is the heating rate in the DSC, and E_a is the apparent activation energy. In order to obtain the frequency factor, A_o, the reaction rate derivation is set to zero as suggested by Prime [14]. The reaction rate, $d\alpha/dt$, is expressed as $A_o\exp(-E_a/RT)\ f(\alpha)h(P)$, where α is the extent of reaction and $f(\alpha)$ is a function of the extent of reaction and can be expressed as $f(\alpha) = (1 - \alpha)^n$, where n is the order of reaction. The last term, $h(P)$, is the function of pressure dependence of the reaction and is often important for reactions involving gases as reactants and/or byproducts [13]. As shown in Figure 4-1, epoxy curing by hydrolyzed protein does not involve gases. The pressure dependence term can be ignored. Setting the derivative of $d\alpha/dt$ with respect to time to zero (i.e., $d^2\alpha/dt^2 = 0$) leads to the following relationship:

$$\beta/T_p^2 = (A_oR/E_a)[n(1 - \alpha_p)^{n-1}]\exp(-E_a/RT_p) \quad (4\text{-}2)$$

where α_p is the conversion at the peak temperature. Kissinger [15] demonstrated that the term $n(1 - \alpha_p)^{n-1}$ is independent of heating rate and nearly equal to 1. By taking the natural log of Equation 4-2, we arrive at:

$$\ln(\beta/T_p^2) = \ln(A_o R/E_a) - E_a/RT_p \quad (4\text{-}3)$$

which means that a plot of $\ln(\beta/T_p^2)$ vs $1/T_p$ gives a straight line with a slope of E_a/R. The y-intercept is $\ln(A_o R/E_a)$. Since this relationship is arrived at following an approximation of the term $n(1 - \alpha_p)^{n-1}$ to unity, a small error in activation energy measurement is to be expected. For nonisothermal experiments, different heating rates may result in different values for α_p for the same reaction. The isoconversional method is another useful method to probe the progress of the reaction at different conversion rates and provide additional insight into the reaction. Similar to Equation 4-3, the activation energy at different extents of reaction is obtained as follows:

$$\ln(\beta_i/T_{\alpha,i}^2) = \text{Constant} - E_\alpha/RT_\alpha \quad (4\text{-}4)$$

where $T_{\alpha,I}$ is the temperature at which α is reached for each heating rate [13]. The reaction model, $f(\alpha)$, and reaction order are obtained by selecting an adequate model as follows. As mentioned earlier, $d\alpha/dt = A_o \exp(-E_a/RT) f(\alpha)$. For constant

heating rate scans, $d\alpha/dt = \beta_i d\alpha/dT$, so that a plot of $\ln[(\beta_i d\alpha/dT)/f(\alpha)]$ vs $1/T$ for constant values of α and an adequate model for $f(\alpha)$ is expected to yield a straight line. The slope is $-E_a/R$, and the y-intercept is $\ln A_o$. The reaction model and its parameters are selected such that the correlation coefficient is maximized [10, 13]. In the Arrhenius equation, the temperature-dependent rate constant, $k(T)$, is expressed as $k(T) = A_o \exp(-E_a/RT)$. At low temperatures, exp $\exp(-E_a/RT)$ is the dominant term, and the reaction rate is slow. At higher temperatures, whereas $\ln A_o$ is dominant, and the rate constant is significantly increased. In order to correlate the changes in activation energy and $\ln A_o$ for the different systems in this study to practical applications, the temperature at which one system's reaction rate constant becomes higher than the rate of a system with a lower activation energy is determined by setting $k_1(T_{eq})$ to $k_2(T_{eq})$ and solving for T_{eq}. The relationship is:

$$T_{eq} = (E_{a1} - E_{a2})/R(\ln A_{o1} - \ln A_{o2}) \quad (4\text{-}5)$$

where T_{eq} is the temperature at which both reactions have equal rate. This relationship is useful only when one reaction, X, has higher activation energy and $\ln A_o$ than those of another reaction, Y ($E_{a1} > E_{a2}$ and $\ln A_{o1} > \ln A_{o2}$) and f(α) is the same for both reactions. At low temperatures, reaction Y proceeds at a higher rate than reaction X. At a sufficiently high temperature, the trend is reversed, and the higher activation energy is compensated for by $\ln A_o$.

4.2 EXPERIMENTAL SECTION

4.2.1 Instrumentation

Thermal Analysis Instruments, DSC 2910, routinely calibrated with indium and zinc standards, was utilized for our work. Aluminum hermetic sample pans and lids were used for experiments. The lid was inverted and sealed on top of the pan. Sample and reference pans were manually placed in the DSC cell. Curing was carried out by heating samples from room temperature to 300 °C at varying rates (2, 5, 10, 15, 20, and 25 °C min−1) under the flow of nitrogen. Samples in the mass range of 2 – 5 mg for DGEBA-protein hydrolysates and 5 – 8 mg for PPGDE-protein hydrolysates were used. The peak temperature for each run was obtained by TA Instruments Universal Analysis 2000 software. The "Peak Max" was selected because it gives the peak value relative to the linear baseline, which corrects for changes in the heat flow caused by heat capacity variations during the scan. The "Signal Max" would give the temperature at the absolute peak of the heat flow signal without correction to the baseline. For most runs, the difference between the two methods is within 1 °C. For each heating rate, three thermal scans were carried out, and the average peak temperature was used for calculations.

4.2.2 Materials

NaCl (99%, mol wt 58.44 g/mol), Na_2HPO_4 (99.6%, mol wt 268.07 g/mol), KH_2PO_4 (99.8%, mol wt 136.09 g/mol), $MgCl_2$ (99%, mol wt 95.21 g/mol), and

hexane (99.9% HPLC grade, mol wt 86.18 g/mol) were purchased from Fisher Scientific Co. SDS (99+ %, mol wt 288.38 g/mol) was obtained from Sigma-Aldrich, St. Louise, MO, U.S.A. Filter paper (Whatmann 4, diameter 11 cm, pore size 20 – 25 μm) was purchased from Whatmann, UK. DGEBA (Araldite 506) and PPGDE (M_n = 380 g/mol) were purchased from Sigma Aldrich. Protein hydrolysates were obtained via thermal hydrolysis (one set at 180 °C and one set at 220 °C) of SRM obtained from Sanimax Industries, Inc. (Montreal, QC, Canada). For the two sets of hydrolyzed SRM, one set of protein hydrolysates was water extracted, and another set was salt-solution extracted in order to produce four different sets of protein hydrolysates. Hydrolysis and extraction were carried out as outlined in our previous work [3, 4]. Salt-free protein hydrolysates obtained at 180 and 220 °C hydrolysis are henceforth referred to as PEP180 and PEP220, respectively, and protein hydrolysates which contain salts due to extraction method (by salt solution) are PEP180SA and PEP220SA.

4.2.3 Hydrolysis and Extraction

Distilled water was added to dry SRM (1:1 mass ratio). Hydrolysis was carried out in a dedicated 5.5 L stainless steel pressure vessel (Parr Instrument 4582, Moline, IL, U.S.A.) capable of handling pressure up to 20.7 MPa. The total volume of SRM solution was 3.6 L per cycle, continuously stirred at 200 rpm. Two sets of SRM were hydrolyzed at 1200 kPa for 40 min, but two temperatures were selected. One set was hydrolyzed at 180 °C, and another set was hydrolyzed

at 220 °C. Protein hydrolysates were extracted from the insoluble components of hydrolyzed SRM with a salt solution consisting of 100 g of the hydrolyzed sample with 450 mL of salt solution consisting of 18 g NaCl, 0.23 g $MgCl_2$, 4.10 g KH_2PO_4, and 4.30 g Na_2HPO_4, according to the method of Park et al. [16] with agitation at 200 rpm for 30 min in a shaker (Innova lab shaker, New Brunswick, Canada). Salt-free protein hydrolysates were extracted by the dissolution of 40 g of hydrolyzed protein in 180 mL of Milli-Q water and agitated at 200 rpm for 30 min followed by centrifugation at 7000g for 30 min and vacuum filtration (Whatman filter paper no 4) to remove insoluble tissues and bone particles. The filtered supernatant was then extracted with 540 mL of hexane to remove lipids. The raffinate was then freeze-dried under reduced pressure, and the total nitrogen was quantified using the Dumas method [17].

4.3 RESULTS AND DISCUSSION

Hydrolysis was carried out at 220 °C in order to study the effect of curing epoxy resins with protein hydrolysates of lower molecular weight compared to protein hydrolysates obtained from hydrolysis at 180 °C. Figure 4-2 shows the reduction in the molecular size of protein hydrolysates hydrolyzed at 220 °C, as determined by the SDS-PAGE technique. The majority of protein hydrolysates obtained from 180 °C hydrolysis were concentrated between 3.5 kDa and 6.5 kDa; hydrolysis at 220 °C resulted in protein hydrolysates mainly concentrated in the range 1.4-3.5 kDa.

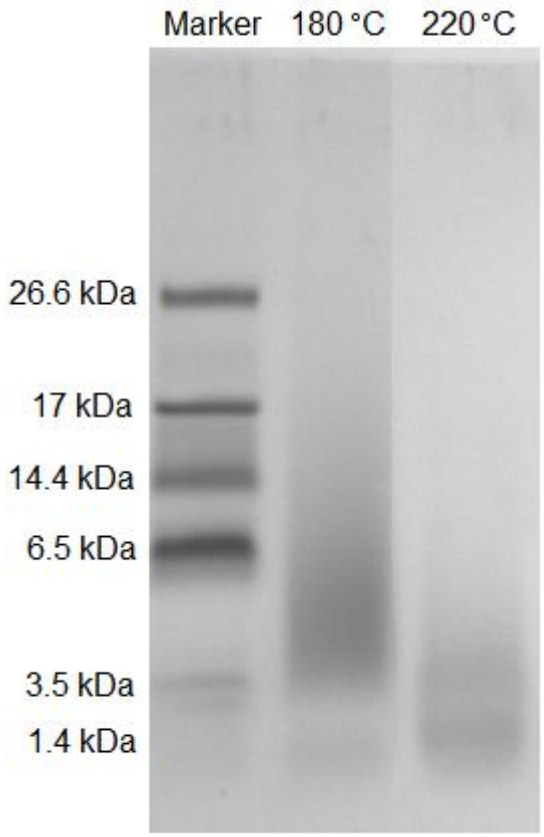

Figure 4-2. SDS PAGE of 180 °C and 220 °C hydrolyzed SRM

The curing of epoxy resins with protein hydrolysates was studied by DSC at six different heating rates. Figure 4-3 illustrates how peak temperature, T_p, is increased as the heating rate is increased. Four different rates are shown here for clarity. The sample was for the curing of DGEBA with PEP180SA (mass ratio of 1:1). The correlation coefficient, R, was > 0.98 for all systems presented in this study.

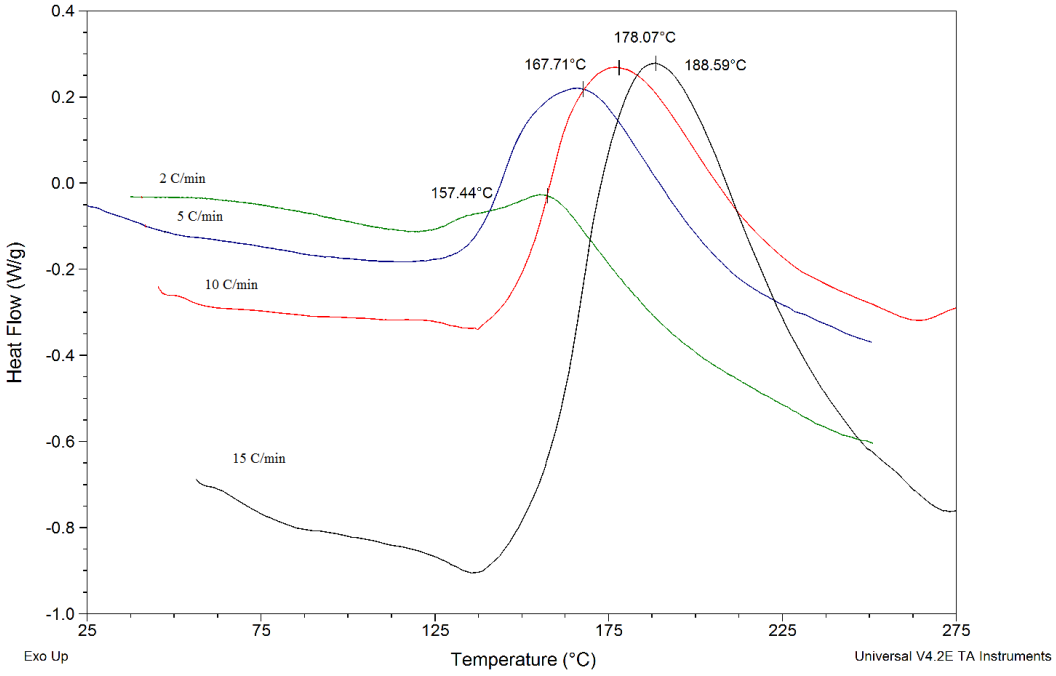

Figure 4-3. Typical DSC curves for the curing of 1:1 DGEBA with PEP180SA (1:1 mass ratio) at four different heating rates: 2, 5, 10, and 15 ºC min^{-1}

Kissinger plots (see example shown in Figure 4-4) were used to obtain the activation energy from the data presented in Figure 4-3.

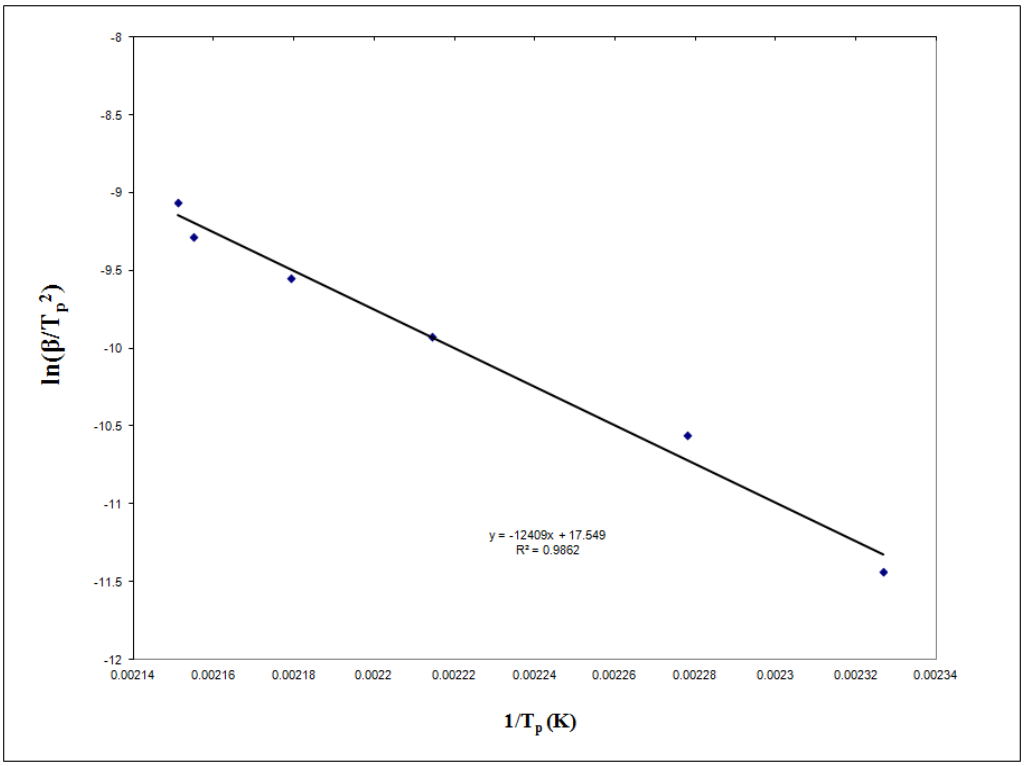

Figure 4-4. Kissinger plot for the curing of DGEBA with PEP180SA

Table 4-1. Effect of Mass Ratio on the Apparent Activation Energy and Frequency Factor for Curing of DGEBA with PEP180SA.

Epoxy:PEP180SA	$\ln A_o$	E_a, kJ mol^{-1}
Mass Ratio	Kissinger	Kissinger
1:1	27.226	104.0
3:2	25.022	95.5
7:3	22.432	87.0

Table 4-1 summarizes results obtained for the curing of DGEBA with PEP180SA. Activation energy was found to be dependent on mass ratio. An increase in epoxy concentration resulted in a reduction of activation energy. For 1:1 mass ratio, the mixture is highly viscous. When more DGEBA is added and the protein hydrolysates are dispersed more freely, viscosity is reduced. We

suspect the additional energy for a higher protein hydrolysate fraction is mainly to compensate for the mixing/viscosity barrier, salt effect, and molecular size of protein hydrolysates.

Table 4-2. Effect of Mass Ratio on the Apparent Activation Energy and Frequency Factor for Curing of DGEBA with PEP180.

Epoxy:PEP180	$\ln A_o$	E_a, kJ mol^{-1}
Mass Ratio	Kissinger	Kissinger
1:1	No Mixing	No Mixing
3:2	17.989	75.1
7:3	17.784	74.0

The same mass ratios were studied using the salt-free PEP180, and interesting results were obtained. No results were obtained for 1:1 mass ratio due to the immiscibility of protein hydrolysates with DGEBA. Contrary to results in Table 4-1, mass ratio had no impact on activation energy (see Table 4-2). The salt fraction in protein hydrolysates is the same for all salt-solution extracted protein hydrolysates. This means that the higher the fraction of protein hydrolysates in the curing reaction, the more is the effect of salt. As for salt-free protein hydrolysates, their ratio to epoxy in curing does not change the electrolyte concentration, which explains why kinetic parameters were determined to be independent of epoxy-to-protein hydrolysate mass ratio. Activation energy was also significantly lower for salt-free reactions and comparable to previous studies on DGEBA curing with short-chain molecules. In particular, Roşu et al. [9] calculated $\ln A_o$ value of 17.953 and activation energy of 69.5 kJ mol^{-1}. We expected the activation energy

of salt-free protein hydrolysates to be higher due to two factors. First, the presence of salts was observed to enhance miscibility of protein hydrolysates with DGEBA. Second, solubility and mechanical properties of salt-free protein hydrolysate-based networks were poorer than their counterparts from PEP180SA. The compensation for higher activation energy is due to the frequency factor, A_o, which is 2 orders of magnitude larger for PEP180SA. However, it is suspected that salts have adverse effects on the reaction as well. The bonds that ions form with reactive groups (e.g., COO^-, NH_3^+) of protein hydrolysates need to be broken up prior to bond formation with DGEBA. The additional activation energy in the presence of salts may be attributed to breaking the bonds between salt ions and protein hydrolysate reactive sites. The higher frequency makes up for the higher activation energy as temperature reaches 63 °C as calculated by Equation 4-5. Salts are expected to bind to protein residues which are expected to react with DGEBA. Activation energy is higher as energy is needed to replace these ions with DGEBA. The reason they lead to a better reaction may be attributed to enhanced miscibility.

The next set of experiments involved water-extracted protein hydrolysates obtained via hydrolysis of SRM at 220 °C. As was the case for PEP180 and as shown in Table 4-3, the change in mass ratio had no impact on $\ln A_o$ or activation energy which was 10% lower than the results reported for PEP180 in Table 4-2.

Table 4-3. Effect of Mass Ratio on the Apparent Activation Energy and Frequency Factor for Curing of DGEBA with PEP220.

Epoxy:PEP220	$\ln A_o$	E_a, kJ mol^{-1}
Mass Ratio	Kissinger	Kissinger
1:1	17.122	68.6
3:2	16.251	65.3
7:3	17.089	68.2

Since all variables are the same except for molecular weight, the decreased activation energy can be attributed to curing DGEBA with smaller protein hydrolysate molecules, enhancing miscibility with the epoxy. The value of $\ln A_o$ for PEP180/DGEBA reactions is only slightly higher than that for PEP220/DGEBA. The reduction in activation energy is therefore expected to enhance curing. The small decrease in the frequency factor does not lead to a lower reaction rate for temperatures below 700 °C as estimated from Equation 4-5.

The next set of experiments involved salt-water-extracted protein hydrolysates obtained via hydrolysis of SRM at 220 °C. Activation energy and the frequency factor were again observed to be higher for this set of experiments (Table 4-4) when compared to those of salt-free protein hydrolysates (Table 4-3). Activation energy increased as the mass fraction of protein hydrolysates (hence, salt concentration) was increased. When compared to results in Table 4-1 for salt-water extracted protein hydrolysates, activation energy decreased for SRM

hydrolyzed at the higher temperature. Once again, the effect of curing DGEBA with smaller protein hydrolysate molecules on activation energy was observed.

Table 4-4. Effect of Mass Ratio on the Apparent Activation Energy and Frequency Factor for Curing of DGEBA with PEP220SA.

Epoxy:PEP220SA	$\ln A_o$	E_a, kJ mol^{-1}
Mass Ratio	Kissinger	Kissinger
1:1	22.832	89.4
3:2	20.434	80.2
7:3	18.274	74.9

The model-free isoconversional method was used to further analyze results. We started with salt-free reactions for simplicity. The activation energy values for curing reactions of 3:2 and 7:3 mass ratios of DGEBA to protein hydrolysates, obtained via hydrolysis at 180 °C, were determined by the Kissinger method to be 75.1 and 74.0 kJ/mol, respectively. For the first reaction, α_p for 2 °C/min and 5 °C/min heating rates was 0.51 and reduced to 0.45 as the heating rate was increased.

The correlation coefficients for 0.05, 0.1, and 0.15 were below 0.98 and higher than 0.98 for the rest. As Figure 4-5 shows, activation energy decreased by roughly 1.2 kJ/mol for every 0.05 incremental increase in conversion. The average activation energy obtained from the isoconversional method was 76.7 ± 6.8 kJ/mol, fairly close to the value obtained by the Kissinger equation for α_p

(75.1 kJ/mol). The trend indicates that activation energy for the rate-determining step decreased slightly as the reaction moved forward. The trend is also consistent with observations obtained by Sbirrazzuoli et al. when excess curing groups are reacted with epoxy. A small decrease in activation energy with excess curing groups is because the predominant reaction is curing, whereas for stoichiometric quantities, the decrease in activation energy is more pronounced as the rate-determining step at higher conversions is diffusion of small molecules into the cross-linked polymer [18]. The dependency of $\ln A_o$ on conversion was similar for the same reaction, with an average of 18.479 ± 2.544 (17.989 at α_p).

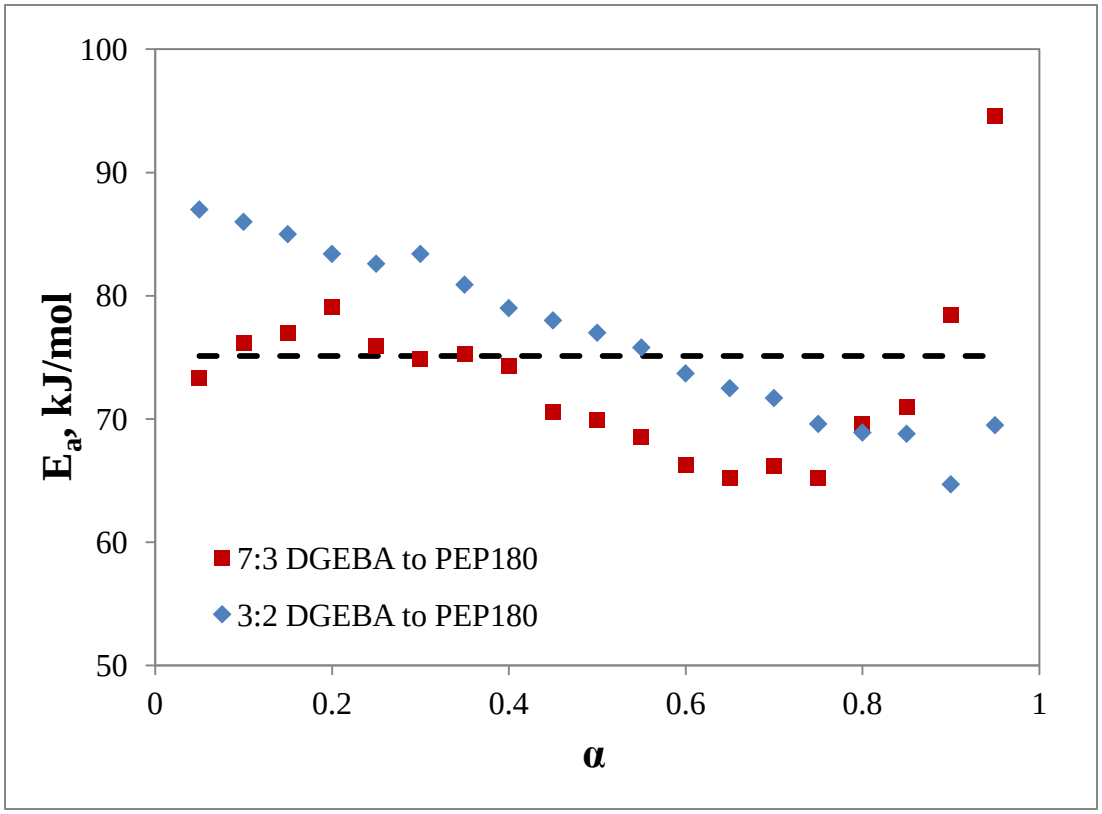

Figure 4-5. Dependency of activation energy on conversion for DGEBA and PEP180 reaction

The decrease in the frequency factor may be attributed to the decrease in the number of reactive sites as conversion is increased. The comparison between activation energy as a function of conversion for the curing of DGEBA with PEP180 at two different mass ratios is shown in Figure 4-5. The correlation coefficient for 7:3 was higher than 0.99 for conversions in the range 0.2 – 0.85 but was lower than 0.97 for conversions outside this range. The average activation energy value of 73.2 ± 6.8 kJ/mol was slightly lower than what was obtained at α_p (74.0 kJ/mol). A slight decrease in activation energy was again observed at higher conversions until 0.8 conversion. As Figure 4-6 shows, $\ln A_o$ also followed a similar dependency with an average of 17.669 ± 1.915 (17.784 at α_p). Despite a significant increase in DGEBA concentration, the average decrease in activation energy was less than 5 kJ/mol.

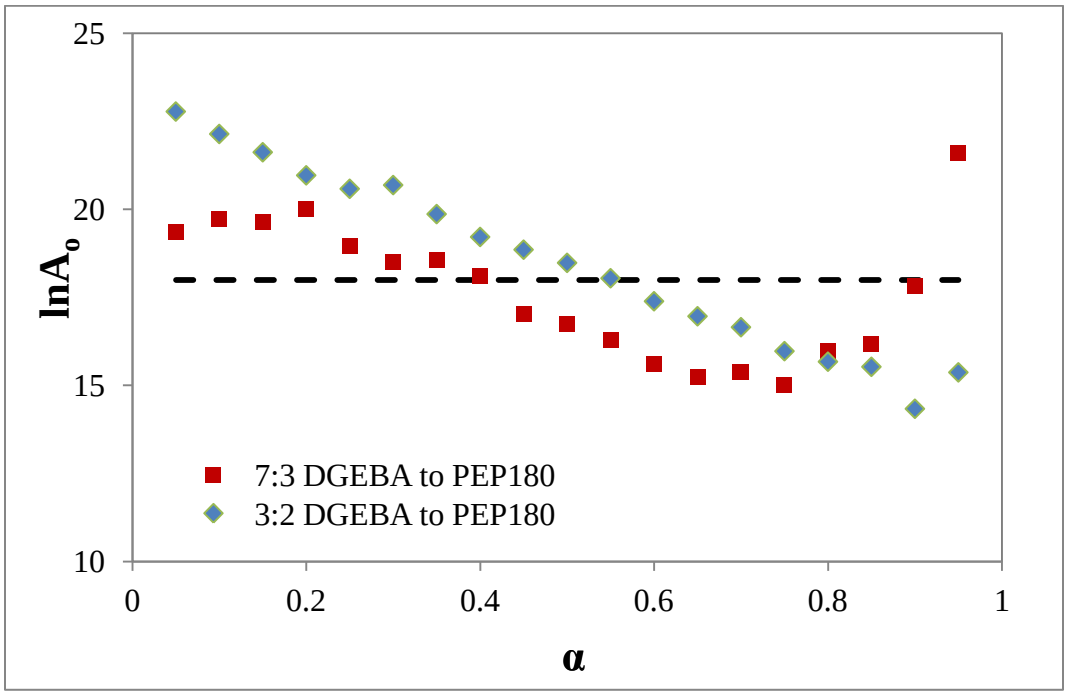

Figure 4-6. Dependency of $\ln A_o$ on conversion for DGEBA and PEP180 reaction

The dependency of activation energy for curing DGEBA with PEP220 at 1:1 and 3:2 mass ratios showed similar trends to those observed with PEP180, but with smaller decrease at higher conversions (Figure 4-7). As DGEBA concentration was increased, a significant decrease in activation energy was observed at higher conversions. Results for 7:3 epoxy to protein hydrolysate ratio were comparable to results obtained by Sbirrazzuoli et al. when stoichiometric quantities of primary amines were used instead of excess quantities of amines for curing of epoxy [18]. They reported a drop in activation energy to 20 kJ/mol, which is too small for reaction activation energy but corresponds to a vitrification process in which the rate-determining step switches from chemical to diffusion controlled as small epoxy molecules have to diffuse through an increasingly cross-linked network to find reactive sites [13]. Our results do not correspond to such a low activation energy even at 0.95 conversion, but the significant drop in activation energy may be attributed to fewer reactive groups available for the curing of DGEBA. The average values for activation energy were 69.4 ± 3.4, 68.7 ± 1.6, and 61.3 ± 6.3 kJ/mol for 1:1, 3:2, and 7:3 DGEBA to PEP220 mass ratios, respectively. These results are comparable to the average activation energy obtained at α_p for the three mass ratios in Table 4-3 (67.4 kJ/mol).

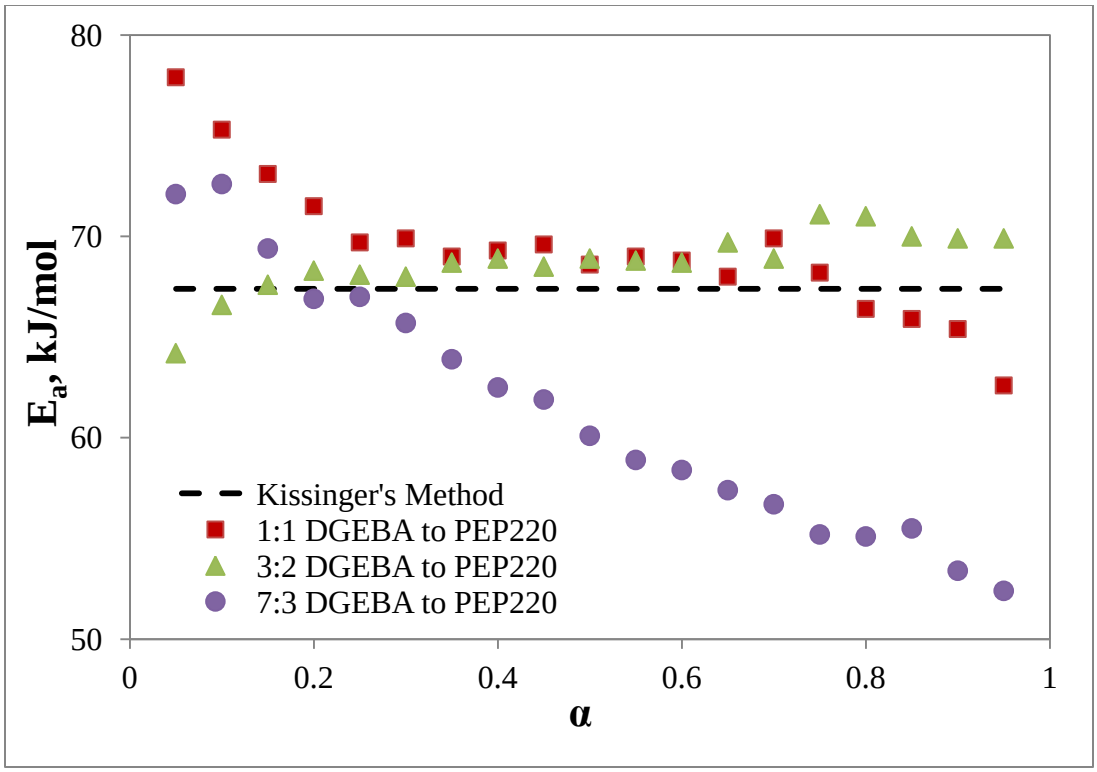

Figure 4-7. Dependency of activation energy on conversion for DGEBA and PEP220 reaction

The frequency factor for the three sets of reactions had similar dependency on conversion as did the activation energy. The average values for ln Ao were 17.262 ± 1.5, 17.184 ± 0.26, and 14.972 ± 2.3 for 1:1, 3:2, and 7:3 DGEBA to PEP220 mass ratios, respectively. These results are comparable to the values obtained at αp for the three mass ratios in Table 4-3 (16.821). For 1:1 and 3:2 DGEBA to PEP220 mass ratios, the frequency factor was nearly constant for the range $0.2 < \alpha < 0.8$, whereas a significant decrease was observed when small amounts of PEP220 were used for curing DGEBA (Figure 4-8).

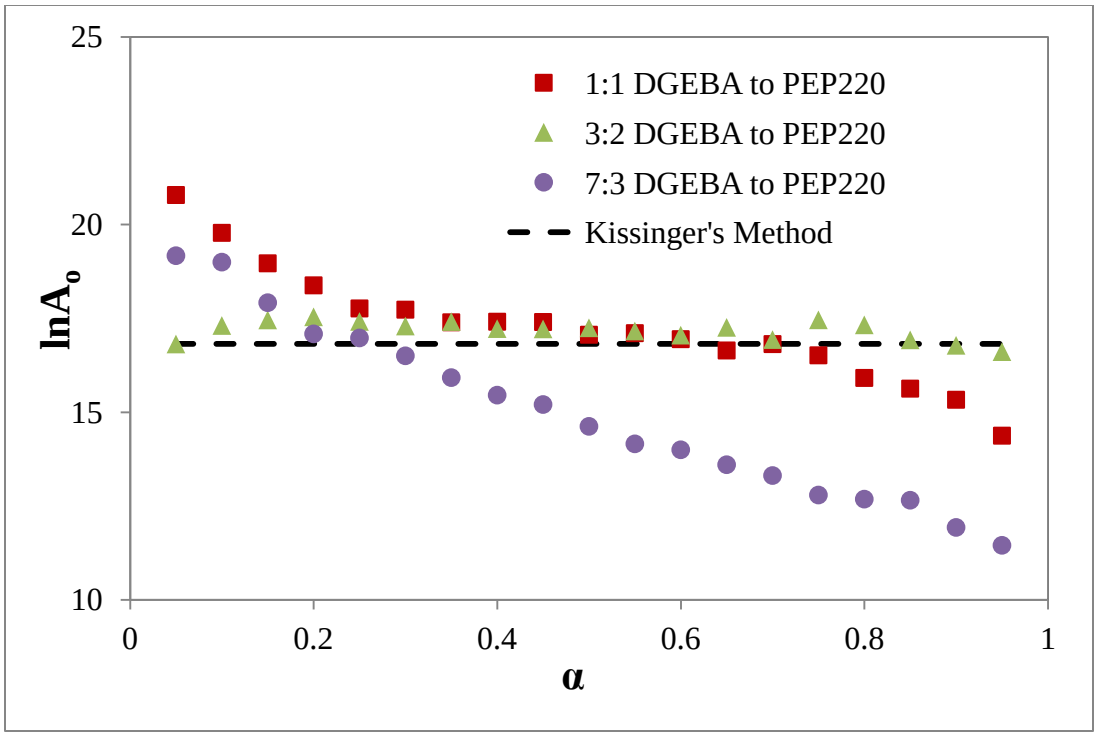

Figure 4-8. Dependency of lnA_o on conversion for DGEBA and PEP220 reaction

All plots for conversion against time for any heating rate exhibited the autocatalytic model. An example is shown in Figure 4-9. The Sestak−Berggren model, $f(\alpha) = \alpha^m(1 - \alpha)^n[1 - \ln(1 - \alpha)]^p$, can adequately model autocatalytic reactions [9, 10, 13] The truncated form, for p = 0, can be simplified further by adding a constraint. Since reactions rarely have an order exceeding 2, m + n = 2, and a plot of $\ln[(\beta_i d\alpha/dT)/\alpha^{2-n}(1 - \alpha)^n]$ vs $1/T$ yields a straight line from which activation energy and lnA_o are calculated from the slope and y-intercept, respectively, and n is selected such that the correlation coefficient is at its maximum value [10] An example is shown in Figure 4-10.

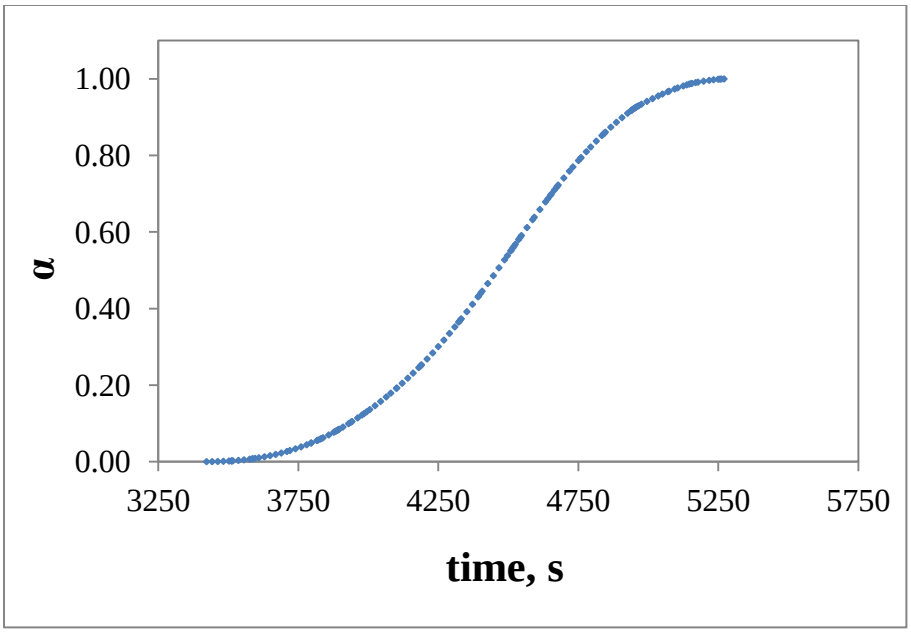

Figure 4-9. Conversion rate as a function of time for 3:2 DGEBA to PEP180 at 2 ºC/min

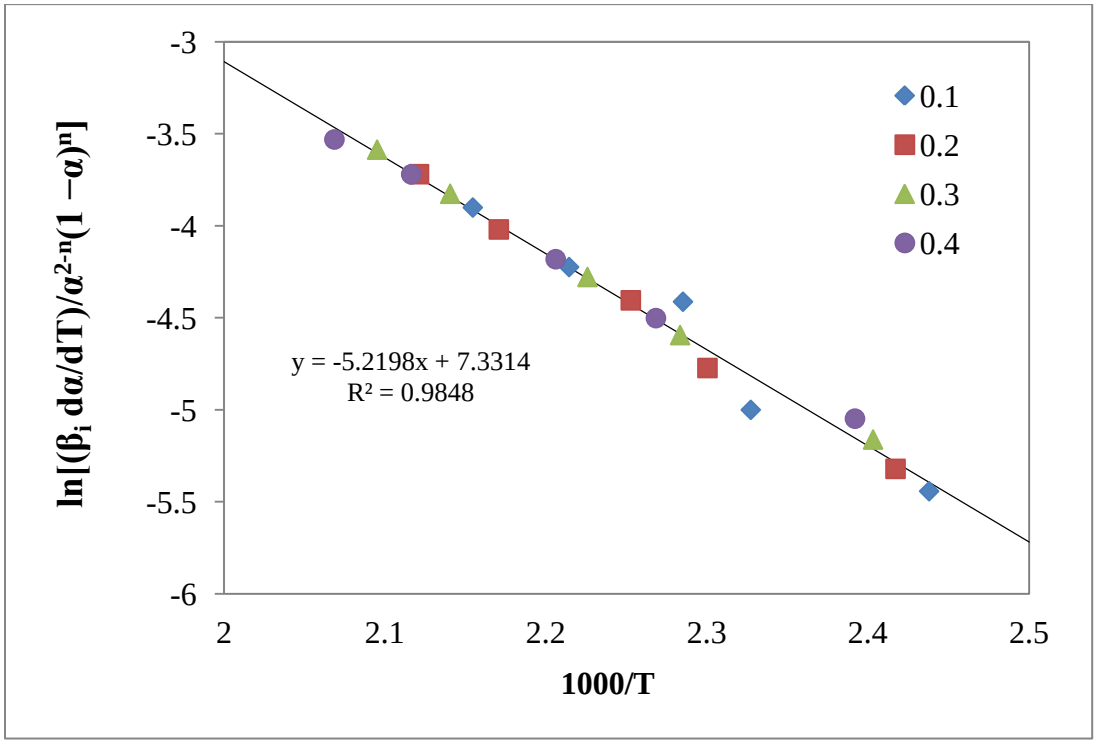

Figure 4-10. Plot for modified autocatalytic model at different conversions for reaction at 7:3 DGEBA to PEP220 mass ratio

The reaction order, n, is selected for each set of reactants such that the correlation coefficient, r, is maximized. The y-intercept is $\ln A_o$ and the slope is E_a/R. The reaction order was found to be insensitive of mass ratio of reactants but decreased when DGEBA was cured with molecules of smaller size. Values for $\ln A_o$ as determined by the autocatalytic model were closer to corresponding values calculated by the isoconversional method at $\alpha = 0.95$ than values calculated at α_p, with the exception of the second set in Table 4-5. This may be attributed to experimental error at 0.95 conversions. The value of $\ln A_o$ at 0.85 conversion was 16.184. Nonetheless, it may be suggested that $\ln A_o$ as $\alpha \rightarrow 1.0$ is more suitable than the average value to analyze and model reaction mechanisms. Activation energy values were nearly the same as obtained from the Kissinger method at α_p with the exception of the reaction in which small amounts of PEP220 were used for DGEBA curing. However, the model generated fits experimental results as shown in Figures 4-11 and 4-12. The model was found to be suitable for conversions up to 0.7.

Table 4-5. Summary of results for Frequency Factor, Activation Energy, and Reaction Order Calculated from the Autocatalytic Model for DGEBA cured with Salt-free Protein Hydrolysates.

DGEBA	$\ln A_o$	E_a, kJ mol^{-1}	n	r	$\ln A_o$ at 0.95
3:2 PEP180	14.231	73.6	1.54	0.993	15.370
7:3 PEP180	14.071	72.6	1.50	0.989	21.584
1:1 PEP220	14.590	63.0	1.37	0.98	14.376
3:2 PEP220	13.393	65.0	1.31	0.986	16.614
7:3 PEP220	7.331	43.4	1.28	0.992	11.454

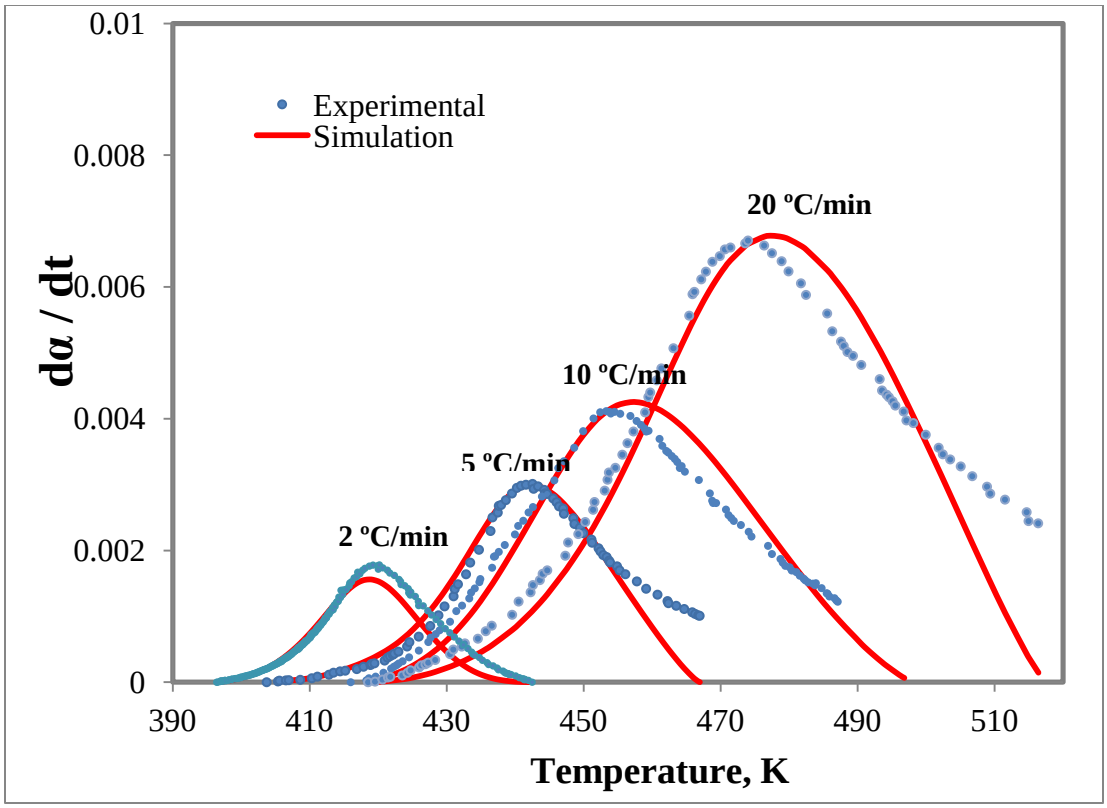

Figure 4-11. Plot for reaction rate, dα/dt, as a function of temperature for experimental results and model for reaction of 7:3 DGEBA to PEP220 mass ratio at different heating rates

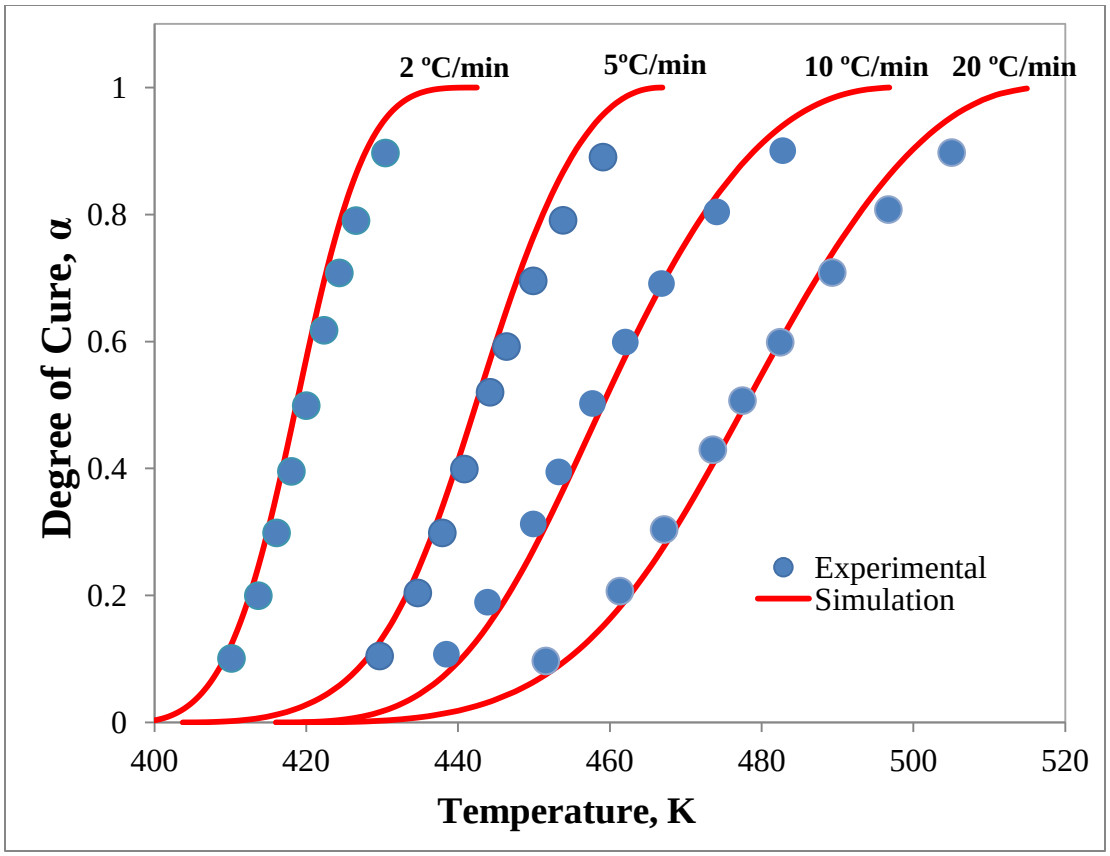

Figure 4-12. Plot for conversion, α, as a function of temperature for experimental results and model for reaction of 7:3 DGEBA to PEP220 mass ratio at different heating rates

Analysis for DGEBA curing with salt-solution-extracted protein hydrolysates confirmed our hypothesis that salts had a negative impact but also showed that analysis is not as straightforward as salt-free systems. As Figure 4-13 shows, activation energy values at varying conversions were significantly lower than values obtained by the Kissinger method at α_p. The average values for activation energy were 71.6 ± 4.3, 53.2 ± 6.4, and 52.9 ± 6.4 kJ/mol for 1:1, 3:2, and 7:3 DGEBA to PEP220SA mass ratios, respectively.

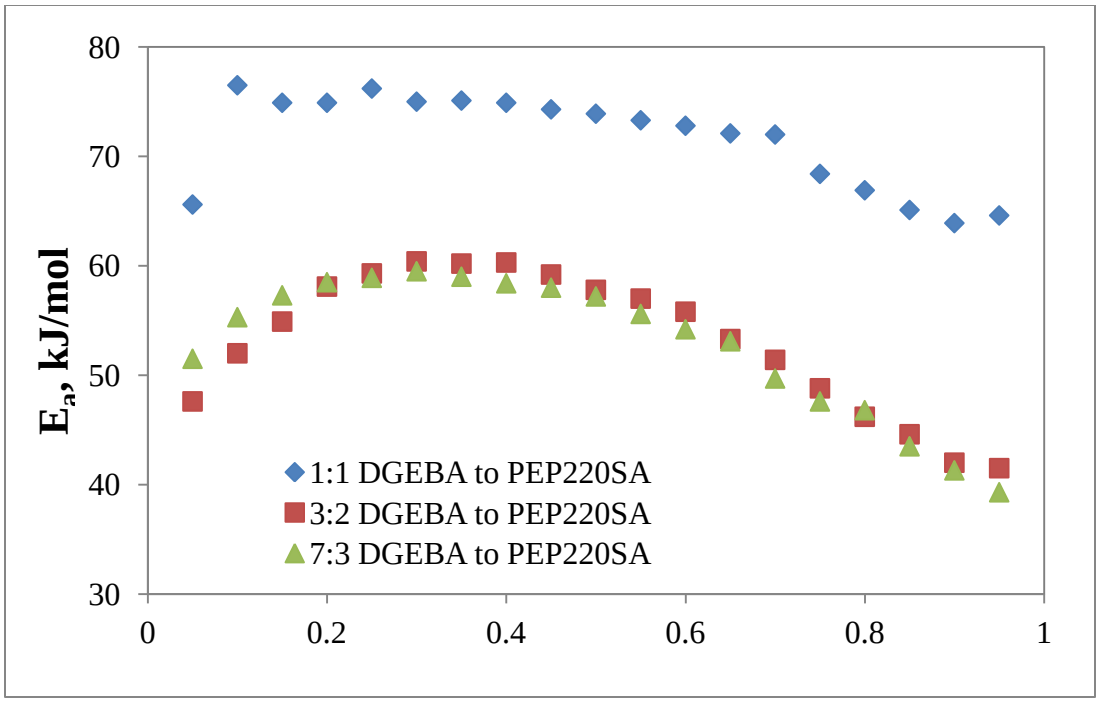

Figure 4-13. Dependency of activation energy on conversion for DGEBA and PEP220SA reaction

As Table 4-6 shows, the reaction order was determined to be higher in the presence of salts. This makes curing peaks wider, hence the reactions take longer to complete. Values for activation energy obtained by the autocatalytic model were higher than the average values from the isoconversional method, yet significantly lower than values calculated at α_p. As a fraction of activation energy from the Kissinger method, they were determined to be 0.86, 0.82, and 0.86 for 1:1, 3:2, and 7:3 DGEBA to PEP220SA mass ratios, respectively; i.e. 15% increase in activation due to the presence of salts. This negative impact offsets any gain obtained from improved miscibility for DGEBA and hydrolyzed proteins. The frequency factor, activation energy, and reaction order decreased as the fraction of DGEBA was increased. Results for PEP180SA were less reliable

as activation energy values and frequency factors changed in opposite trends to what was observed for all other systems, and were markedly different from values obtained by the Kissinger method at α_p.

Table 4-6. Summary of results for Frequency Factor, Activation Energy, and Reaction Order Calculated from the Autocatalytic Model for DGEBA cured with Salt-solution Extracted Protein Hydrolysates.

DGEBA	$\ln A_o$	E_a, kJ mol^{-1}	N	r
1:1 PEP180SA	10.326	56.2	1.65	0.986
3:2 PEP180SA	12.158	62.0	1.52	0.974
1:1 PEP220SA	15.823	77.0	1.66	0.987
3:2 PEP220SA	12.748	65.8	1.58	0.988
7:3 PEP220SA	12.319	64.1	1.55	0.974

Activation energy values calculated from three different methods for reactions involving salt-free curing groups were in reasonable agreement. The same cannot be said with respect to hydrolyzed materials extracted with salt solutions. Parameters obtained from the autocatalytic model were the most suitable to provide a model in reasonable agreement with experimental results (Figures 4-14, 4-15, 4-16, and 4-17). The model is suitable only up to the peak reaction rate and deviates significantly for the latter stages of the reaction. The tail at the end of DSC peaks shift the degree of cure at the peak temperature, α_p, from 0.5 and it was observed that heating rate had a significant effect: at higher heating rates, α_p decreased to as low as 0.3, thereby affecting the apparent activation energy obtained by the Kissinger method when peak temperatures were used.

Generally, we found modeling with salt-free protein hydrolysates to be closer to experimental results.

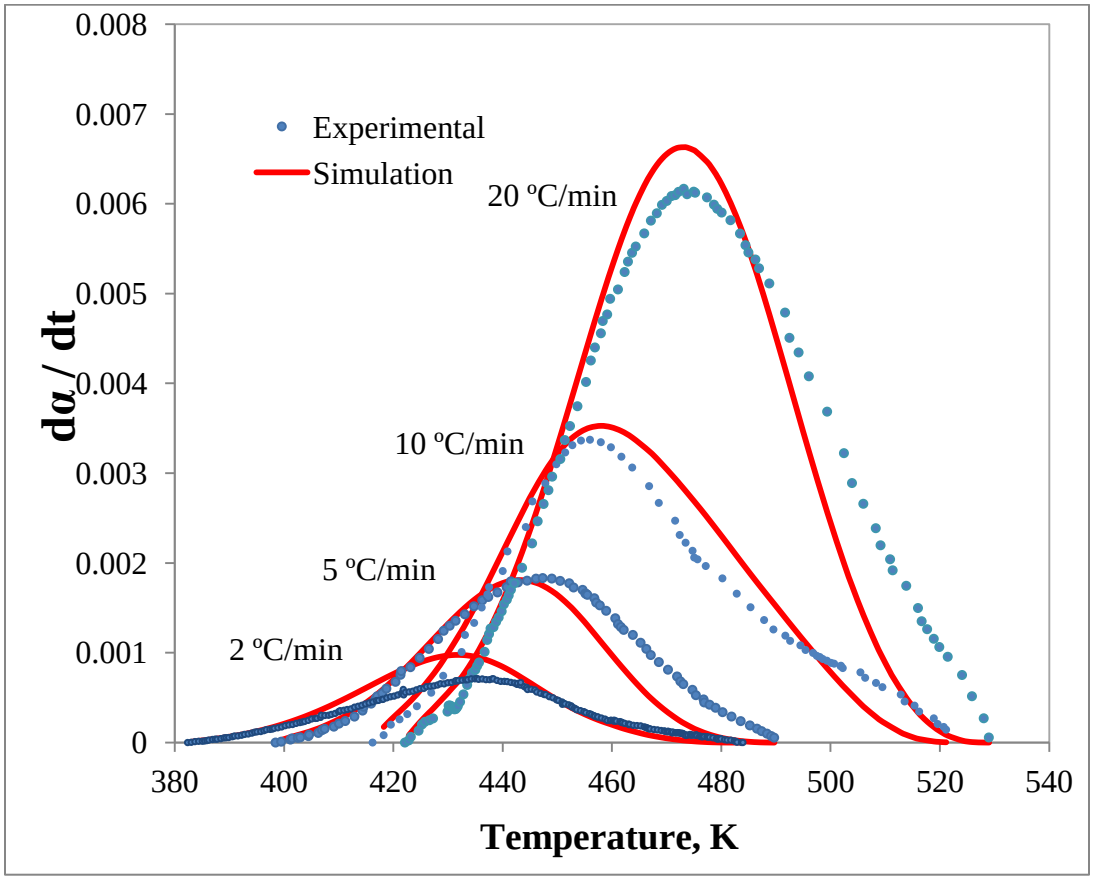

Figure 4-14. Plot for reaction rate, dα/dt, as a function of temperature for experimental results and model for reaction of 1:1 DGEBA to PEP220SA mass ratio at different heating rates

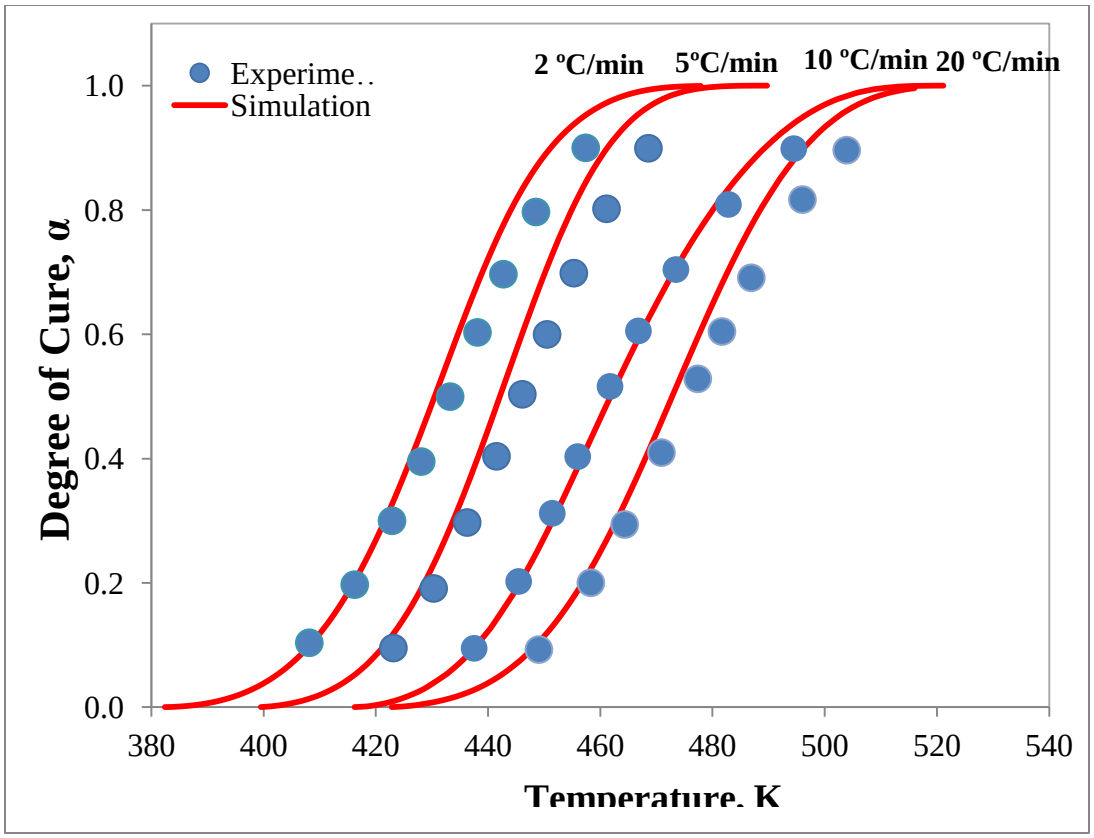

Figure 4-15. Plot for conversion, α, as a function of temperature for experimental results and model for reaction of 1:1 DGEBA to PEP220SA mass ratio at different heating rates

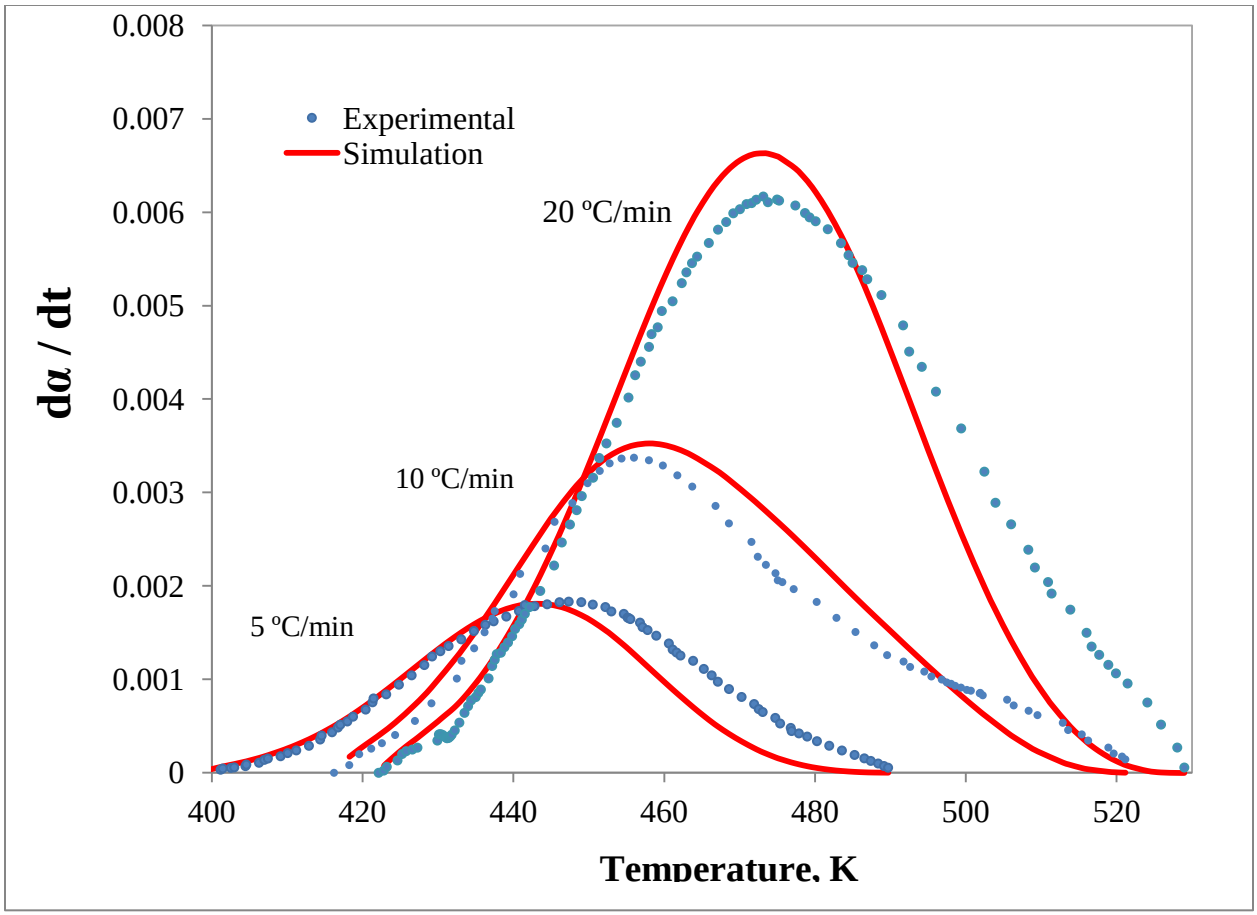

Figure 4-16. Plot for reaction rate, dα/dt, as a function of temperature for experimental results and model for reaction of 7:3 DGEBA to PEP220SA mass ratio at different heating rates

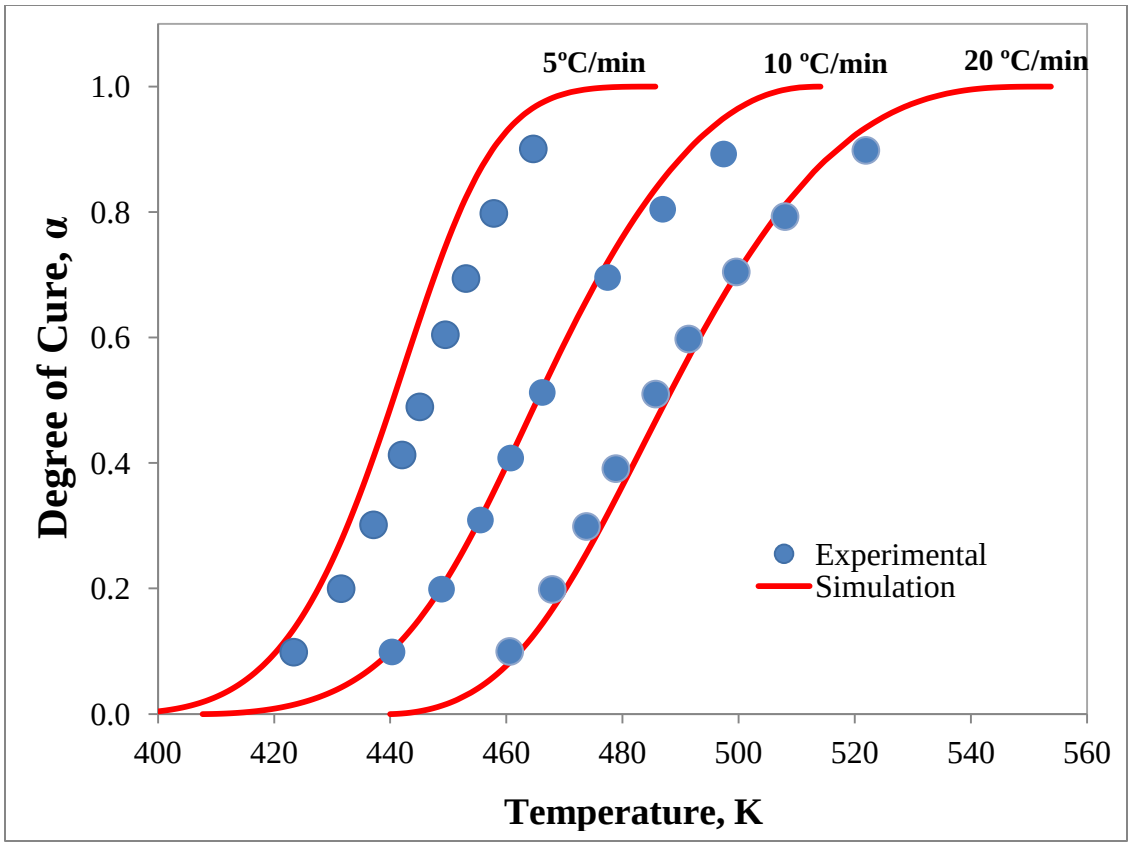

Figure 4-17. Plot for conversion, α, as a function of temperature for experimental results and model for reaction of 7:3 DGEBA to PEP220SA mass ratio at different heating rates

We attempted to obtain parameters for $f(\alpha)$ by using conversions at the latter stages of reactions. As an example shown in Figure 4-18, plots $\ln[(\beta_i d\alpha/dT)/\alpha^{2-n}(1-\alpha)^n]$ vs $1/T$ at high conversions did not produce straight lines.

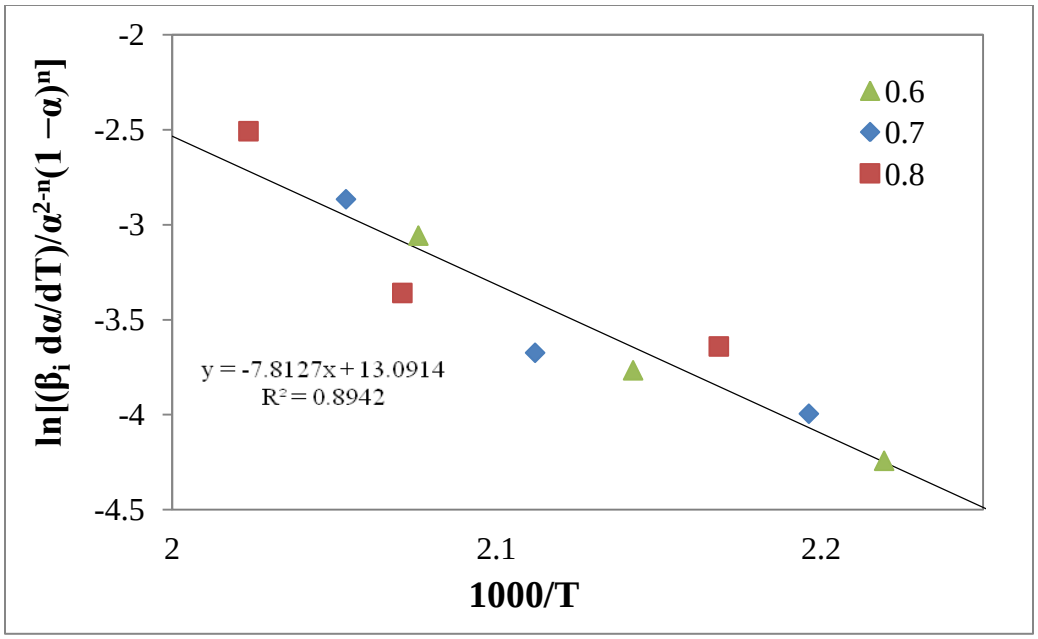

Figure 4-18. Plot for modified autocatalytic model at different conversions for reaction at 1:1 DGEBA to PEP220SA mass ratio at conversions above 0.5

Activation energy was 65 kJ/mol (compared to 77 kJ/mol), $\ln A_o$ was 13.1 (compared to 15.8), and reaction order increased to 1.71 (from 1.66) for 1:1 DGEBA to PEP220SA for maximum correlation coefficient; the correlation was nonetheless poor compared to results obtained at low degrees of cure. The modified model only provided slightly better agreement with experimental data at conversions near peak reaction rates (Figure 4-19) but was not suitable for modeling reaction rates at low conversions. As conversion increased further, the modified model approached the model obtained earlier.

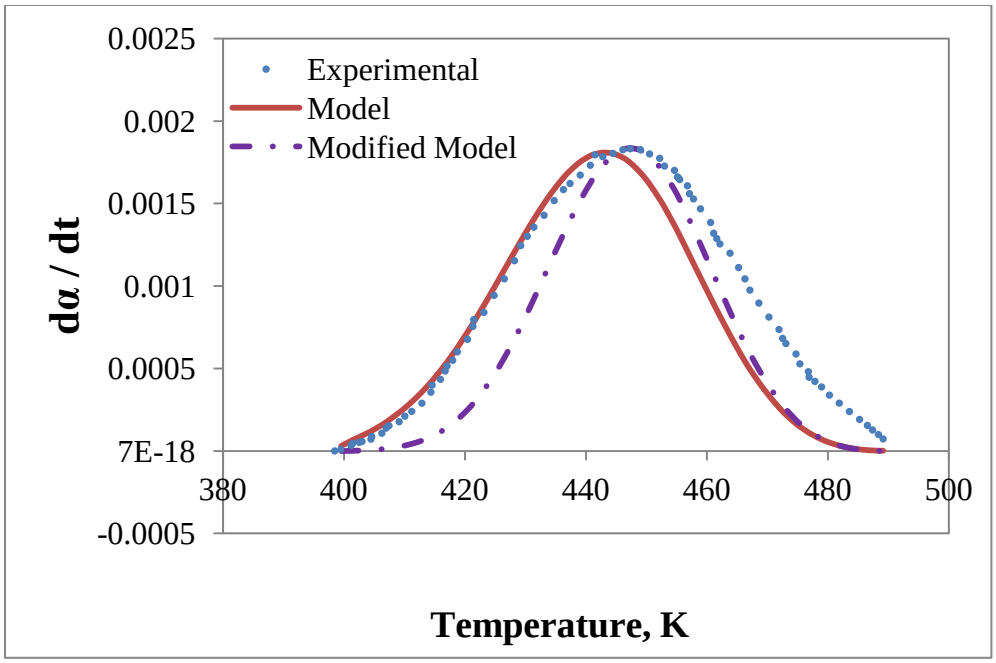

Figure 4-19. Plot for reaction rate, dα/dt, as a function of temperature for experimental results and model for reaction of 3:2 DGEBA to PEP220SA mass ratio at different heating rates

Heats of reaction showed dependence on heating rate with tendency to be the smallest for 2 and 5 °C/min heating rates. Faster heating rates consistently led to larger heats of reaction. Figure 4-20 shows measurements obtained for DGEBA curing with two sets of salt-extracted protein hydrolysates. Mass ratio was 1:1. Heats of reaction were also larger when for protein hydrolysates of larger molecular size, 213 ± 27 J/g for PEP180SA and 160 ± 27 J/g for PEP220SA. On DGEBA molar basis in samples, these values are 72.4 ± 9.2 kJ/mol (PEP180SA) and 54.4 ± 9.2 kJ/mol (PEP220SA) expressed in terms of oxirane mole equivalent. These values were similar to measurements for other reactions investigated in this work and are summarized in Table 4-7.

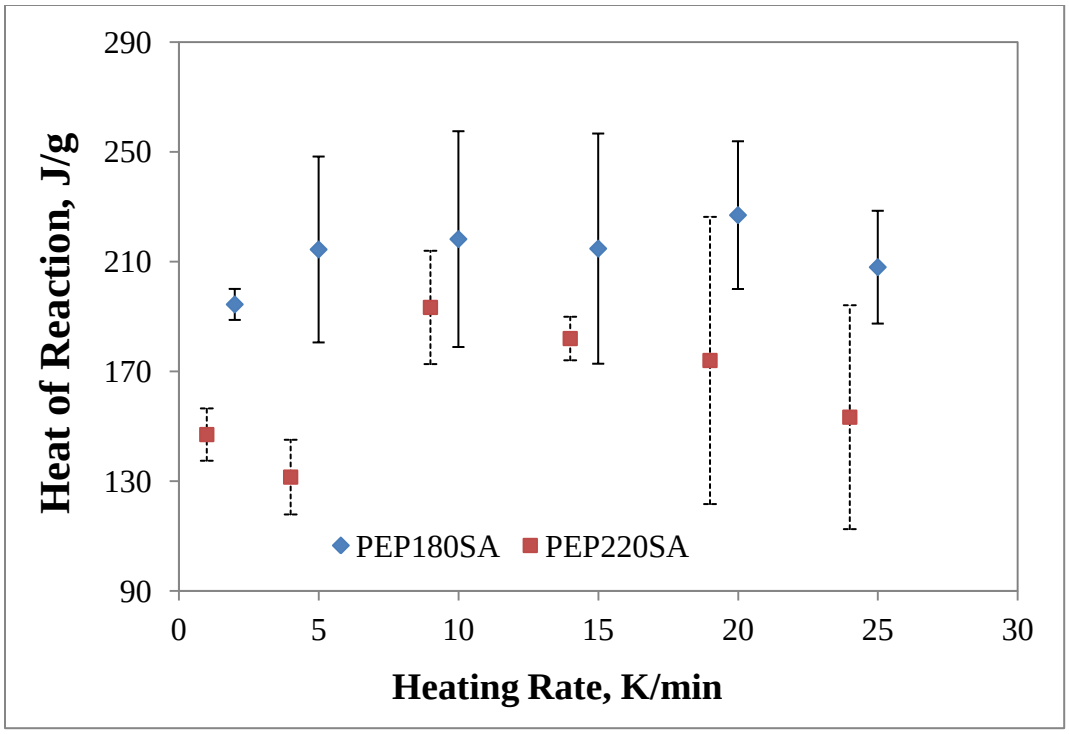

Figure 4-20. Heats of Reaction dependency on heating rate for DGEBA curing with PEP180SA and PEP220SA (1:1 mass ratio). Values for PEP220SA reactions were shifted for clarity

Table 4-7. Heats of Reaction with DGEBA expressed in terms of 1 mol of Oxirane.

	ΔH, kJ/mol	ΔH, kJ/mol	ΔH, kJ/mol
Mass Ratio	1:1	3:2	7:3
PEP180SA	72.4 ± 9.2	37.7 ± 6.1	32.5 ± 9.3
PEP180	No mixing	48.3 ± 11.6	39.8 ± 10.4
PEP220SA	54.4 ± 9.2	46.2 ± 17.4	36.4 ± 12.1
PEP220	56.8 ± 11.9	55.0 ± 9.9	32.5 ± 11.1

Typical heats of reaction for 1 mol of epoxy rings with primary and secondary amines are 83 and 131 kJ/mol, respectively, and 65 kJ/mol with hydroxyl groups [19]. Heats of reaction measured here were lower than expected

values for secondary amines, likely due to abundant presence of primary amines and hydroxyl groups as well as carboxylic and sulfhydryl, lowering the apparent heat of reaction. The curing of DGEBA with proteinacious materials is a complex reaction due to the presence of at least five different curing groups, as well as the hydroxyl group from the epoxy resin that is formed when the oxirane receives a proton from curing groups. Heats of reaction need to be measured more accurately at optimal heating rates or isothermal conditions with carefully varied masses. It is also clear that increasing the mass fraction of the epoxy resin resulted in a decrease in the heat of reaction. In agreement with observations from dependency of activation rate on the degree of curing for different mass concentrations, heats of reaction here also indicate that 1:1 mass ratio provided enough reactive groups for the curing of DGEBA. On the other hand, at 7:3 DGEBA to protein hydrolysates mass ratio did not provide enough curing groups, as evidenced from lower heats of reaction and decreasing activation energy at high conversions (Figures 4-7 and 4-13).

Araldite 506, the DGEBA epoxy used in this study, has a viscosity exceeding 500 cP. In order to elucidate the effect of viscosity, we selected a low viscosity epoxy resin for comparison. Polypropylene glycol diglycidyl ether, PPGDE, has a viscosity of ~50 cP. Both epoxy resins have similar molecular weight (340 g mol^{-1} for DGEBA and 380 g mol^{-1} for PPGDE) and chemical structure. The main difference is the presence of benzyl groups in DGEBA whereas linear alkanes make up the backbone of PPGDE. As it is not a good

solvent for protein hydrolysates, PPGDE to protein hydrolysate mass ratio of 3:2 was used, as the 1:1 mixture did not mix well enough to carry out curing experiments. As was the case with DGEBA, activation energy was higher for reactions with salt solution-extracted protein hydrolysates (approximately 10 kJ/mol at all conversions). As Figure 4-21 shows, activation energy decreased as the extent of curing increased for both reactions. The average activation energy obtained from the isoconversional method was 60.9 ± 6.8 kJ/mol for curing PPGDE with PEP180SA and 49.9 ± 7.0 kJ/mol for PPGDE curing with PEP180.

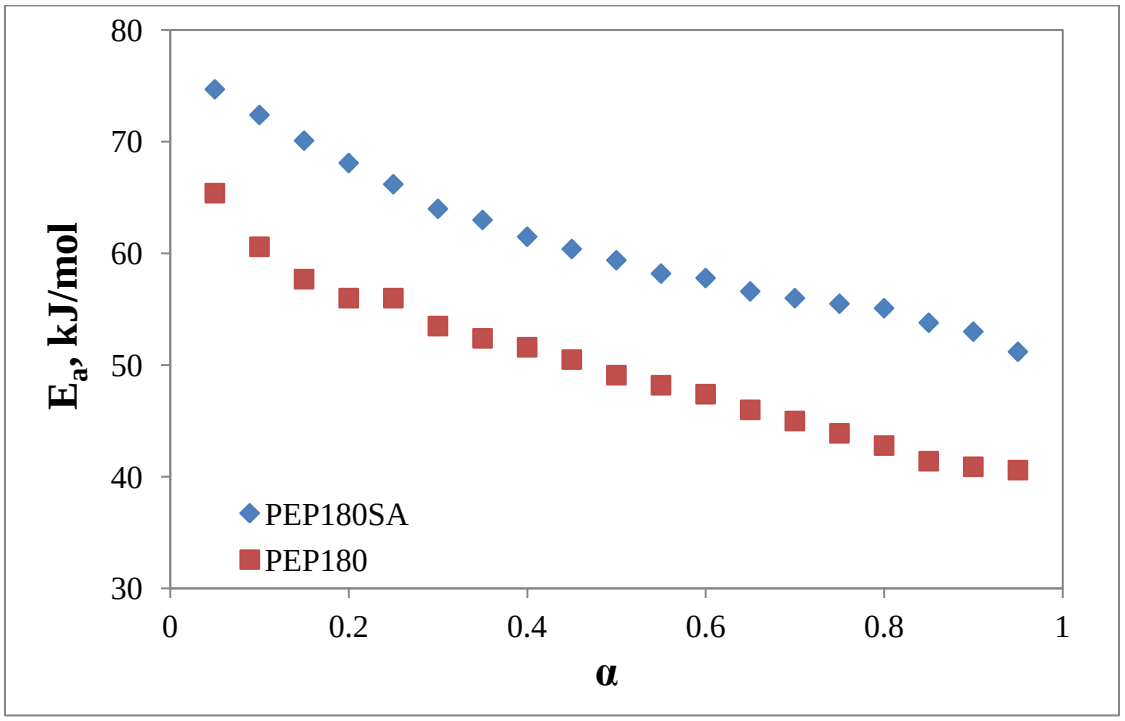

Figure 4-21. Dependency of activation energy on conversion for PPGDE curing with two sets of protein hydrolysates at 3:2 mass ratio

The dependency of the frequency factor on conversion followed the same trend (Figure 4-22) as did the activation energy. The average values for $\ln A_o$ were

11.235 ± 2.2 for PEP180 and 15.068 ± 2.5 for PEP180SA. At 0.95 conversion, $\ln A_o$ was 9.432 for PEP180 and 11.300 for PEP180SA. These values were higher than results obtained from the autocatalytic model (see Figure 4-23).

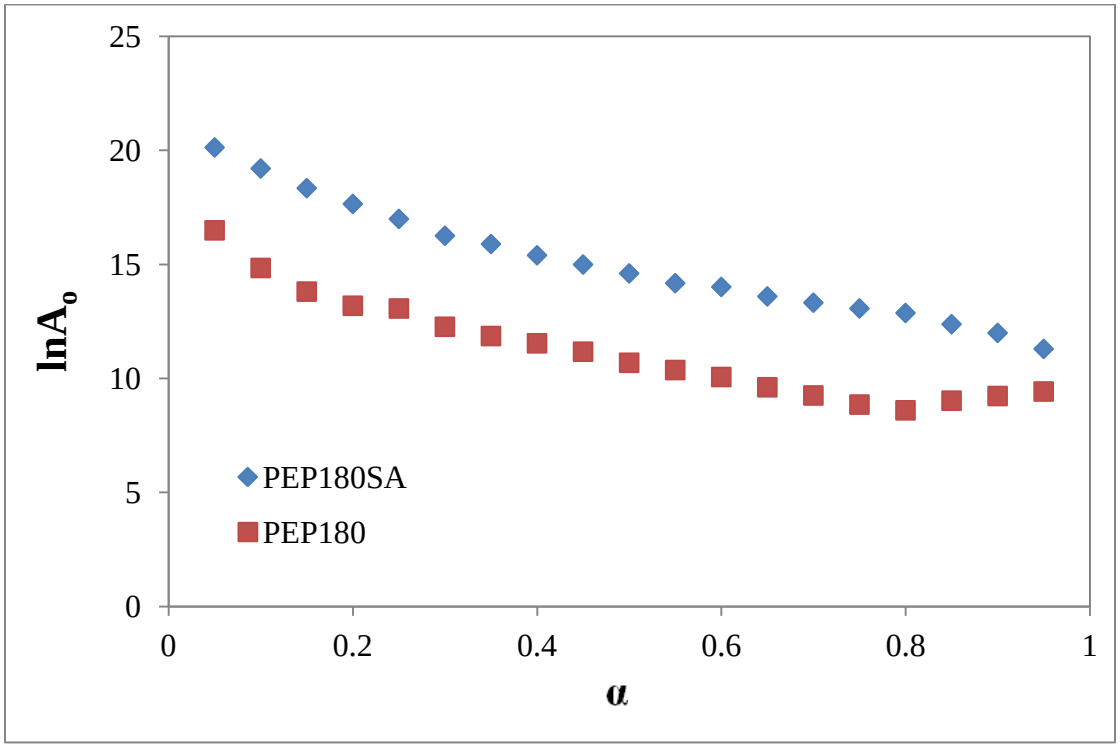

Figure 4-22. Dependency of the frequency factor on conversion for PPGDE curing with two sets of protein hydrolysates at 3:2 mass ratio

The autocatalytic model was also a suitable fit for experimental results and was used to obtain the reaction order, effective activation energy, and the frequency factor (Figure 4-24).

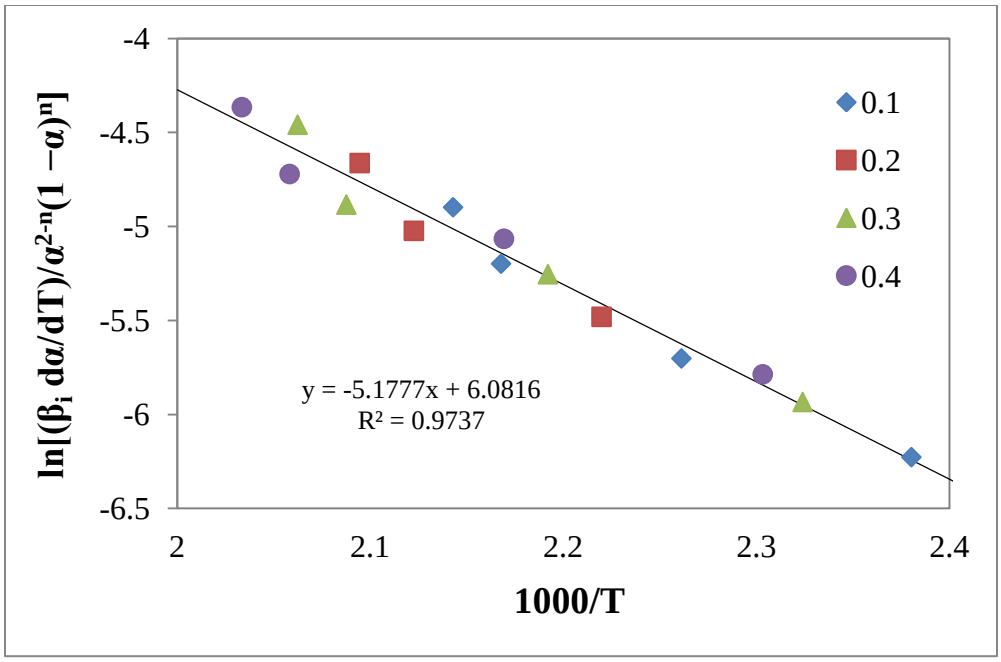

Figure 4-23. Plot for modified autocatalytic model at different conversions for reaction at 3:2 PPGDE to PEP180 mass ratio

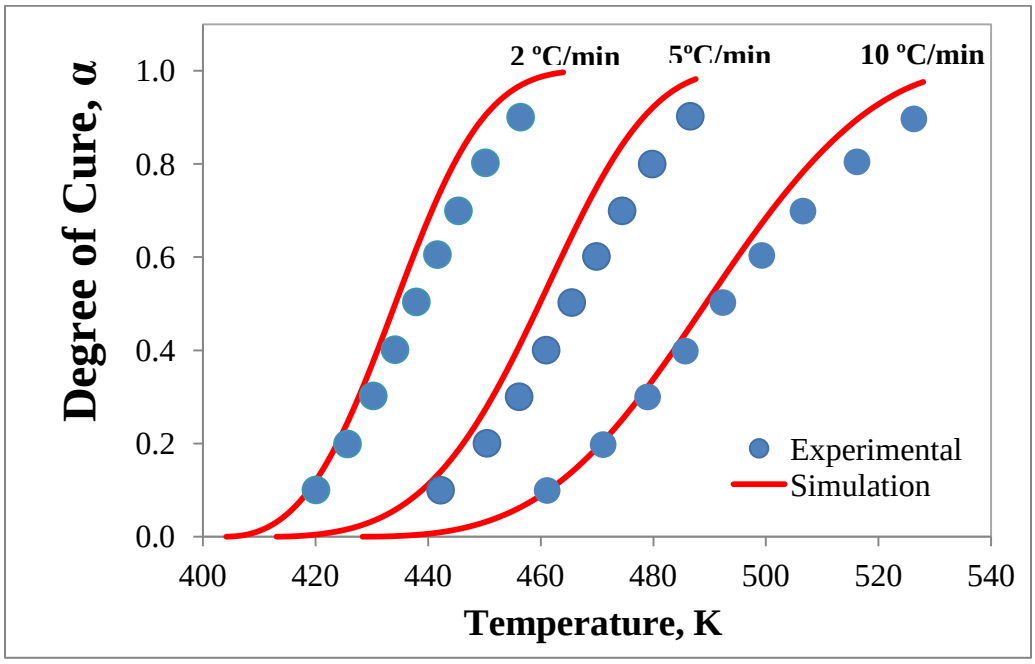

Figure 4-24. Plot for conversion, α, as a function of temperature for experimental results and model for reaction of 3:2 PPGDE to PEP180 mass ratio at different heating rates

As Table 4-8 shows, activation energy for PPGDE curing with hydrolyzed protein was significantly lower than for curing DGEBA. PPGDE can also be used for the cross-linking of biowaste materials, such as hydrolyzed SRM in this study.

Table 4-8. Summary of results for Frequency Factor, Activation Energy, and Reaction Order Calculated from the Autocatalytic Model for PPGDE Reactions.

PPGDE	$\ln A_o$	E_a, kJ mol^{-1}	n	r	ΔH, kJ/mol
3:2 PEP180	6.082	43.0	1.45	0.987	43.1 ± 5.1
3:2 PEP180SA	8.646	48.3	1.43	0.962	38.3 ± 15

Lacking aromatic rings, PPGDE can provide cross-linking and flexibility as well as lower activation energy. It can be co-utilized with a high-viscosity, cross-linking reagent or other chemicals with lower reactivity such as diamides and dialdehydes for value recovery from waste biomass.

4.4 CONCLUSION

We used DSC to study the cure kinetics of DGEBA epoxy resin with four sets of biowaste protein hydrolysate materials. Activation energy was decreased by ~10% for cross-linking with smaller protein hydrolysates obtained at higher hydrolysis temperature. The autocatalytic model was used to obtain reaction parameters to fit experimental data. The presence of salts was found to have increased activation energy and the frequency factor of the reaction. As the fraction of protein hydrolysates relative to epoxy was increased, the effect of salt on activation energy was larger. The curing of DGEBA with salt-free protein

hydrolysates had a lower activation energy, which did not change when more protein hydrolysates were reacted with DGEBA. Activation energy measured by the Kissinger method, the isoconversional method, and the autocatalytic model gave approximately the same results for curing two epoxy resins, DGEBA and PPGDE, with salt-free protein hydrolysates. Measurements for curing with salt solution- extracted protein hydrolysates led to an increase by 15% in activation energy obtained from the best-fit autocatalytic model compared to the average value from the isoconversional method. Despite the fact salts enhanced miscibility between protein hydrolysates and epoxy resins, the increase of additional bonds (salt−protein hydrolysate) which needed to be broken up, as measured by activation energy, offset the miscibility advantage of salts. The increase of DGEBA mass fraction to salt-containing protein hydrolysates enhanced miscibility and reduced viscosity, but activation energy was consistently higher in comparison to salt-free systems. The curing of a low-viscosity epoxy resin (PPGDE) had significantly lower activation energy. The effect of reduced viscosity on activation energy was more significant than the molecular size of the curing agent. This work demonstrates that DSC can be used in order to gain valuable insight into reaction kinetics of various complex systems by only using 50 mg for each sample set. DSC technique is inexpensive and efficient for investigating reaction kinetics of compounds which are expensive to purchase or laborious to synthesize in large quantities.

4.5 REFERENCES

(1) Canadian Food Inspection Agency. *Enhanced Animal Health Protection from BSE*. **2010**, Canada. [Online] Available at: http://www.inspection.gc.ca/animals/terrestrial-animals/diseases/enhanced-feed-ban/eng/1299870250278/1334278201780 [Accessed 26 November 2012].

(2) Fedorowicz, E. M.; Miller, S. F.; Miller, B. G. Biomass Gasification as a Means of Carcass and Specified Risk Materials Disposal and Energy Production in the Beef Rendering and Meat Packing Industries. *Energy Fuels.* **2007**, *21*, 3225-3232.

(3) Mekonnen, T.; Mussone, P.; Stashko, N.; Choi, P.; Bressler, D. Recovery and Characterization of Proteinacious Material Recovered from Thermal and Alkaline Hydrolyzed Specified Risk Materials. *Process Biochem*. **2013**, *48*, 885-892.

(4) El-Thaher, N.; Mekonnen, T.; Mussone, P.; Bressler, D.; Choi, P. Effects of Electrolytes, Water, and Temperature on Cross-linking of Glutaraldehyde and Hydrolyzed Specified Risk Material. *Ind. Eng. Chem. Res*. **2013**, *52*, 4987-4993.

(5) Mekonnen, T.; Mussone, P.; El-Thaher, N.; Choi, P.; Bressler, D. Thermosetting Proteinacious Bioplastics from Hydrolyzed Specific Risk Material. *Macromol. Mater. Eng*. **2013,** DOI: 10.1002/mame.201200429

(6) Grenier-Loustalot, M. F.; Grenier, P.; Horny, P.; Chenard, J. Y. Reaction Mechanism, Kinetics and Network structure of the DGEBA-DDS System. *Brit. Polym. J*. **1988**, *20*, 463-476.

(7) Stevens, G. C. Cure Kinetics of a Low Epoxide/Hydroxyl Group-Ratio Bisphenol A Epoxy Resin-Anhydride System by Infrared Absorption Spectroscopy. *J. Appl. Polym. Sci.* **1981,** *26*, 4259-4278.

(8) Hartman, M. E.; Hockswender, T. R. Process of Making Epoxy Resins Modified with Mercaptocarboxylates. US Patent 4153586. Ppg Industries, Inc. **1979.**

(9) Roşu, D.; Caşcaval, C. N.; Mustaţă, F.; Ciobanu, C. Cure Kinetics of Epoxy Resins Studied by non-isothermal DSC Data. *Thermochim. Acta.* **2002,** *383*, 119-127.

(10) Hong, I.; Lee, S. Cure Kinetics and Modeling the Reaction of Silicone Rubber. *J. Ind. Eng. Chem.* **2013,** *19*, 42-47.

(11) Boey, F. Y. C.; Qiang, W. Experimental Modeling of the Cure Kinetics of an Epoxy-hexaanhydro-4-methylphthalicanhydride (MHHPA) System. *Polymer* **2000,** *41*, 2081-2094.

(12) Ozawa, T. A New Method of Analyzing Thermogravimetric Data. *Bull. Chem. Soc. Jpn.* **1965,** *38*,1881-1886.

(13) Vyazovkin, S.; Burnham, A. K.; Criado, J. M.; Perez-Maqueda, L. A.; Popescu, C.; Sbirrazzuoli, N. ICTAC Kinetics Committee Recommendations for

Performing Kinetic Computations on Thermal Analysis Data. *Thermochim. Acta.* **2011,** *520*, 1-19.

(14) Prime, R. B. Differential Scanning Calorimetry of the Epoxy Cure Reaction. *Polym. Eng. Sci.* **1973,** *13*, 365-371.

(15) Kissinger, H. E. Reaction Kinetics in Differential Thermal Analysis. *Anal. Chem.* **1957,** *29*, 1702-1706.

(16) Park, S. K.; Bae, D. H.; Hettiarachchy, N. S. Protein Concentrate and Adhesives from Meat and Bone Meal. *J. Am. Oil Chem. Soc.* **2000**, *77*, 1223-1227.

(17) Garcia, R. A.; Rosentrater, K. A.; Flores, R. A. Characteristics of North American Meat and Bone Meal Relevant to the Development of non-feed Applications. *Appl. Eng. Agric.* **2006**, *22*, 729-736.

(18) Sbirrazzuoli, N.; Vyazovkin, S.; Mititelu, A.; Sladic, C.; Vincent, L. A Study of Epoxy-Amine Cure Kinetics by Combining Isoconversional Analysis with Temperature Modulated DSC and Dynamic Rheometry. *Macromol. Chem. Phys*. **2003**, *204*, 1815-1821.

(19) Langmaier, F.; Mokrejs, P.; Kolomazník, K. ; Mládek, M. ; Karnas, R. Cross-linking Epoxide Resins with Hydrolysates of Chrome-tanned Leather Waste. *J. Therm. Anal. Calorim.* **2007,** *88*, 857-862.

CHAPTER 5[3]

5.0 DENATURANTS AND CATALYSIS

Cross-linking of proteins with epoxy resins has been studied for well over 20 years. Epoxy resins react by accepting a proton to the epoxy ring to form a hydroxyl group. Therefore, they can react with primary and secondary amines (converting them into secondary and tertiary amines, respectively), hydroxyl groups (converting them into ethers), and carboxylic groups (converting them into esters). Sulfhydryl groups similarly react with epoxy rings [1]. These five groups of reactants are abundantly found in proteins. Because no gas byproducts are released from the reaction, curing exhibits no pressure dependence.

As an alternative to glutaraldehyde, epoxy resins have been proposed in order to improve properties of the final product. Among the cited examples is better resistance to calcification in bioprosthetic materials [2, 3]. Collagen cross-linking with 1,4-butanediol diglycidyl ether was reported to reduce degradation by enzymatic activity of collagenase [4]. In a recently published study, we employed differential scanning calorimetry to investigate the curing kinetics of bisphenol A diglycidyl ether (DGEBA) with protein-rich biomass waste materials derived from beef rendering by-products via hydrolysis and extraction [1]. Hydrolysis of proteins is generally desirable for subsequent reactivity because

[3] A version of this chapter has been accepted for publication. El-Thaher et al. *ACS Sustainable Chemistry and Engineering*. October 2, **2013**.

enzymes are destroyed, thereby avoiding undesirable enzymatic activity in proteins, and the native structure (α-helices and β-sheets) is converted into a denatured state (random coils) [5]. Reactive sites are more accessible in denatured proteins than in proteins in their native structure [6]. Hydrolysis is also an important pretreatment to render hazardous protein sources safe to handle prior to value recovery in subsequent modifications. For example, beef byproducts that may contain prions, the causative agent of mad cow disease, must be hydrolyzed in order to inactivate the prions [7]. On the other hand, an increased degree of hydrolysis (at increased temperatures) consumes more energy and produces smaller molecules of hydrolyzed proteins. Reduced molecular size can be detrimental for applications such as adhesion [6], coagulation [8], and flocculation [9], for which larger molecules are more desirable, albeit in their extended state. Even when hydrolysis is sufficient to completely break down α-helices and β-sheets and form random coils, proteins can still coil into structures of reduced surface area in solvents to avoid certain types of interactions, e.g. hydrophobic interactions in aqueous solutions. Therefore, the use of an adequate denaturant is still important to enhance cross-linking reactions involving hydrolyzed proteins.

The utilization of denaturants instead of increased hydrolysis temperatures can offset the impact of increased energy and the larger size of hydrolyzed protein molecules obtained at moderate levels of hydrolysis. The aim of this study was to investigate the effect of denaturing compounds, urea and sodium dodecyl sulfate (SDS), on the kinetics of curing DGEBA with hydrolyzed proteins and to

compare the results to the effect of triethylamine (TEA), a well-known epoxy ring opening catalyst. TEA was selected as a catalyst because it lacks functional groups known to be reactive with DGEBA. As a tertiary amine, it is only expected to accelerate the reaction by opening the epoxy ring of DGEBA in the initial stages of curing, which is why TEA is generally considered an initiator [10]. As TEA does not react, its concentration is expected to remain constant for the duration of curing. Additionally, TEA is not expected to compete with hydrolyzed protein molecules, an important factor for the correct analysis of results.

Urea and SDS are protein denaturants. As an example of their prior use in value-added applications based on protein-based materials, urea and SDS have been shown to improve adhesive strength and water resistance in wood adhesion applications by uncoiling protein molecules, thereby increasing wood-protein interactions [6]. SDS and urea are known to disrupt protein-protein interactions [11]. As intra- and inter-molecular protein interactions are reduced, more reactive sites may become available for cross-linking with DGEBA. Diffusion of DGEBA molecules can also be expected to increase in the presence of denaturants. This work demonstrated, in quantitative terms, an energy-saving approach to the chemical cross-linking of protein feedstock recovered from waste agricultural streams into value-added polymeric materials.

5.1 EPOXY CURING BY DIFFERENTIAL SCANNING CALORIMETRY

The DSC nonisothermal technique was used in this work to obtain the curing thermal data. When cross-linking is studied with a calorimetric instrument, released energy is recorded for the duration of the reaction. The reaction rate, $d\alpha/dt$, can be expressed as $k(T)f(\alpha)h(P)$, where $k(T)$ is the temperature-dependent rate constant, α is the extent of reaction, $f(\alpha)$ is a function of the extent of reaction, and $h(P)$ is the function of pressure dependence of the reaction and is often important for reactions involving gases as reactants and/or byproducts [12]. The term can be dropped for this study because no gases are involved in the reaction. The reaction rate can then be expressed as:

$$d\alpha/dt = A_o \exp(-E_a/RT) f(\alpha) \quad (5\text{-}1)$$

where E_a is the activation energy, A_o is the frequency factor, R is the universal gas constant, and T is the temperature. For constant heating rate scans in DSC, $d\alpha/dt$ can be expressed as $\beta_i \, d\alpha/dT$, where is β_i the heating rate. So a plot of $\ln[(\beta_i \, d\alpha/dT)/f(\alpha)]$ vs. $1/T$ for constant values of α and an adequate model for $f(\alpha)$ is expected to yield a straight line. The slope is $-E_a/R$ and the y-intercept is $\ln A_o$. The reaction model and its parameters are selected such that the correlation coefficient is maximized [12, 13]. Curing epoxy resins generally exhibits autocatalysis, which can be adequately modeled by using the Sestak-Berggren

model [1, 12-14]. The conversion function, $f(\alpha)$, has the form $\alpha^m(1-\alpha)^n[-\ln(1-\alpha)]^p$. The truncated form, for p = 0, can be simplified further by adding a constraint that because reactions rarely have an order exceeding 2, m + n = 2, and a plot of $\ln[(\beta_i\, d\alpha/dT)/\alpha^{2-n}(1-\alpha)^n]$ vs. $1/T$ yields a straight line [1, 13]. The overall order of reaction (m + n) for epoxy-amine reactions is 2 but for epoxy-hydroxyl reactions the sum is closer to 1.5 [15]. Vyazovkin and Sbirrazzuoli have noted that for unconstrained fits, the sum has been found to exceed 2.5 in some cases [16]. For cases where the constraint (m + n = 2) does not lead to a good fit, a multiple linear regression as described by Jubsilp et al. can be used to determine values for m and n [17].

The isoconversional method is another useful method to probe the progress of the reaction at different conversion rates and provide additional insight into the reaction as the degree of curing increases. Activation energy at different extents of reaction is obtained from the following relationship:

$$\ln(\beta_i/T_{\alpha,i}^2) = \text{Constant} - E_\alpha/RT_\alpha \qquad (5\text{-}2)$$

where $T_{\alpha,i}$ is the temperature at which α is reached for each heating rate, β_i, and E_a is the activation energy at α [12].

5.2 EXPERIMENTAL SECTION

5.2.1 Instrumentation

Thermal Analysis Instruments DSC 2910, routinely calibrated with indium and zinc standards, was utilized for our work. Aluminum hermetic sample pans and lids were used for experiments. The lid was inverted and sealed on top of the pan. Sample and reference pans were manually placed in the DSC cell. Curing was carried out by heating samples from room temperature to 300 °C at varying rates (5, 10, 15, and 25 °C min^{-1}) under nitrogen. Samples in the mass range of 2–5 mg for curing with the additives urea and TEA were found to be appropriate. For scans where SDS was the additive, samples of no more than 1 mg were found to be appropriate. This is because at a larger sample size, the material expanded outside the sealed pan, and results were not reproducible.

5.2.2 Materials

Bisphenol A diglycidyl ether (Araldite 506, epoxide equivalent weight 172–185 Da), triethylamine (99.5%), and sodium dodecyl sulfate (ReagentPlus 98.5%) were purchased from Sigma Aldrich. Urea (U-15 ACS) was purchased from Fisher Scientific Co. Protein hydrolysate was obtained via thermal hydrolysis (at 220 °C) of SRM obtained from Sanimax Industries, Inc. (Montreal, QC, Canada). Protein hydrolysis and recovery by water extraction were carried out as outlined in our previous work [1, 18]. Water-extracted protein hydrolyzed at 220 °C was used for this study (PEP220). Molecular weight was concentrated between 1.4

and 3.5 kDa. As our earlier work demonstrated [1], curing kinetics with salt-extracted samples were difficult to interpret due to the ionic interactions with reactive groups of protein hydrolysate. Additionally, the higher hydrolysis temperature led to lower molecular weight (< 9 kDa), and therefore improved miscibility with DGEBA.

5.2.3 Sample preparation

DGEBA was first mixed with the additive (SDS or TEA) and stirred at room temperature to disperse the additive throughout the epoxy resin and ensure homogeneity. Hydrolyzed protein was then added to the DGEBA-additive mixture. For urea, which is not readily soluble in DGEBA, urea was crushed into small particles and then added to DGEBA. The mixture was then heated at 60 ºC until urea was dissolved in DGEBA, prior to adding the hydrolyzed protein. For all three sets, the mass ratio of DGEBA to hydrolyzed protein was 3:2. The amount of added TEA was 1% by mass of the final epoxy-protein mass. The amounts of urea and SDS used were the molar equivalent to 1% TEA (2.9% for SDS and 0.6% for urea).

5.3 RESULTS AND DISCUSSION

All plots for conversion against time for any heating rate exhibited the autocatalytic model. An example is shown in Figure 5-1. The truncated Sestak-

Berggren model, $f(\alpha) = \alpha^m(1 - \alpha)^n$, can adequately model autocatalytic reactions [1, 12-14]. The model can be simplified further by adding a constraint that because reactions rarely have an order exceeding 2, m + n = 2, and a plot of $\ln[(\beta_i\, d\alpha/dT)/\alpha^{2-n}(1 - \alpha)^n]$ vs. $1/T$ yields a straight line from which the activation energy and $\ln A_o$ are calculated from the slope and y-intercept respectively. The reaction order, n, is selected such that the correlation coefficient, r, is at its maximum value [1, 13]. An example is shown in Figure 5-2.

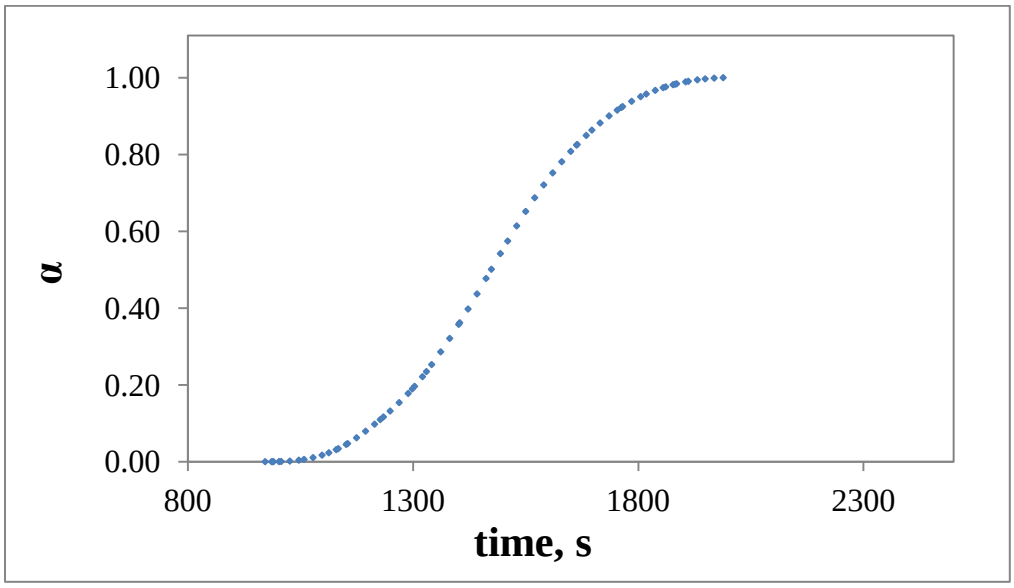

Figure 5-1. Conversion rate as a function of time for 3:2 DGEBA to PEP220 mass ratio at 5 ºC/min in the presence of triethylamine

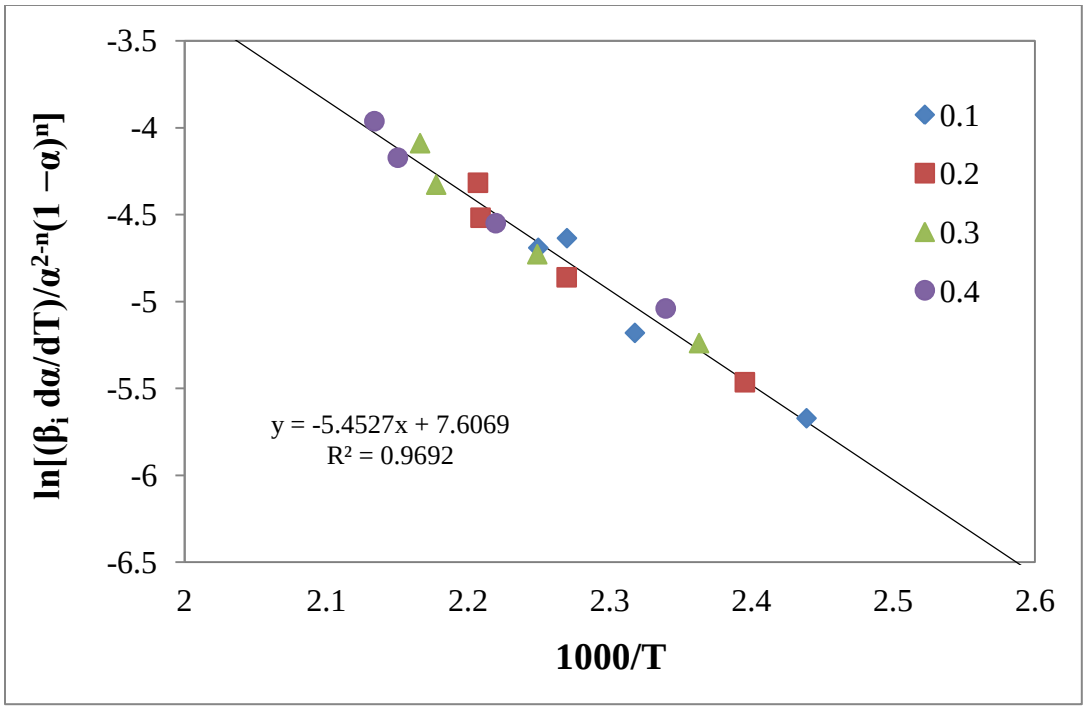

Figure 5-2. Plot for modified autocatalytic model at different conversions for reaction at 3:2 DGEBA to PEP220 mass ratio in the presence of triethylamine

Reaction parameters are summarized in Table 5-1 and are compared with results obtained in an earlier study in which no additives were used.

Table 5-1. Summary of Results for Frequency Factor, Activation Energy, and Reaction Order Calculated from the Autocatalytic Model for DGEBA Cured with Hydrolyzed Proteins.

Additive	$\ln A_o$	E_a, kJ mol^{-1}	n	r
no additive (ref 1)	13.393	65.0	1.31	0.986
triethylamine	6.524	41.5	1.50	0.988
sodium dodecyl sulfate	7.406	43.8	1.67	0.986
urea	15.746	75.0	1.65	0.981

Predictably, the use of the initiator TEA has resulted in a significant reduction in the activation energy, compared to the curing reaction without any additives. The results for denaturants SDS and urea were contrasting. The addition of SDS also decreased the activation energy whereas the presence of urea led to a pronounced increase in activation energy. While the effect of SDS demonstrated that denaturing proteins for cross-linking reactions is as important as targeting the reactive arm of epoxy resins, urea addition was counter-productive. One possible explanation for this is that urea amine groups may interact with the epoxy rings (hydrogen bonding or curing) instead of with the hydrolyzed proteins. Epoxy-urea interactions may therefore offset any benefit from potential protein denaturing. On the other hand, our results showed that SDS was effective in disrupting the hydrophobic interactions among the hydrophobic segments of hydrolyzed proteins [11], and possibly also disrupted such interactions with DGEBA's hydrocarbon backbone. This aspect of SDS may have contributed to increased collisions between reactive groups from the hydrolyzed proteins and epoxide ring of DGEBA.

The reaction order increased for all three reactions in that additives were used compared to the value for epoxy-hydrolyzed protein curing. The use of denaturants, though, caused a more significant increase in the reaction order.

The curing of epoxy resins with materials which contain five different reactive groups (primary and secondary amines, hydroxyls, carboxylic acids, and sulfhydryl groups) is a complex reaction, given the presence of hydroxyl and amine reactive groups that have different reaction orders for curing epoxy rings [15]. Nonetheless, kinetic parameters (Table 5-1) obtained from the truncated Sestak-Berggren model provided simulations which were in reasonable agreement with experimental data (Figures 5-3, 5-4, 5-5, 5-6, 5-7, and 5-8).

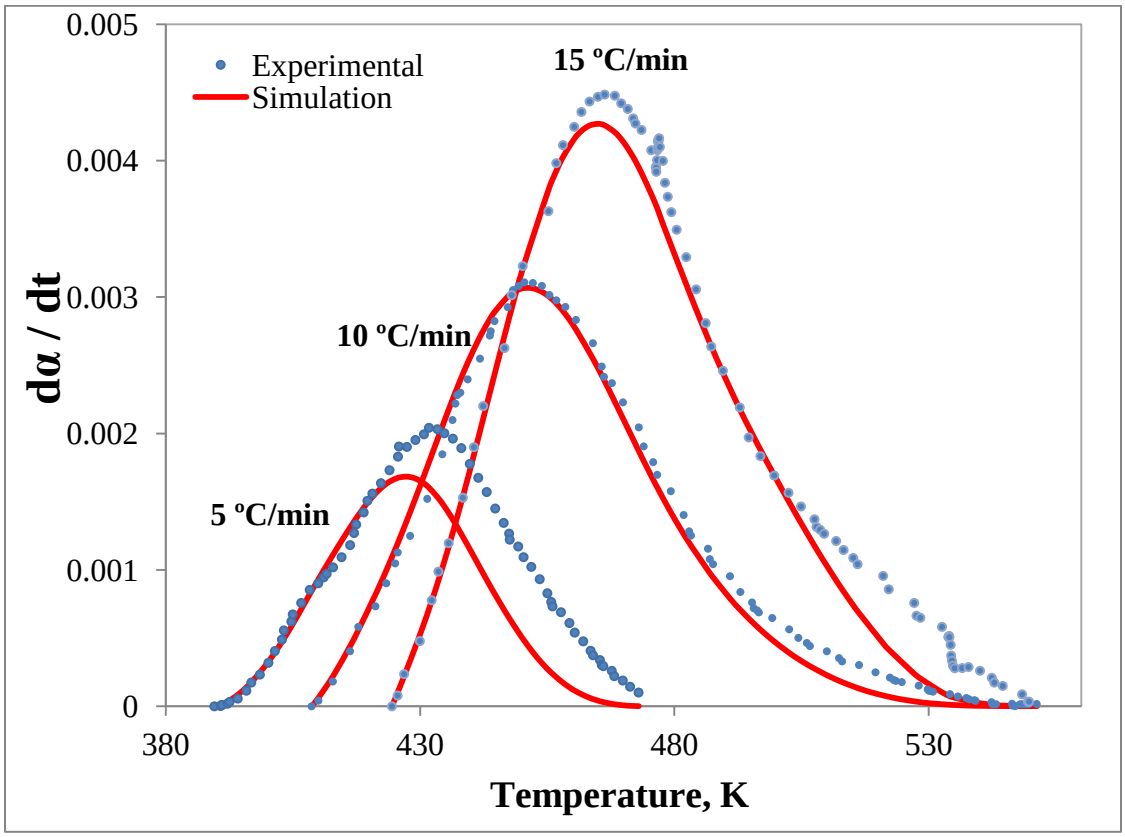

Figure 5-3. Plot for reaction rate, dα/dt, as a function of temperature for experimental results and model for the reaction of DGEBA–PEP220–TEA at different heating rates

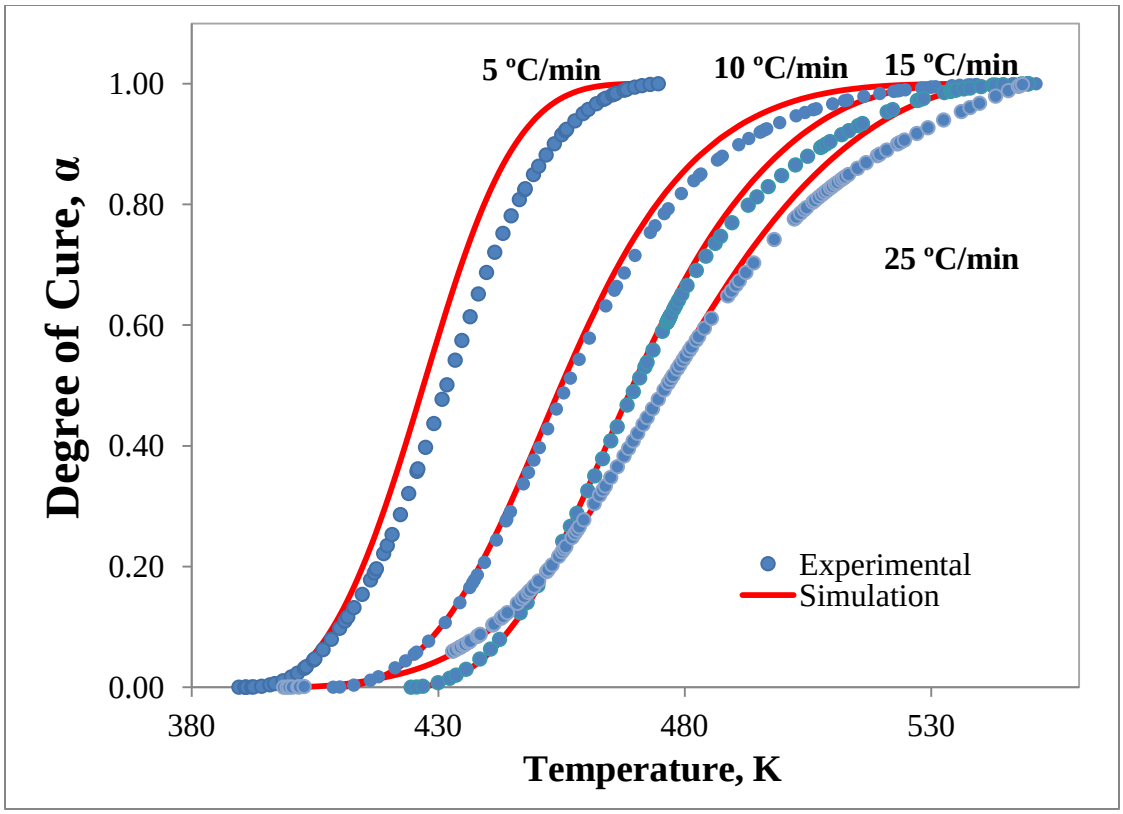

Figure 5-4. Plot for conversion, α, as a function of temperature for experimental results and model for the reaction of DGEBA–PEP220–TEA at different heating rates

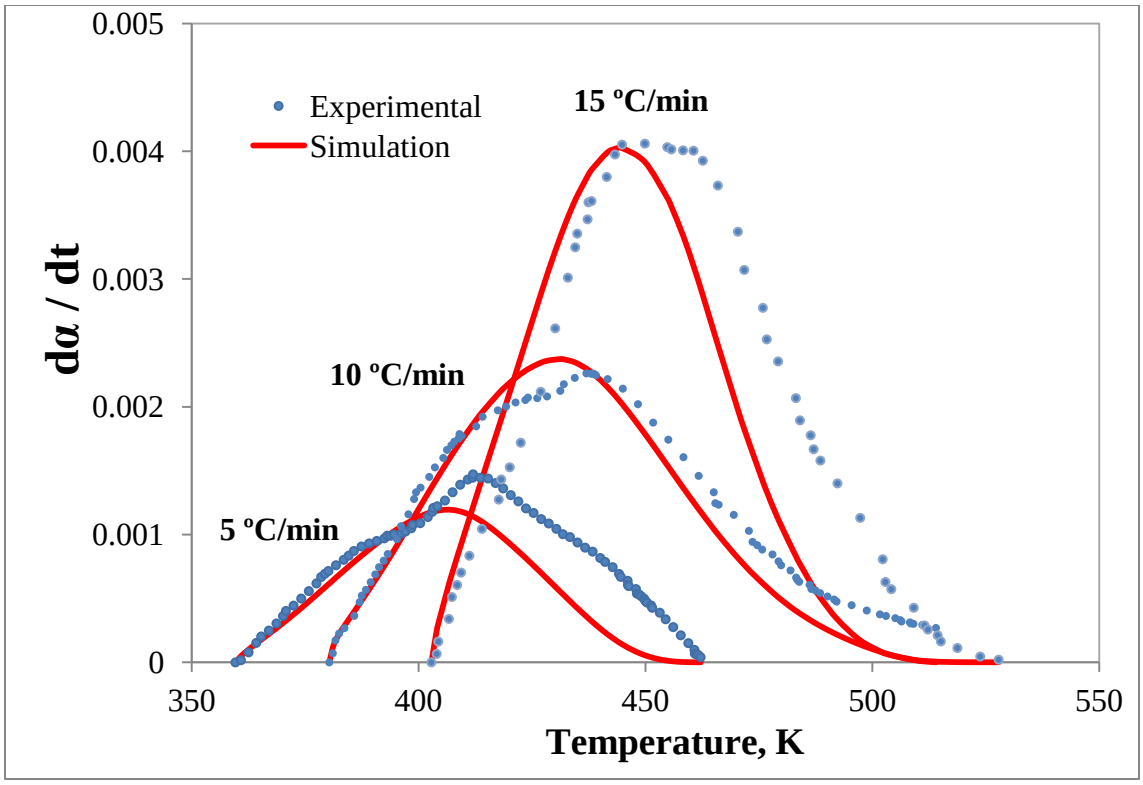

Figure 5-5. Plot for reaction rate, dα/dt, as a function of temperature for experimental results and model for the reaction of DGEBA–PEP220–SDS at different heating rates

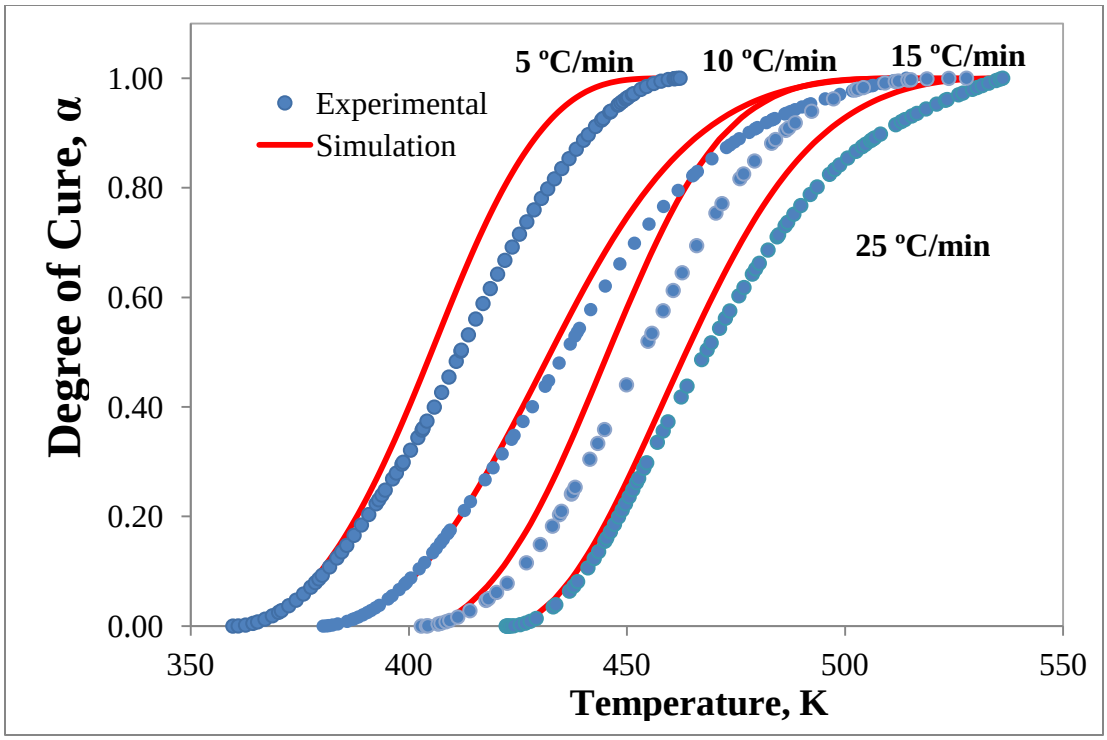

Figure 5-6. Plot for conversion, α, as a function of temperature for experimental results and model for the reaction of DGEBA–PEP220–SDS at different heating rates

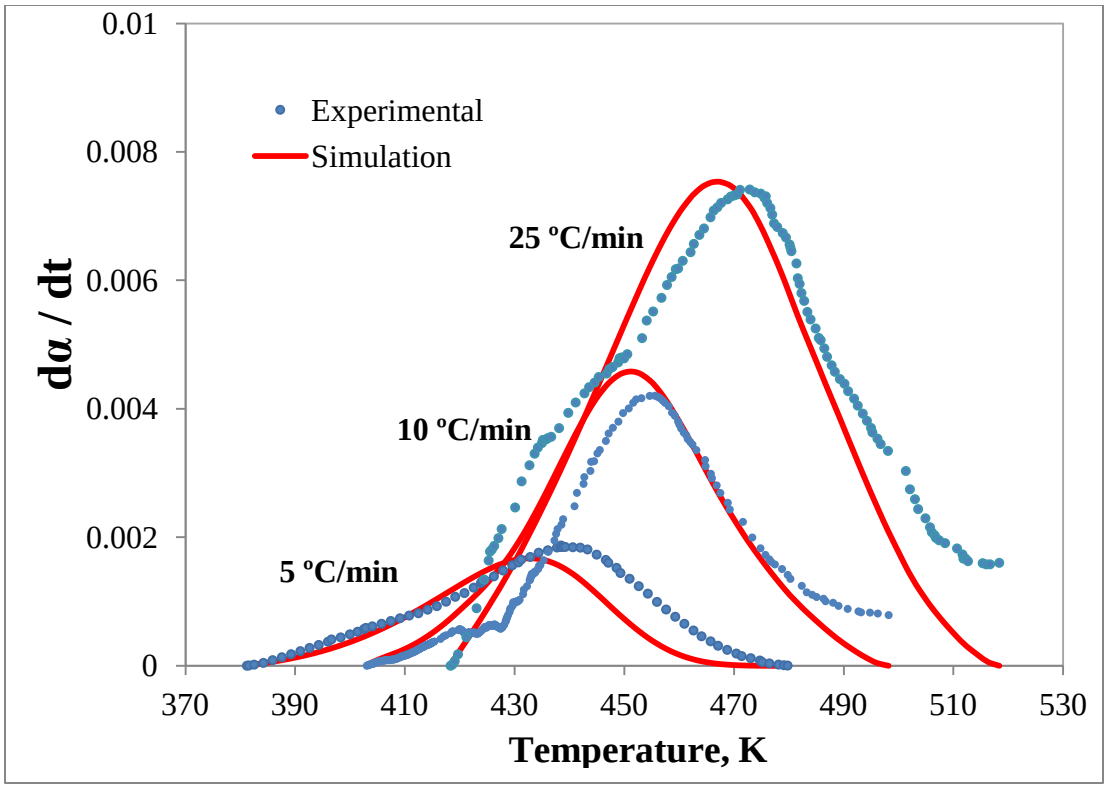

Figure 5-7. Plot for reaction rate, dα/dt, as a function of temperature for experimental results and model for the reaction of DGEBA–PEP220–urea at different heating rates

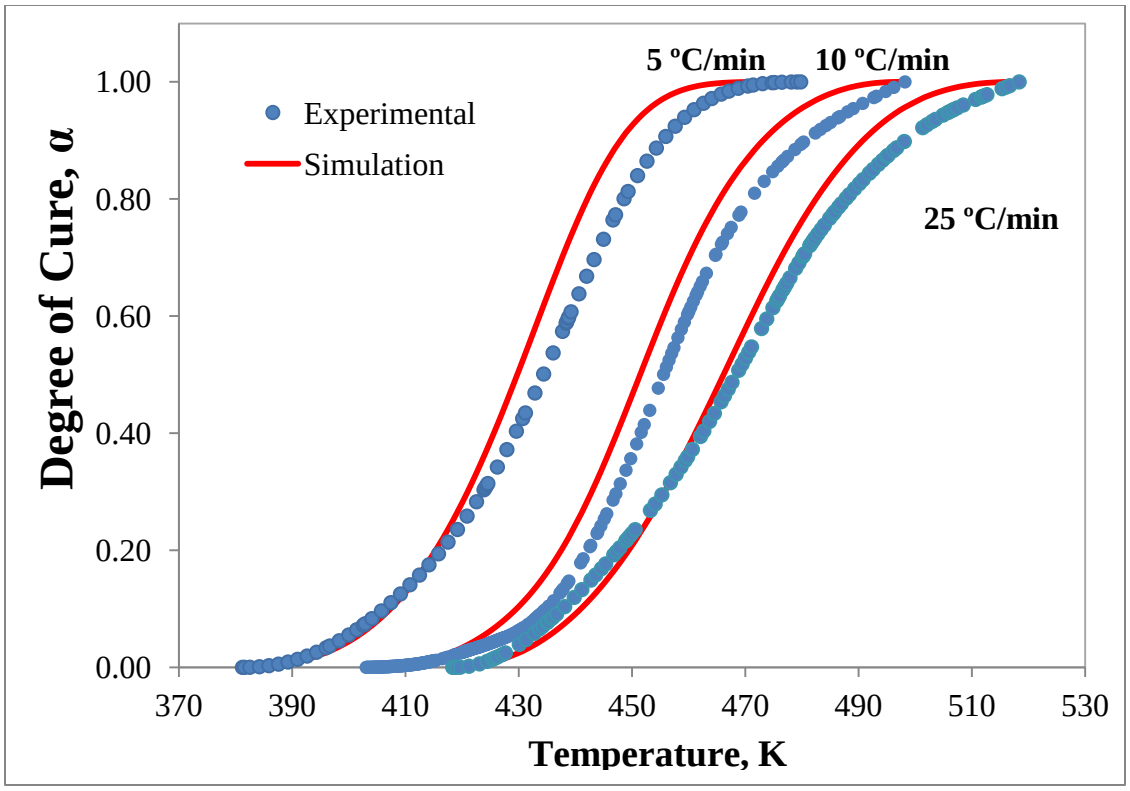

Figure 5-8. Plot for conversion, α, as a function of temperature for experimental results and model for the reaction of DGEBA–PEP220–urea at different heating rates

The model-free isoconversional method was used to further analyze results. Values for the activation energy and the pre-exponential factor were calculated from Equation 2 at increments of 0.05 for degrees of cure in the range from 0.05 to 0.95, and the plots are shown in Figures 5-9 and 5-10, respectively.

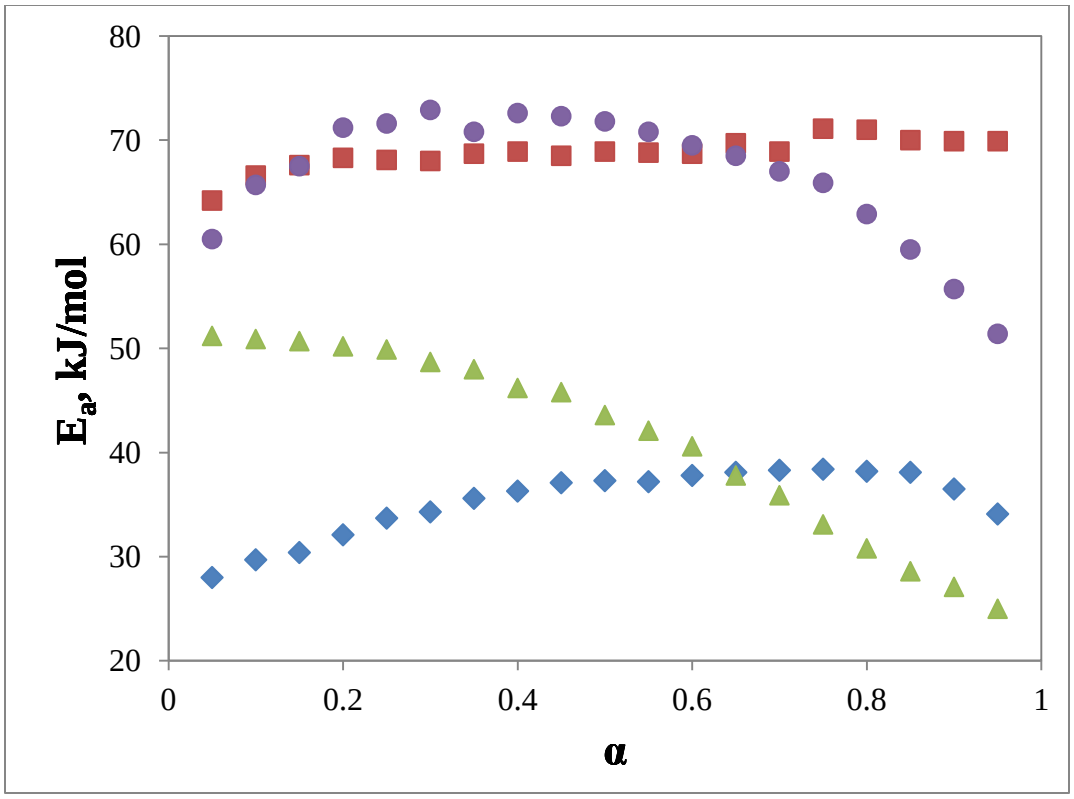

Figure 5-9. Dependency of activation energy on conversion for DGEBA and PEP220 reaction without additives (■ – Ref 1) and in the presence of TEA (▲), SDS (♦), and urea(●)

Activation energy values for urea-added curing were slightly higher than values for curing without additives up to conversions of 0.65, remaining nearly constant for the range of 0.1 – 0.75 and decreasing until reaction completion. Because the amount of urea added to the reaction was rather small (0.6% w/w), had urea reacted with DGEBA, the activation energy should not be consistently higher when compared to the neat system. This result suggests that urea hindered the reaction continuously, making it more likely that there was hydrogen bonding with the epoxy ring oxygen.

SDS-added curing exhibited an activation energy dependency on conversion in contrast to results obtained for curing in the presence of urea. The activation energy slightly increased over the course of the reaction. In fact, activation energy values in the initial stages of the reaction indicated diffusion was the likely rate-determining step. On the basis of this, it may be suggested that hydrolyzed protein denaturing was the predominant process at low degrees of curing. The lack of vitrification as the degree of curing increased for the reaction in the presence of SDS may also suggest that the formed gel remained in the rubbery state, not the glassy state in which vitrification is expected to occur [16], further confirming the role of SDS as a denaturant.

In the presence of an initiator that opens the epoxy ring, the curing of DGEBA proceeded to completion at a high rate up to conversions of 0.5 and then exhibited vitrification at higher conversions as the rate-determining step changes from a chemical-controlled process to a diffusion-controlled process [12]. The activation energy underwent a small decrease as conversion increased up to 0.5, and then a higher rate of activation energy decrease occurred until completion of the curing. The average values for the activation energy obtained from the model-free method were 66.7 ± 6.2 kJ/mol for urea-added curing, 41.4 ± 8.9 kJ/mol for TEA-added curing, and 35.3 ± 3.2 kJ/mol for SDS-added curing. The correlation coefficient, r, for isoconversional plots exceeded 0.98 in the conversions range of 0.05 – 0.65 for urea, 0.2 – 0.95 for TEA, and 0.05 – 0.85 for SDS. In agreement with results obtained from the truncated Sestak-Berggren model, addition of the

denaturant SDS, but not urea, resulted in a significant reduction in activation energy. This decrease in activation energy was more than obtained by reducing the molecular size of proteins by carrying out hydrolysis at higher temperatures [1], thereby demonstrating that utilization of a suitable denaturant is a cost-saving alternative to an energy-intensive hydrolysis process in which proteins are subjected to a higher degree of hydrolysis without significantly improving reactivity in subsequent reactions.

Dependencies of $\ln A_o$ on conversion (Figure 5-10) had trends similar to dependencies of activation energy on conversion. The average values for $\ln A_o$ obtained from the model-free method were 17.1 ± 2.1 for urea-added curing, 9.5 ± 3.1 kJ/mol for TEA-added curing, and 8.2 ± 0.69 kJ/mol for SDS-added curing.

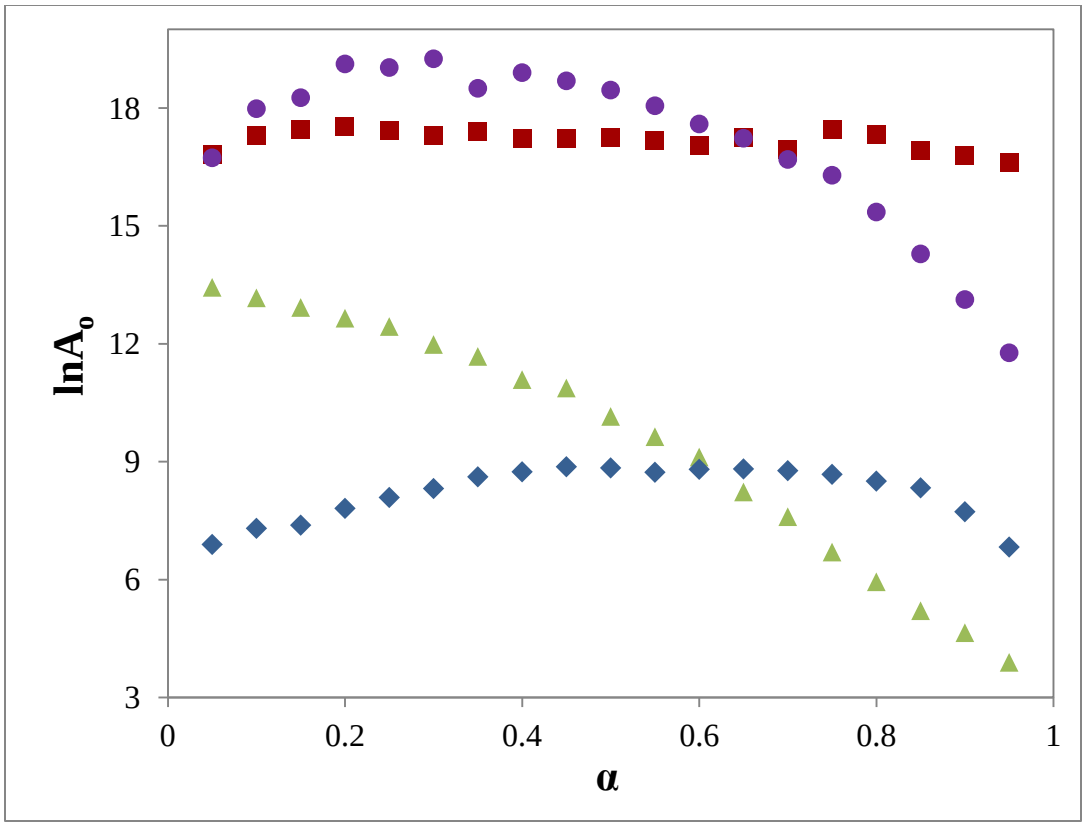

Figure 5-10. Dependency of lnA_o on conversion for DGEBA and PEP220 reaction without additives (■ – Ref 1) and in the presence of TEA (▲), SDS (♦), and urea(●)

Table 5-2. Heats of Reaction with DGEBA expressed in terms of 1 mol of Oxirane.

Additive	ΔH, kJ/mol
no additive (ref 1)	55.0 ± 9.9
triethylamine	64.3 ± 15.7
sodium dodecyl sulfate	97.5 ± 20.9
urea	60.9 ± 17.7

Heats of reaction, ΔH, were obtained by integrating the exothermic peaks. Values for the three reactions investigated in this work, expressed in terms of 1 mol of oxirane, are listed in Table 5-2. Heats of reaction in the presence of urea and triethylamine were comparable to results obtained earlier for the curing of DGEBA with hydrolyzed proteins without any additives. When SDS was used, the heat of reaction has increased. Typical heats of reaction for 1 mol of epoxy rings with primary and secondary amines are 83 and 131 kJ/mol, respectively, and 65 kJ/mol with hydroxyl groups [19]. The increase in reaction heat in the presence of SDS further supports earlier findings that denaturation has the potential to allow DGEBA molecules increased access to reactive sites of the hydrolyzed protein. This increase in reaction heat is an indication that more primary and secondary amines cured the epoxy rings instead of the hydroxyl group. When DGEBA has limited reactive sites, subsequent reactions may occur between unreacted epoxy rings and hydroxyl groups which were formed from the curing of epoxy rings. The presence of SDS enhanced DGEBA-protein reactions at the expense of DGEBA-DGEBA reactions.

5.4 CONCLUSION

DSC was used to investigate DGEBA curing with hydrolyzed proteins in the presence of two protein denaturants and an epoxy ring-opening catalyst (TEA). The addition of either TEA or SDS lowered the activation energy, whereas urea addition led to a slight increase in activation energy. Additionally, SDS increased

the heat of reaction by increasing the availability of primary and secondary amines for curing DGEBA. The heat of reaction in the presence of urea and TEA remained the same compared to the neat epoxy-protein reaction. This work demonstrated the use of SDS as an energetically efficient alternative to provide uncoiled proteins for curing DGEBA rather than producing lower molecular weight protein hydrolysate by increasing the degree of hydrolysis. Cure kinetics in the presence of urea illustrate the importance of selecting an adequate denaturant, such that it interacts with protein molecules instead of the cross-linking reagent.

5.5 REFERENCES

(1) El-Thaher, N.; Mekonnen, T.; Mussone, P.; Bressler, D.; Choi, P. Nonisothermal DSC Study of Epoxy Resins Cured with Hydrolyzed Specified Risk Material. *Ind. Eng. Chem. Res.* **2013**, *52*, 8189−8199.

(2) Imamura, E.; Noishiki, Y.; Koyanagi, H.; Miyata, T.; Furuse, M. (Koken Co., Ltd). Bioprosthetic Valve. US Patent 5,080,670, 1992.

(3) Imamura, E.; Sawatani, O.; Koyanagi, H.; Noishiki, Y.; Miyata, T. Epoxy Compounds As a New Cross-Linking Agent for Porcine Aortic Leaflets: Subcutaneous Implant Studies in Rats. *J. Card. Surg.***1989**, *4*, 50-57.

(4) Zeeman, R.; Dijkstra, P. J.; van Wachem, P. B.; van Luyn, M. J. A.; Marc Hendriks, M.; Cahalan, P. T.; Feijen, J. Successive Epoxy and Carbodiimide Cross-linking of Dermal Sheep Collagen. *Biomaterials* **1999**, *20*, 921-931.

(5) Sunphorka, S.; Chavasiri, W.; Oshima, Y.; Ngamprasertsith, S. Kinetic Studies on Rice Bran Protein Hydrolysis in Subcritical Water. *J. Supercrit. Fluids* **2012**, *65*, 54-60.

(6) Kumar, R.; Choudhary, V.; Mishra, S.; Varma, I. K.; Mattiason, B. Adhesives and Plastics Based on Soy Protein Products. *Ind. Crop. Prod.* **2002**, *16*, 155-172.

(7) Somerville, R. A.; Fernie, K.; Smith, A.; Andrews, R.; Schmidt E.; Taylor, D. M. Inactivation of a TSE Agent by a Novel Biorefinement System. *Process Biochem.* **2009**, *44*, 1060-1062.

(8) Walles, W. E. Role of Flocculant Molecular Weight in the Coagulation of Suspensions. *J. Colloid Interface Sci.* **1968**, *27*, 797-803.

(9) Hunter, R. J. *Foundations of Colloids, 2nd Edition*; Oxford University Press: Oxford, 2001.

(10) Samios, D.; Castiglia, S.; Pesce da Silveira, N.; Stassen, H. Network Formation Studied by Temperature Scanning Brillouin Scattering and Differential Scanning Calorimetry Techniques. I. The Cure of 1,4=Butanediol Diglycidyl Ether with cis=1,2=Cyclohexanedicarboxylic Anhydride Initiated by Triethylamine. *J. Polym. Sci. Part B Polym. Phys.* **2003**, *33*, 1857-1866.

(11) Verbeek, C. J. R.; van den Berg, L. E. Development of Proteinous Bioplastics Using Bloodmeal. *J. Polym. Environ.* **2011**, *19*, 1-10.

(12) Vyazovkin, S.; Burnham, A. K.; Criado, J. M.; Perez-Maqueda, L. A.; Popescu, C.; Sbirrazzuoli, N. ICTAC Kinetics Committee Recommendations for Performing Kinetic Computations on Thermal Analysis Data. *Thermochim. Acta.* **2011,** *520*, 1-19.

(13) Hong, I.; Lee, S. Cure Kinetics and Modeling the Reaction of Silicone Rubber. *J. Ind. Eng. Chem.* **2013,** *19*, 42-47.

(14) Roşu, D.; Caşcaval, C. N.; Mustaţă, F.; Ciobanu, C. Cure Kinetics of Epoxy Resins Studied by non-isothermal DSC Data. *Thermochim. Acta.* **2002,** *383*, 119-127.

(15) Oh, J. H.; Jang, J.; Lee, S. H. Curing Behavior of Tetrafunctional Epoxy Resin/Hyperbranched Polymer System. *Polymer* **2001**, *42*, 8339-8347.

(16) Vyazovkin, S.; Sbirrazzuoli, N. Kinetic Methods to Study Isothermal and Nonisothermal Epoxy-Anhydride Cure. *Macromol. Chem. Phys.* **1999**, *200*, 2294-2303.

(17) Jubsilp, C.; Punson, K.; Takeichi, T.; Rimdusit, S. Curing Kinetics of Benzoxazine-epoxy Copolymer Investigated by Non–isothermal Differential Scanning Calorimetry. *Polym. Degrad. Stabil.* **2010**, *95*, 918-924.

(18) Mekonnen, T.; Mussone, P.; Stashko, N.; Choi, P.; Bressler, D. Recovery and Characterization of Proteinacious Material Recovered from Thermal and Alkaline Hydrolyzed Specified Risk Materials. *Process Biochem*. **2013**, *48*, 885-892.

(19) Langmaier, F.; Mokrejs, P.; Kolomazník, K.; Mládek, M.; Karnas, R. Cross-linking Epoxide Resins with Hydrolysates of Chrome-tanned Leather Waste. *J. Therm. Anal. Calorim.* **2007,** *88*, 857-862.

CHAPTER 6

6.0 GENERAL DISCUSSION AND CONCLUSIONS

This work investigated pathways to convert protein-rich waste biomass into stable, insoluble cross-linked networks, with the aim of recovering value from agricultural waste materials by producing value-added polymers for industrial applications. Glutaraldehyde, a well-known but poorly understood cross-linking reagent, was determined to be a suitable cross-linker, although its reaction chemistry is complex. Previous researchers have proposed different mechanisms for glutaraldehyde reactions with amine groups. We summarized the major reactions into five types, put forth a hypothesis based on a theoretical examination of literature, and experimentally demonstrated the validity of the simplified pathway. The role of water, a previously unexamined parameter, was shown to have competing effects on the reaction. It is a reaction medium for mixing hydrolyzed proteins with glutaraldehyde, a hydrogen source to enhance the reaction, and a by-product which shifts equilibrium to the reactants' side. This investigation demonstrates that the controlled removal of water is of paramount importance to improve cross-linking amine groups with glutaraldehyde.

Figure 6-1 is an illustration of the role of water. As we discussed earlier (Figure 1-3), we proposed a simplified reaction mechanism, based on theoretical analyses of reported reactions, for the reaction of glutaraldehyde and amines in order to help understand the overall reaction. The simplified mechanism was

experimentally shown to be an adequate representation for the cross-linking reactions of amines and glutaraldehyde.

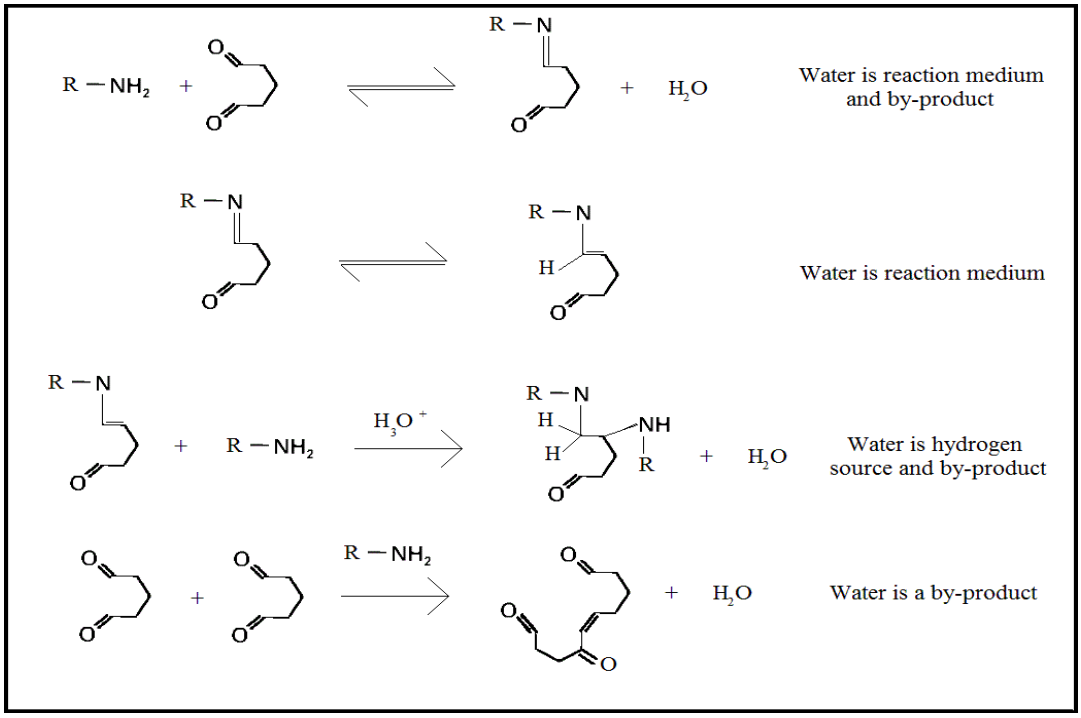

Figure 6-1. The role of water in glutaraldehyde-amine reactions as solvent, hydrogen source, and byproduct

The extent of hydrolysis and protein hydrolysate molecular weight, viscosity, electrolyte content, mass ratio of the protein-rich biomass to the cross-linking reagents, and the role of denaturants were also studied. Kinetics models, obtained by the non-isothermal differential scanning calorimetry technique, for cross-linking hydrolyzed proteins with epoxy resins have provided additional insight on the effect of various reaction parameters on the conversion process. Figure 6-2 summarizes our findings. Increased viscosity and presence of salts

were both found to increase the cross-linking activation energy whereas mass ratio, with the exception of significant amounts of excess reactant, was found to have a very small effect on activation energy.

The presence of salts led to increased activation energy during cross-linking but the final product had lower solubility and reduced swelling in water. One explanation for higher activation energy is that the bonds ions form with reactive groups (e.g. COO^-, NH_3^+) of protein hydrolysates need to be broken up prior to the reaction with DGEBA. The additional activation energy in the presence of salts may be attributed to breaking bonds between salt ions and protein hydrolysate reactive sites. Another plausible explanation is that cations and anions form bridges, i.e. electrostatic forces that prevent molecules from sliding across one another, thereby increasing the activation energy. These electrostatic forces are also responsible for the lower solubility and swelling of networks formed by cross-linking salt solution extracted proteins with epoxy resins. This can be tested this further by extracting proteins with distilled water containing $Fe(OH)_2$ or $Fe(OH)_3$ and not use any anions. If the polymer swells, it means anions are needed for efficient binding. If the swelling is not severe, the polymer can be potentially used for selective sorption of negatively charged molecules. Binding and swelling may thus be controlled. Excessive binding makes pore-formation difficult whereas excessive swelling leads to failure.

High temperature hydrolysis is expensive and leads to low yields of total amino acids and at the same time does not fully un-coil proteins for their effective utilization. Therefore, in order to alleviate the high cost of SRM conversion into feed-stock, a future direction could be to utilize safe protein biomass which can be hydrolyzed at mild temperatures (120 ºC or lower) and used along hydrolyzed SRM to off-set the high cost of hydrolysis and low yield of amino acids. Denaturants are then adequately chosen to by-pass the need for higher degrees of hydrolysis.

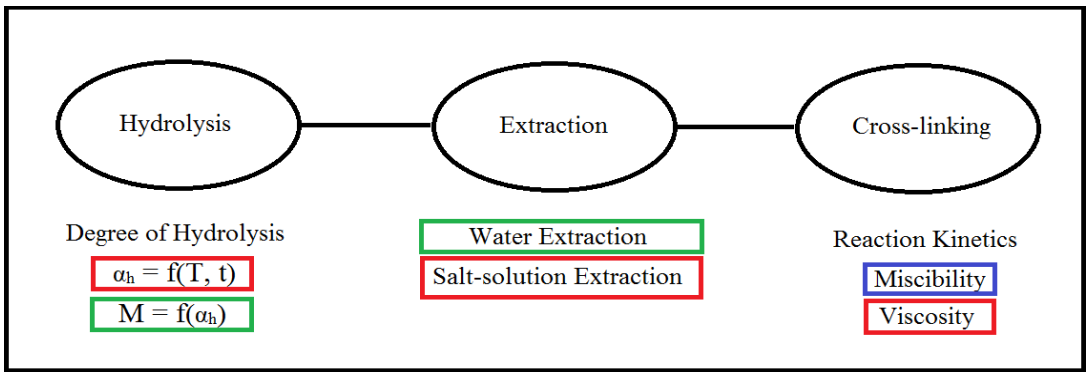

Figure 6-2. The impact of each parameter from each unit step on the overall process

Selection of adequate denaturant lowers activation energy more efficiently than decreasing the molecular size of protein hydrolysate by carrying out hydrolysis at higher temperatures, an important finding for a more energy-efficient overall conversion process. This approach achieves higher amino acid

yields, larger molecules, and an overall lower operational cost. In the case of epoxy cross-linking, sodium dodecyl sulfate was found to be effective in lowering activation energy by disrupting hydrophobic interactions. On the other hand, another well-known denaturant, urea, increased activation energy because it interacted with oxirane, the reactive site of epoxy resins. The implication of this result is that denaturants have to be chosen on the basis they only interact with protein molecules and not with the cross-linking reagent.

6.1 FUTURE WORK

Safety regulations related to Specified Risk Material (SRM) dictate specific treatment methods prior to their disposal or utilization in value-added applications. The two hydrolysis methods investigated in this work require significant amount of energy. The improved reactivity of the hydrolyzed protein-derived materials obtained at high degrees of hydrolysis was shown to be comparatively small. The implication of this finding is that a better alternative can be obtained from protein-rich biomass derived from safe sources. The degree of hydrolysis, and in turn the cost of this step, can be reduced. The use of denaturants can also help reduce the cost associated with high hydrolysis temperatures. In addition to that, a bio-hydrolysis method can be explored as another alternative. The breakdown of biomass by bacteria and/or enzymes may cost less. Under anaerobic conditions, bacteria produce methanol. This helps to increase the value recovery of the overall process.

It is also recommended that the kinetics of hydrolysis are investigated for different types of biomass. The aim of this approach is to determine which type of biomass requires less energy. The fraction of β-sheets in the biomass is expected to be proportional to energy consumption. The thermal hydrolysis method can also be combined with a subsequent step of bacterial hydrolysis in order to minimize energy consumption and the duration of the combined hydrolysis process. The breakdown of β-sheets by heat and/or denaturants followed by bacterial digestion may provide the most energy-saving approach for hydrolysis.

This body of work investigated the addition of two denaturants, urea and sodium dodecyl sulphate (SDS), as discussed in Chapter 5. It is recommended that other additives be investigated as well. Additives such as chaotropic compounds, e.g. guanidinium thiocyanate, in addition to organic and inorganic protein denaturants, among others, can also be explored. It is plausible that any of these compounds has the potential to improve the recovery of the protein-rich material during the extraction step in addition to the improved reactivity in the next step. It is also recommended to evaluate the effect of the mass of these additives on the overall process.